

12th International Conference on

ENVIRONMENTAL DEGRADATION



of Materials in Nuclear Power Systems-Water Reactors

August 14-18, 2005

Snowbird Resort
Salt Lake City, Utah, USA

FINAL TECHNICAL PROGRAM *With Abstracts*

Sponsored by:

TMS

The Minerals, Metals &
Materials Society

NACE
INTERNATIONAL
Informing the World on Corrosion Control



Co-sponsored by:

The Japan Institute of Metals
Japan Society of Corrosion Engineering
The Society of Materials Science, Japan

Welcome to the 12th International Conference on Environmental Degradation of Materials in Nuclear Power Systems-Water Reactors!

TABLE OF CONTENTS

Organizing Committee.....	3
Social Functions.....	3
Snowbird Resort Facilities.....	4
Proceedings and Policies.....	4
Cliff Lodge Floor Plan.....	5
Technical Program.....	6
Conference at a Glance.....	Back Cover

CORPORATE SPONSORS

The Environmental Degradation Organizing Committee and TMS thank the following corporations for their sponsorship:

- Atomic Energy of Canada LTD, Chalk River
- Battelle
- Dominion Engineering Inc.
- EPRI
- Framatome ANP
- General Electric-Global Research Center
- General Electric-Nuclear Energy
- General Electric-Nuclear, Wilmington
- Hitachi LTD
- Korean Atomic Energy Research Institute
- Mitsubishi Heavy Industries LTD
- Nippon Nuclear Fuel Development Co. LTD
- Pacific Northwest National Laboratory
- Ringhals
- Studsvik Nuclear Aktiebolag
- TEPCO
- Toshiba Co.
- U.S. Nuclear Regulatory Commission

TECHNICAL SCOPE AND THRUST

Purpose

Environmentally induced materials problems cause a significant portion of nuclear power plant outage time and are of great economic and safety concern both for operating light water reactors that continue to age and for the next-generation systems that are currently being designed. The purpose of this conference is to foster the exchange of ideas about such problems and their remedies in nuclear power plants using water coolants.

Focus

The conference focuses on the degradation of nickel base alloys, stainless steels, pressure vessel and piping steels, zircalloys, and other alloys in water environments relevant to reactor vessels and internals, steam generators, fuel cladding, irradiated components, fuel storage containers, and balance of plant components and systems. A new topic for the 12th conference is materials degradation issues for supercritical water-cooled reactors and other generation IV water-cooled nuclear energy systems.

Format

The established conference format allows scientists and engineers concerned with environmental degradation processes (corrosion, mechanical, and radiation effects) to exchange views and present their latest results through a combination of invited and contributed presentations.

The conference is of interest to utility engineers, reactor vendor engineers, plant architect engineers, and consultants involved in design, construction, and operation of water reactors, as well as researchers concerned with the fundamental nature of materials degradation.



ORGANIZING COMMITTEE

Larry Nelson

GENERAL MEETING CHAIR
GE Global Research Center

Peter King

TECHNICAL PROGRAM CHAIR
Babcock & Wilcox Canada Ltd.

Todd Allen

ASST. TECHNICAL PROGRAM CHAIR
University of Wisconsin-Madison

PROGRAM COMMITTEE

Peter Andresen, *GE Global Research Center*

Steve Bruemmer, *Pacific Northwest National Laboratory*

Gene Carpenter, *U.S. Nuclear Regulatory Commission*

Paul Doherty, *University of Waterloo*

Peter Ford, *GE Global Research Center (retired)*

Barry Gordon, *Structural Integrity Associates Inc.*

Ron Horn, *GE Nuclear Energy*

Il Soon Hwang, *Seoul National University*

Natraj Iyer, *Westinghouse – Savannah River*

Rich Jacko, *Westinghouse Electric Corp.*

Christer Jansson, *SwedPower AB*

Renate Kilian, *Framatome ANP GmbH*

Al McIlree, *EPRI*

Bill Mills, *Bechtel Bettis Inc.*

Peter Scott, *Framatome ANP*

Tetsuo Shoji, *Tohoku University*

Ed Simonen, *Pacific Northwest National Laboratory*

Robert Tapping, *AECL Chalk River Nuclear Labs*

Charlie Thompson, *Lockheed-Martin*

Francois Vaillant, *Electricite de France*

Gary Was, *University of Michigan*

Toshio Yonezawa, *Mitsubishi Heavy Industries Ltd.*

SOCIAL FUNCTION HIGHLIGHTS

Welcoming Reception

Sunday, August 14
6 to 7 p.m.

Cliff Lodge, Golden Cliff/Eagle's Nest

Authors' Breakfast

Daily

Monday, August 15 - Thursday, August 18
7 to 8 a.m.

Magpie A/B

Authors' breakfast is for authors, chairs, and organizers. Authors are required to attend only on the morning of their presentation in order to coordinate last minute changes and to receive instructions before presentations begin.

Conference Banquet

Wednesday, August 17
6:30 to 9:30 p.m.

La Caille Restaurant

The restaurant, surrounding gardens and vineyards are a creation of David Johnson, Steven Runolfson and Mark Haug, the owners. They spent over twenty years creating what is commonly referred to as a "must see" in the Salt Lake area. Just 20 minutes from downtown, the internationally acclaimed restaurant reverses time to the rural valleys of Bordeaux, Champagne, and Alsace. Many visitors have remarked about its beauty, decor, and wildlife. La Caille's signature wine comes from its vineyards and is bottled on-site.

Round-trip transportation is provided from the Snowbird Resort to La Caille Restaurant. Buses depart from the resort at 6 p.m.



INTERNET ACCESS

Wireless Internet access is available in the meeting rooms throughout the conference.

SNOWBIRD RESORT RECREATION AND FACILITIES

Throughout the village there are seven restaurants, five lounges, a full service pharmacy, post office, grocery deli, internet café, liquor store, other concessions and several unique gift shops.

The paved walkways from each lodge make getting around the resort convenient for guests. The Barrier Free Trail is a one-mile round-strip nature walk that begins at the Skier's bridge and climaxes at the observation deck overlooking the Gad Valley. Adults and children of all ages can enjoy this low impact hike. The trail is also wheelchair accessible.

The Snowbird Activity Center and many of the mountain's favorite activities are accessible from the plaza deck next to the famous aerial TRAM.

There is something for everyone at Snowbird with the Cliff Spa, tennis courts, fish pond, playground, horseback riding, ATV tours, Alpine Slide, ZipRider, Bungy trampoline, and more.

AIRPORT TRANSPORTATION

Canyon Transportation vans provide transportation between the Snowbird Resort and the Salt Lake City Airport. Arrangements can be made and confirmed through Snowbird Central Reservations at (800) 453-3000. Round-trip transportation is \$50 per person. Reservations are required.

Taxi service is also available at a cost of approximately \$90 to \$100 for a one-way trip.

POST-CONFERENCE PROCEEDINGS

Conference proceedings will be published as a CD-ROM planned for completion in October 2005. One copy of the proceedings will be shipped to each full registrant when the CD is available. Additional proceedings CD-ROMs can be ordered at the registration desk or by contacting TMS Customer Service, (724) 776-9000, ext. 256. The cost of each volume is \$102 (shipping and handling included).

AMERICANS WITH DISABILITIES ACT



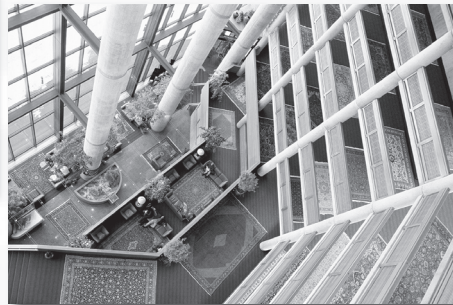
TMS strongly supports the federal Americans with Disabilities Act (ADA) which prohibits discrimination against, and promotes public accessibility for, those with disabilities. In support of, and in compliance with, ADA, we ask those requiring specific equipment or services to notify an individual at the conference registration desk.

AUDIO/VIDEO RECORDING POLICY

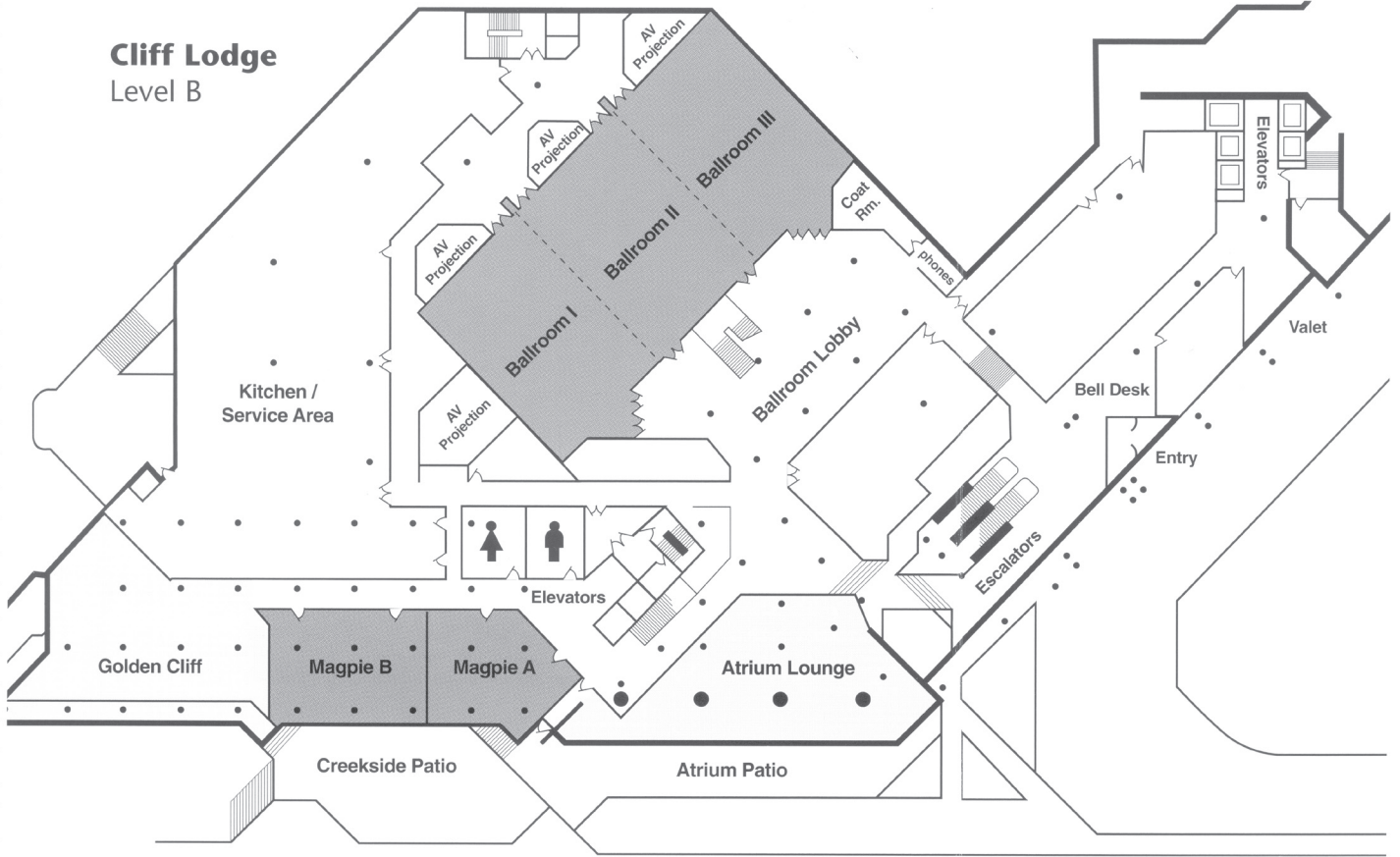
TMS reserves the right to all audio and video reproductions of presentations at TMS sponsored meetings. Recording of sessions (audio, video, still photography, etc.) intended for personal use, distribution, publication, or copyright without the express written consent of TMS and the individual authors is strictly prohibited.

REFUND POLICY

The deadline for all refunds was July 25, 2005. No refunds are issued at the meeting.



Cliff Lodge Level B



Cliff Lodge Level C



Technical Program

12th International Conference on Environmental Degradation of Materials in Nuclear Power Systems-Water Reactors

BWR SCC and Modeling - I

Monday AM Room: Ballroom I
August 15, 2005 Location: Cliff Lodge

Session Chairs: Lawrence Nelson, GE Global Research Center; Kenro Takamori, Tokyo Electric Power Company

8:00 AM

Advances in Electrochemical Corrosion Potential Monitoring in Boiling Water Reactors: *Sam Hettiarachchi*¹; ¹General Electric

Electrochemical corrosion potential (ECP) monitoring gained critical attention in the early 80's since the recognition of elevated ECP being an important factor that can enhance the susceptibility of structural materials to undergo stress corrosion cracking (SCC) in operating boiling water reactor (BWR) environments. Since then, many BWRs have performed HWC mini-tests to confirm the effectiveness of hydrogen water chemistry (HWC) in lowering the ECP of reactor internals below -230 mV(SHE), the industry accepted HWC specification value to achieve potential SCC mitigation. Currently, there are over 40 BWRs worldwide that have monitored ECP or continuously monitoring ECP under a variety of water chemistry conditions. In addition, ECP measurements have been made at least at eight different locations in the BWR heat transport circuit that has enabled a better understanding of the redox conditions prevailing in different parts of the BWR. The measurements have also helped the ECP modeling efforts to improve their predictive capability. The paper will highlight the evolution of ECP monitoring efforts from early 80's to date, including improved understanding of ECP mapping in the BWR heat transport circuit. In addition, the paper will address the unique ECP response of the lower plenum to hydrogen addition. The paper will also include the post-NobleChem™ ECP response of about 20 BWRs, that have applied NobleChem™ and monitored ECP.

8:25 AM

Effects of Hydrogen Peroxide and Oxygen on Corrosion of Stainless Steel in High Temperature Water: *Shunsuke Uchida*¹; Tomonori Satoh¹; Yoshiyuki Satoh¹; Naoshi Usui²; Yoichi Wada²; ¹Tohoku University; ²Hitachi, Ltd.

Static and dynamic responses of stainless steel specimens exposed to H₂O₂ and O₂ in high temperature water were evaluated by analyzing ECP and FDCI (frequency dependent complex impedance). The oxide films on the specimens were characterized by multilateral surface analyses, e.g., LRS, SIMS, XPS and direct electric resistance measurement. As a result of evaluation, it was confirmed that 1) corrosive condition of BWR normal water chemistry (NWC) was simulated by 100 ppb H₂O₂ without co-existing O₂, while that of hydrogen water chemistry (HWC) was simulated by 10 ppb H₂O₂, 2) ECP under HWC was as high as that under NWC, while dissolution rate of oxide film under HWC was much lower than that under NWC, 3) combination effects of electric resistance and dissolution rate of oxide caused same level ECP for both NWC and HWC, and 4) distinct weight loss of the specimen exposed to 100 ppb H₂O₂ was observed.

8:50 AM

Effect of the Plastic Strain Level Quantified by EBSP Method on the Stress Corrosion Cracking of L-Grade Stainless Steels: *Yoshinori Katayama*¹; Motoji Tsubota¹; Yoshiaki Saito¹; ¹Toshiba Corporation

SCC in L-grade stainless steel components with heavy surface cold work has been reported. Plastic strain introduced by the cold work during fabrication process is important factor for SCC. In order to clarify the relation between SCC susceptibility in high temperature water and plastic strain, misorientation obtained from EBSP (Electron Backscattering Pattern) method has been carried out. Misorientation vs. hardness (HV) curve was divided into two stages, and the boundary hardness around HV300 was reported to be a critical hardness for the TGSCC susceptibility. In the case of HV<300, misorientation by EBSP was considered to be relating to the dislocation density and have linear relationship between the plastic strain, hardness, yield strength. In this report, the effect of water chemistry has been also investigated, and it was found out that SCC of L-grade stainless steels with heavy cold work occurred regardless of water condition.

9:15 AM

Correlation between Deformation-Induced Microstructures and TGSCC Susceptibility in Low Carbon Austenitic Stainless Steels: *Akihiko Kimura*¹; Hideki Ohkubo¹; Tomohiro Noda¹; ¹Kyoto University

Microstructural observations were done for cold rolled SUS304L and SUS316L steels after slow strain rate tests in a hot water in order to correlate the TGSCC susceptibility with the deformation-induced microstructures. Slow strain rate tests were carried out at 561K in a pressurized hot water with dissolved oxygen of 8 ppm. EPR tests also carried out following the JIS standard. The EPR-DOS was remarkably reduced by cold work. Deformation-induced phase transformations were investigated by magnetic field measurements and TEM microstructural examinations. A magnetic field experiments revealed that a small amount of martensite phase was observed in SUS316L after cold work and several tens percent of one in SUS304L. TEM examinations also revealed that many twins were formed by the cold roll. With increasing cold work, the engineering strain and the reduction in area of SUS304L were markedly reduced, and TGSCC occurred. The role of deformation-induced microstructural changes in the TGSCC will be discussed based on the EPR tests, slow strain rate tests and microstructural examinations.

9:40 AM Break

BWR SCC and Modeling - II

Monday AM Room: Ballroom I
August 15, 2005 Location: Cliff Lodge

Session Chairs: Lawrence Nelson, GE Global Research Center; Kenro Takamori, Tokyo Electric Power Company

10:30 AM

The Initiation of Environmentally Assisted Cracking in BWR High Temperature Water: *Shengchun Wang*¹; Yoichi Takeda¹; Kazuhiko Sakaguchi¹; Tetsuo Shoji¹; ¹Tohoku University

The initiation of environmentally assisted cracking (EAC) usually takes a long time in LWR high temperature water. To understand where EAC tends to initiate and how it initiates, i.e. the initiation mechanism, would be significant in proactively preventing harmful deep cracks and to the development of materials of high EAC resistance. The initiation of EAC from stainless steel specimens of surface work hardening layers in BWR high temperature water has been proposed to be a repeating process of oxidation/film rupture based on a previous work of ours. The surface work hardening layer and local stress concentration, e.g. at a scratch site, were shown to influence the EAC initiation. Meanwhile, in that work, the role of slip lines is required to be made clear to further the understanding of the development of crack embryos. Those slip lines were already introduced by the applied tensile stress. The present work was focused on specimens without surface work hardening layers. The surface oxide film rupture was examined by TEM. It was shown that those slip lines are not obviously sensitive to EAC in high temperature water. Factors affecting EAC initiation in BWR high temperature water were discussed.

10:55 AM

Stress Corrosion Cracking of Type 316 and 316L Stainless Steels in High Temperature Water: *Nobuhisa Ishiyama*¹; Masami Mayuzumi¹; Yoshihiro Mizutani¹; Junichi Tani²; ¹Tokyo Institute of Technology; ²Central Research Institute of Electric Power Industry

Recently, stress corrosion cracking (SCC) was observed in lots of Japanese BWR components made of L grade stainless steels (SS) with very low carbon content. The cracking morphology changes from trans-granular (TG) type in the immediate surface area to inter-granular type along the cracking path. SCC of grade SS is quite different from the conventional IGSCC of type 304 SS with a weld sensitization structure. SCC test was conducted by the creviced bent beam (CBB) method in high temperature water containing 8 ppm dissolved oxygen (DO). The test specimen was prepared by adding cold rolling and/or heat treatment at a temperature range from 873K to 1073K. Degree of sensitization was measured by an electro-chemical potentio-kinetic method, together with hardness to discuss the SCC test results. The maximum SCC susceptibility was observed in a as-cold rolled condition for both Type 316 and 316L SS.

11:20 AM

Crack Growth Behaviors of Low Carbon 316 Stainless Steels in 288°C Pure Water: *Mikiro Itow*¹; Masao Itatani¹; Masaaki Kikuchi¹; Norihiko Tanaka¹; ¹Toshiba Corporation

In recent years in Japan, the components in BWR primary systems made of low carbon 316 stainless steels, such as core shroud and PLR piping, have suffered from stress corrosion cracking (SCC) and it has become more important to assess the integrity and to predict the lifespan of these components. The Nuclear Plant Operation and Maintenance Code has been developed and is going to be applied for nuclear power system components. According to the code, if a crack is detected in a component, the evaluation of crack growth due to SCC is required. A prerequisite for performance of the evaluation is preparation of a crack growth rate database, that is, data on the relationship between crack growth rate and stress intensity factor (K). In order to reduce incubation time for stress corrosion crack initiation and to obtain appropriate crack growth rate data, environmental pre-cracking accompanied by intergranular morphology is considered to be applicable to the SCC growth testing. In this study, to clarify the loading condition to introduce intergranular cracking for low carbon 316 stainless steel, the crack growth tests of 316NG were carried out in 288°C pure water under high corrosion potential condition simulating a BWR reactor water environment. The target Kmax value was 30MPa^m^{0.5} and the loading mode was gentle cyclic waveforms with high R ratio (0.8-0.9) and low frequency (0.0001Hz). The fracture morphology of the specimen tested at R=0.9 was completely intergranular but that tested at R=0.8 was mixed mode of intergranular and transgranular morphologies. Based on the literature data and the results obtained in this study, the relationship between fracture morphology and loading mode was discussed. Also, SCC and corrosion fatigue growth rates were discussed by means of time domain analysis.

11:45 AM

Influence of Heat Treatment, Aging and Neutron Irradiation on the Fracture Toughness and Crack Growth Rate in BWR Environments of Alloy X-750: *Anders Jenssen*¹; Pål Efsing²; Johan Sundberg¹; ¹Studsvik Nuclear AB; ²Ringhals AB

During the refueling outage of 1999, defects were detected in brackets of the core spray system in Barsebäck units 1 and 2. The brackets were made of Alloy X-750 heat treated according to AMS 5598 (solution annealed at 980°C/1 h, followed by aging at 730°C/8 hrs and 620°C/8 hrs). Continued operation of the reactors was granted after an extensive flaw tolerance analysis. One limitation identified in the analysis was the relative paucity of relevant crack growth rate and fracture toughness data on Alloy X-750 in the conditions used in the components, as well as for modern heat treatments. For this reason crack growth rate and fracture toughness tests were initiated. The material conditions covered in these tests were archive and irradiated material (~1·10¹⁹ n/cm², E>1 MeV) of the same heat and heat treatment condition (AMS 5598), as well as another heat in an improved heat treatment condition (1080°C/1 h, followed by aging at 715°C/30 h). Crack growth rate testing was performed in simulated BWR normal water chemistry and hydrogen water chemistry, while fracture toughness testing was done in air at 288°C. The results from these tests will be presented and discussed.

PWR Primary - I

Monday AM
August 15, 2005

Room: Ballroom II
Location: Cliff Lodge

Session Chairs: David Morton, Lockheed Martin (KAPL); Toshio Yonezawa, Mitsubishi Heavy Industries, Ltd.

8:00 AM

Influence of Surface Films on the Susceptibility of Alloy 600 to SCC in PWR Primary Water: *Thomas M. Devine*¹; Todd S. Mintz¹; ¹University of California

The susceptibility of Inconel 600 to stress corrosion cracking (SCC) in the primary water of a pressurized water reactor (PWR) is strongly dependent on potential. In the present paper we assess the validity of the hypothesis that the potential dependency of SCC is related to the influence of potential on the identities of the surface films that form on Inconel 600. That is, according to the hypothesis, SCC requires the presence of a particular surface film. The identities of the surface films that develop at different potentials on Inconel 600 in PWR primary water (2 ppm LiOH + 1200 ppm H₃BO₃) at 288°C were investigated in situ by surface enhanced Raman spectroscopy (SERS). The in situ results were supplemented by ex situ Auger electron spectroscopy. To help identify the components of the films that grow on Inconel 600, the films that form on unalloyed nickel, chromium, and iron in 288°C PWR primary water were also investigated in situ by SERS. The main results of the in situ SERS investigation of the surface films are as follows. (1) No films were formed on Inconel 600 at

potentials below the region of potential in which SCC occurs. (2) A chromium-rich oxide forms on Inconel 600 in the SCC region. (3) NiO forms as the potential is increased immediately above the region of SCC susceptibility. (4) At still higher potentials, films of (Fe,Cr)₂O₃ and Ni_{3-x}Fe_xO₄ form. The results are consistent with concept that specific films affect SCC susceptibility.

8:25 AM

Oxidation of Ni Base Alloys in PWR Water: Oxide Layers and Associated Damage to the Base Metal: *Pierre Combrade*¹; Marc Foucault¹; Peter M. Scott¹; Eric Andrieu²; Philippe Marcus³; ¹Framatome-ANP; ²ENSIACET; ³Ecole Nationale Supérieure de Chimie de Paris

Knowledge of the oxidation processes on Ni base alloys in PWR primary coolant is of major importance for at least two practical reasons: (i) the activity of the circuit is mainly due to cations released by the corrosion of steam generator tubes and (ii) the oxidation process is at the origin of the initiation of IGSCC cracks on Alloys 600, 82 and 182. Understanding the root causes of this cracking should also allow the safety margins offered by the Alloys 690, 52 and 152 that have replaced the former ones to be predicted more accurately. During the last 8 years, Framatome-ANP has devoted a significant effort to the study of the oxidation of Alloys 600 and 690 in PWR primary coolant by supporting several PhD theses. The present paper summarizes these studies and our present understanding of the oxidation of Ni base alloys in PWR primary water. The main findings can be summarized as follows: (1) The oxide is made of 3 layers: (i) an internal layer a few nm thick of Cr₂O₃ that is probably the main protective layer, (ii) an intermediate layer of a spinel-type, Cr-rich oxide containing both Ni and Fe whose protective character is not clear, and (iii) an external layer made of nickel ferrite that forms only in metal cation saturated environment. The composition and thickness of these oxide layers is strongly dependent on the hydrogen content of the water. (2) On bare metal surfaces, the oxidation exhibits several growth stages that seem to be typical of Ni base alloys: (i) the Cr₂O₃ internal layer is formed very rapidly on the bare surface and its thickness increases with the Cr content of the alloy, (ii) the oxide growth stops for a period of time that increases with the Cr content of the alloys, probably due to a lack of Cr at the metal/oxide interface, (iii) the oxide layer starts growing again and, for long oxidation times, the oxidation rate is probably controlled by ion transport through the inner oxide layer. (3) The base metal suffers at least two types of damage that probably involve accelerated mass transport due to vacancy injection from the metal/oxide interface: (1) intergranular Cr oxidation and (2) selective oxidation of Cr on the whole surface. These damage processes are believed to play a major role in the initiation of intergranular cracks. (4) The higher Cr alloys exhibit thinner oxide layers and, more interestingly, very limited oxidation damage of the underlying base metal.

8:50 AM

Alloy Oxidation Studies Related to PWSCC: *Fabio Scenini*¹; Roger Newman²; ¹University of Manchester; ²University of Toronto

The intergranular oxidation model of PWSCC has been tested by exposing several Ni based materials to water and steam environments containing hydrogen, at temperatures up to 480°C, and analyzing the resultant complex oxidized surfaces. If the surfaces are mechanically prepared, short-circuit outward diffusion of Cr occurs, and the differences between alloys or alloy conditions (600, 690, 600TT) are minimal. Only on deformation-free surfaces are the differences in oxidation response of the materials displayed clearly. For hydrogen contents greater than that corresponding to the Ni/NiO equilibrium, Alloy 600 shows intergranular oxidation with particulate oxide within each grain; the oxidation morphology is strongly dependent on grain orientation. Oxide-free zones appear near grain boundaries. Thermal treatment to precipitate grain boundary carbides eliminates or strongly modifies the intergranular oxidation and the oxide-free zones. Alloy 690 forms a nearly continuous external oxide.

9:15 AM

Effect of the Chromium Content and Strain on the Corrosion of Nickel Based Alloys in Primary Water of Pressurized Water Reactors: *Frederic Delabrouille*¹; L. Legras²; F. Vaillant²; P. Scott³; B. Viguier⁴; E. Andrieu⁴; ¹Electricité De France, CIRIMAT; ²Electricité De France; ³Framatome-ANP; ⁴CIRIMAT

Chromium contents of nickel-based alloys is known to enhance the corrosion and stress corrosion cracking behavior in high temperature water. A study has been launched to characterize these effects for alloys containing chromium concentrations ranging from 5% to 30%. This present paper compares the growth of oxide scale in these alloys in PWR primary water, and investigates the effects of applied stress. A detailed characterization of the oxide scale is performed by SEM, TEM and SIMS. Increasing chromium content results in an increase in chromium content of the protective oxide scale and decreases the oxide thickness. Applied stress, however acts to increase oxide thickness and decrease the chromium content of the oxide scale.

9:40 AM Break

PWR Primary - II

Monday AM Room: Ballroom II
 August 15, 2005 Location: Cliff Lodge

Session Chairs: David Morton, Lockheed Martin (KAPL); Toshio Yonezawa, Mitsubishi Heavy Industries, Ltd.

10:30 AM

The Mechanisms and Modeling of Intergranular Cracking in Ni-Cr-Fe Alloys Exposed to High Purity Water: *George Young*¹; David Morton¹; Weldon Wilkening¹; John Wuthrich¹; Edward Richey¹; John Mullen¹; Nathan Lewis¹; ¹Lockheed Martin (KAPL)

Nickel-Chromium-Iron Alloys are well known to be susceptible to intergranular cracking at both high ($T > 250^\circ\text{C}$) and low temperatures ($T < 150^\circ\text{C}$) when exposed to high purity water. However, the mechanisms of crack advance and subsequent equations to predict crack growth rates are subject to debate. In the current study, integrating experimental crack growth rate data, fracture mechanics analyses, microstructural characterization, and atomistic modeling provides insight into the key factors and mechanisms that control crack advance. In the high temperature regime, the alloys investigated (Alloy 600, E-182, EN82, X-750) exhibit a large temperature dependence with an apparent activation energy for crack growth of ~ 130 kJ/mol. However, the temperature dependence is insensitive to changes in microstructure, yield strength, or stress intensity factor, indicating that environmental processes (e.g., corrosion and mass transport), not mechanical processes (e.g., crack tip strain rate) control the rate of crack advance. At low temperatures, the crack growth rate exhibits little temperature dependence and occurs via hydrogen embrittlement. In both the high and low temperature regimes, crack growth is accurately described as stable intergranular tearing and experimental findings are well described by the concept of a J-R curve, local to the crack tip process zone, controlling the rate of crack advance. These findings are used to outline the factors which affect low temperature cracking and to construct a mechanistically based, semi-empirical model for high temperature crack advance.

10:55 AM

Crack Initiation in Alloy 600 Tubing in Elevated pH PWR Primary Water: *Richard Jacko*¹; Robert Gold¹; ¹Westinghouse Electric Company

Crack initiation tests were carried out using steam generator tubing specimens to evaluate the effect of primary water pH on the tendency for stress corrosion crack initiation. All exposures were in 325°C water with lithium and boron concentrations selected to simulate at-temperature pH values of 6.9, 7.2 and 7.4. In each environment, a series of eight successive fuel cycles were simulated by approximately 1000-hour exposure cycles. In each of the eight exposure cycles, the Li and B concentrations were "stepped down" in a series of six steps to simulate the boron and lithium changes that occur during a fuel cycle while the dissolved hydrogen concentration was maintained within the range 30-40 $\text{cm}^3/\text{kg H}_2\text{O}$. The eight heats of tubing used in these tests included several heats of mill annealed Alloy 600 with known low resistance to PWSCC, in addition to thermally treated Alloy 600 and a single heat of thermally treated Alloy 690. All tests were periodically interrupted to examine the RUBs for indications of crack initiation. Total test durations extended to 9736 hours. Analysis of the results in terms of the cumulative number of specimens cracked vs. exposure time in each of the environments was done using Weibull statistics. For each set of data the Weibull characteristic life (α) and the Weibull shape factor (γ) were determined. Weibull plots were developed for each test material for which crack initiation was observed. The shortest PWSCC initiation times were consistently observed in the pH 7.2 environment. The longest initiation times were observed in the pH 6.9 solution. The pH 7.4 test results were generally intermediate between the pH 6.9 and pH 7.2 results.

11:20 AM

Initiation of SCC in Alloy 600 Wrought Materials: A Laboratory and Statistical Evaluation: *Jacques Daret*¹; ¹CEA

The susceptibility to SCC initiation of 23 Alloy 600 wrought materials was investigated under representative conditions of PWR primary water, using series of 10 U-bend specimens (constant deformation) per material and orientation. The objective of this program was a tentative correlation between the susceptibility to SCC initiation and one or more of the following characteristics of the materials: carbon content, mechanical properties, grain size, partitioning of inter/intragranular chromium carbides, and grain boundary coverage by carbides. After 36,000 hours of exposure in a recirculating loop, 14 of these materials exhibited SCC initiation, and 12 could be statistically evaluated. Statistical analysis showed that, on all susceptible materials, the probability for initiating a crack on a next specimen is constant with time, when a certain exposure time (incubation) is exceeded. The principal components method also evidenced that incuba-

tion time and cracking probability are independent variables. The paper will present on what they are depending, respectively.

11:45 AM

SCC Initiation Testing of Nickel-Based Alloys Using In-Situ Monitored Uniaxial Tensile Specimens: *Edward Richey*¹; David Morton¹; Maureen Schurman¹; ¹Lockheed Martin (KAPL)

Stress corrosion cracking (SCC) initiation tests have been conducted on Alloy 600, Alloy 600 weld metal EN82H, and X-750 at elevated temperature (315 to 360°C). Tests were conducted with in-situ monitored smooth tensile specimens under a constant load in hydrogenated and aerated environments. The use of uniaxial constant load specimens is a vast improvement over conventional U-bend specimens in which the stress state is difficult to characterize because of stress relaxation issues. Three different loading methods were employed: ring-loading, pressure-loading and active-loading (i.e., electric actuator or dead weights). Three types of in-situ monitors were also investigated: DC-electric potential drop (EPD), linear variable differential transducers (LVDTs) and electrochemical potential noise (EcPN). Out of the three in-situ crack initiation monitors investigated, DC-EPD is the only method that consistently detected the onset of SCC. Each of the three loading methods initiated SCC, and reproducible results were obtained with pressure and active loading. Reproducible results were not found between ring and active loading. Specifically, less SCC occurs in ring loaded specimens compared with active loaded specimens. A load history initiation dependency was observed in oxygenated-sulfate solutions. The thermal activation energy of SCC initiation was measured as 36 kcal/mol in hydrogenated water. SCC initiation was shown to have a similar coolant hydrogen dependency as SCC crack growth. Preliminary results suggest that the fundamental mechanical parameter which controls SCC initiation is plastic strain not stress.

BWR SCC and Modeling - III

Monday PM Room: Ballroom I
August 15, 2005 Location: Cliff Lodge

Session Chairs: Anders Jenssen, Studsvik Nuclear AB; Martin M. Morra, General Electric Global Research

1:30 PM

Effects of Silicon on SCC of Stainless Steels and Alloy 182 Weld Metal: *Peter L. Andresen*¹; Martin M. Morra¹; ¹GE Global Research Center

The effects of silicon on SCC growth rates in high temperature water have been evaluated in 304L/316L stainless steels and alloy 182 weld metal. Si has a pronounced effect on SCC, whether added at 1-5% levels to materials of otherwise normal composition, or to alloys that represent a synthetic irradiated grain boundary composition. At the higher levels (e.g., 3-5% Si), the alloys not only exhibit high growth rates, but show little or no effect of corrosion potential or stress intensity factor. Much less effect of Si has been observed to date on 316L stainless steel than 304L or alloy 182. The relevance of these observations to irradiated and unirradiated alloys is discussed.

1:55 PM

Stress Corrosion Cracking Growth Behavior of Cold Worked Austenitic Stainless Steel in High Temperature Water: *Motoji Tsubota*¹; Yoshinori Katayama¹; ¹Toshiba Corporation

Crack propagation test of type 316L stainless steel, with different hardness level, in high temperature water has been performed, and the relationship between SCC growth rate (da/dt) and hardness (Hv) has been discussed. Intergranular crack propagation was observed in both cold worked material and partially sensitized material, and highly work hardened material showed higher crack propagation rate. Using strain distribution near the crack tip and SCC susceptible plastic zone size, crack propagation rate for the low carbon stainless steel could be described as $da/dt = A \cdot K_2 / (Hvc - Hv)^2$. K: Stress Intensity Factor, Hvc: Critical hardness for SCC (HV300), Hv: Hardness of the base material.

2:20 PM

Finite Element Calculation of Crack Propagation in Type 304 Stainless Steel in Diluted Sulphuric Acid Solution under Stress Corrosion Conditions: *Serguei Gavrilov*¹; Marc Vankeerberghen¹; Johan Deconinck²; ¹SCK-CEN; ²Vrije Universiteit Brussel

Stress corrosion cracking is a synergetic interaction between a stresses material and its environment. A physico-electrochemical simulation tool based on Finite Element (FE) method has been developed to describe such an interaction by incorporation of the mass-transport and the chemical reactions in environment, the electrochemical reactions at the metal surface and the mechano-corrosive interaction at the crack tip. Type 304 stainless steel in dilute sulphuric acid solution system is chosen to simulate the SCC effect in constructive elements in BWR conditions. The effect of the dissolved oxygen concentration, the sulphur content, the temperature, the stress intensity, the crack's length, the fluid flow, sensitization and yield strength were analyzed and compared with experimental observations when it is possible. The FE simulation of one particular case is time-consuming process and requires additional efforts to implement changes in the system in FE framework. To make easy for the final user the parametric study of SS304/H₂SO₄ system the results of many precalculated case are summarized in the data base and an interpolation procedure developed to predict the crack growth rate for an arbitrary set of the system parameters.

2:45 PM

The Electrochemistry of Boiling Water Reactors: Digby D. Macdonald¹; *Han Sang Kim*¹; Mirna Urquidi-Macdonald¹; ¹Pennsylvania State University

Recently, planned or unplanned scrams of nuclear power plants caused by the corrosive degradation of components in the heat transport circuits (HTCs) have increased. This is expected, because damage is cumulative and hence the frequency of corrosion-related failures and outages increases as the operating time of reactors accumulates. In addition, cracking occurs in a wide variety of components, including in the reactor internals, primary coolant circuits, turbine systems, and secondary circuits, and the extent of damage is commonly surveyed by inspection during refueling outages. The damage often occurs in poorly accessible regions of the HTCs and may not be readily detected. The development of a robust predictive methodology would allow prioritization of area inspections and hence would greatly assist the detection and repair of damage. However, the methodology must be accurate in terms of predicted location and severity of damage, in order that "false positives" be held to an absolute minimum. With respect to Boiling Water Reactors (BWRs), the two most important types of cracking in the primary coolant circuits are intergranular stress corrosion cracking (IGSCC) and irradiation assisted stress corrosion cracking (IASCC). Both forms of cracking are essentially electrochemical in nature and hence the

corrosion potential (electrochemical potential, ECP) is possibly the most important parameter in determining the rate of accumulation of damage once the steel has become susceptible. Numerous laboratory and plant studies have shown that sensitized type Type 304 SS will suffer IGSCC only at ECPs above some critical value. The critical potential is found to depend on the degree of sensitization of the steel, temperature, pH, and the type of electrolyte. Clearly, if the ECP and the critical potential are known throughout the heat transport circuit (HTC), the chemistry of the system may be engineered so as to avoid many of the deleterious forms of corrosion. Over the past two decades, we developed computer codes for modeling the water chemistry, ECP, and crack growth rate (CGR) in reactor HTCs, and some of these codes can be used to predict the accumulated damage from stress corrosion cracking in BWRs. The codes incorporate deterministic models for estimating specie concentrations, ECP, and CGR using models whose outputs are constrained to the physically real values by the natural laws (conservation of mass and charge and Faraday's law). The use of the codes will be illustrated with reference to an actual reactor operating under both normal water chemistry (NWC) conditions and hydrogen water chemistry (HWC) conditions by calculating the accumulated damage due to cracks in various locations in the HTC. HWC results in the displacement of the ECP in the negative direction, thereby suppressing the CGR and hence the accumulation of damage. However, the damage that does accumulate is a complex function of various plant operating and water chemistry parameters, and the relative impact of the various parameters will be illustrated in a systematic manner by sensitivity analysis. The authors gratefully acknowledge the support of this work by the DOE/NEER program under Grant No. DE-FG07-021D14334.

3:10 PM

Modelling and Experimental Studies of Intergranular Corrosion in Austenitic Steels: *Roy Faulkner*¹; Paul Moreton²; Ian Armson²; Youfa Yin¹; Jesus Cintas³; Manuel Montes³; ¹Loughborough University; ²Rolls Royce plc; ³University of Sevilla

The experimental part of the paper provides evidence for a correlation between the analysed chromium concentration of several austenitic alloys and the actual chromium content of the grain boundaries in these alloys as measured by high resolution field emission gun transmission electron microscopy. Analysis of composition on the grain boundary plane uses a new deconvolution technique relying on beam diameter parameters and assumptions about the composition profile near to the boundary. Thermodynamic models have been used to forecast the matrix chromium content in the alloys allowing for removal of chromium by other phases existing at temperatures where grain boundary chromium depletion is created. A correlation between the boundary concentration measured and the residual chromium content in the alloy has been established. A triangular shaped depleted zone is shown to give best fits between experiment and theory.

3:35 PM Break

BWR SCC and Modeling - IV

Monday PM Room: Ballroom I
August 15, 2005 Location: Cliff Lodge

Session Chairs: Anders Jenssen, Studsvik Nuclear AB; Martin M. Morra, General Electric Global Research

4:00 PM

Evaluation of the Fracture Research Institute Theoretical Stress Corrosion Cracking Model: *Ernest D. Eason*¹; Raj Pathania²; Tetsuo Shoji³; ¹Modeling & Computing Services; ²Electric Power Research Institute; ³Tohoku University

A theoretical model of stress corrosion cracking (SCC) of Type 304 stainless steel in Boiling Water Reactor environments has been developed by the Fracture Research Institute (FRI) of Tohoku University, incorporating simple models of electrochemistry, material properties, and the mechanics of crack growth. The model is an extension of the well-known Ford model, adding the effect on local strain rate of a growing crack in a hardening material. The objective of the current work was to apply the FRI theoretical model to predict well-controlled laboratory data not used in developing the model, performing a preliminary engineering evaluation by an investigator not involved in the original model development. The model simulations were compared with selected laboratory data on the Type 304 stainless steel heat tested in a recent international Round-Robin study, including constant load and constant K tests in various water environments. Reasonable agreement is obtained between the model predictions and experimental data on 10 SCC growth rate comparisons not used in model development. The ability to simulate 9 FRI development problems was also confirmed. The sensitivity of the results to key input parameters is evaluated, methods of estimating the key non-measurable parameter are presented, and potential extensions to other applications are discussed.

PWR Primary - III

Monday PM Room: Ballroom II
August 15, 2005 Location: Cliff Lodge

Session Chairs: Peter M. Scott, Framatome ANP; Richard J. Jacko, Westinghouse Electric Co. LLC

1:30 PM

Cracking of Alloy 600 Nozzles and Welds in PWRs: A Review of Cracking Events and Repair Service Experience: *Warren Bamford*¹; John F. Hall¹; ¹Westinghouse

Alloy 600 and its compatible weld metals, Alloys 182 and 82, are present in various pressure boundary locations in pressurized water reactors. Similarly, more corrosion resistant Alloy 690 and its weld metals, Alloys 52, 52M and 152, are increasingly present in PWR pressure boundary applications because of repair, replacement or new construction. Depending upon the specific plant designs, these applications are in one or more of the following major components: main loop piping, reactor vessel upper and lower heads, steam generators and pressurizers. Since 1986, service induced cracking of Alloy 600 nozzles and welds, frequently resulting in primary coolant leakage, has become an increasingly common occurrence resulting in the need to repair or replace nozzles and welds or to replace major component (e.g., reactor vessel heads). This paper updates previous reviews by the authors of Alloy 600/182/82 service-induced cracking events. Recognizing the importance of repairs/replacements and the use of alternative and more corrosion resistant materials, the paper reviews the histories of activities such as replacement-in-kind, pressure boundary relocations with half-nozzle repairs and use of mechanical repairs that leave the cracked nozzles in place. The paper addresses briefly approaches used to evaluate flaws left in place and corrosion of carbon/low alloy steels exposed to coolant as the result of repairs. The paper also reviews the service history of materials used in repairs or replacements, including Alloy 600 with enhanced heat treatments, Alloy 182, Alloy 690 and weld metals Alloy 52, 52M and 152.

1:55 PM

Development of Intraspecimen Method for the Application to Life Prediction: Hoi Su Choi¹; Chi Bum Bahn¹; Ji Hyun Kim²; *Il Soon Hwang*¹; ¹Seoul National University; ²Massachusetts Institute of Technology

A proof-of-principle experiment for the intraspecimen method was conducted earlier using four-point bending tests with positive results. The power of area ratio in Weibull model was expected to be unity, while measured value was 0.63. Therefore, more detail study was conducted to investigate the effect of intraspecimen area using uniaxial tension tests. Two heats of Alloy 600, of which the grain sizes were 0.310 and 0.145mm, respectively, were used after sensitization. Test solution was 0.1 M sodium tetrathionate (Na₂S₄O₆•2H₂O). The measured power of area ratio varied from 0.43 to 0.8. To identify the grain boundary nature at the crack initiation site, EBSD (Electron Back Scattered Diffraction) analysis was conducted after the test. It is postulated that difference in high angle boundary population between specimens may be responsible for the observed discrepancy in the measured area ratio power.

2:20 PM

In Search of the True Temperature and Stress Intensity Factor Dependencies for PWSCC: *David Morton*¹; Steven Attanasio¹; Edward Richey¹; George Young¹; ¹Lockheed Martin (KAPL)

This paper discusses the implications of the aqueous hydrogen level SCC functionality on modeling the temperature dependency (thermal activation energy) of nickel alloy SCC. Prior testing has identified a significant effect of hydrogen level on the SCC of nickel-based alloys. A maximum in susceptibility occurs near the Ni/NiO phase transition. This functionality has been fundamentality characterized by the extent that the alloy's electrochemical potential (EcP) deviates from the EcP of the Ni/NiO phase transition (ΔEcP). The implication of this understanding to the determination of SCC thermal activation energies is that thermal activation energy tests need to be conducted at a constant ΔEcP , not at a constant hydrogen level. Thermal activation energies are often biased high when determined from tests conducted at a constant hydrogen level. Recent testing and analyses show that the true (hydrogen level independent) thermal activation energy for Alloy 600, X-750, and EN82 is ~35 kcal/mol. In order to better understand the dependence of the crack growth rate on the applied stress intensity factor, SCC growth tests have been conducted on Alloy 600 as a function of stress intensity factor and specimen size (0.4T to 2T compact tension specimen). Smaller specimens produced faster crack growth rates at high stress intensity factors (e.g., 60 ksi \sqrt{in}) relative to larger specimens tested at the same stress intensity factor. These results suggest that Alloy 600 SCC growth rate stress intensity factor modeling could be biased by a data set largely populated with "small" specimens (1T CT and less) at high stress intensity factors.

2:45 PM

Effects of PWR Water Chemistry on SCC Growth Rates of Alloy 600: *Peter L. Andresen*¹; Martin M. Morra¹; John Hickling²; ¹GE Global Research Center; ²Electric Power Research Institute

The effects of H₂ fugacity and B/Li/pH on SCC growth rates have been evaluated on nickel alloys in high temperature water. Growth rates exhibit a peak vs. H₂ fugacity near the Ni/NiO peak, while no discernible effects of B/Li/pH was observed in the ranges relevant to present or foreseeable PWR operation.

3:10 PM

Crack Growth Rates in Primary Side Materials in Elevated pH PWR Water: *Richard J. Jacko*¹; Robert E. Gold¹; ¹Westinghouse Electric Company

A comprehensive test program was conducted to assess the effects of various primary water pH environments on the crack growth rates of a range of materials typically deployed in the primary system of PWRs. The environments used for this program included pH 6.9, 7.2 and 7.4 simulated primary water chemistries (all pH values calculated for an average primary loop temperature of 310°C.) Compact tension specimens prepared from Alloy 600 CRDM penetration materials, Alloys X-750, Alloy 718, and the weld metal Alloy 182, were tested at temperatures ranging from 325°C to 360°C. The water chemistry was altered during several of the test series from one pH to another (and back) in order to discern subtle environmental effects on crack growth behavior. A number of the tests were carried out using active monitoring by reverse DC-potential drop to follow crack growth; crack growth in specimens that were not actively monitored was determined by periodic interim inspections. The results of these tests were contrasted with the available literature database; generally good agreement was observed. Within the normal scatter observed for crack growth rate tests, no significant effect of the environment on crack propagation was observed within the pH range 6.9 through 7.4.

3:35 PM Break**PWR Primary - IV**

Monday PM Room: Ballroom II
August 15, 2005 Location: Cliff Lodge

Session Chairs: Peter M. Scott, Framatome ANP; Richard J. Jacko, Westinghouse Electric Co. LLC

4:00 PM

Evaluation of Crack Growth Rate for Alloy 600 Vessel Penetration in Primary Water Environments: *Yutaka Yamamoto*¹; Masayoshi Ozawa¹; Kiyotomo Nakata¹; Kentaro Yoshimoto²; Masahiko Toyoda²; Junichiro Okuda²; ¹Japan Nuclear Energy Safety Organization; ²Mitsubishi Heavy Industries, Ltd.

Recent leakage at Alloy 600 reactor vessel (RV) penetration reported in several PWR plants is one of the major issues in order to maintain the structural integrity of RV. In such a region, Alloy 600 would be subjected to work hardening due to thermal strain during welding and enhanced in susceptibility to primary water stress corrosion cracking (PWSCC). In this study, mocked-up models partially simulated the RV penetration were made and the degree of plastic strain near J-groove welds was estimated by hardness measurement. The 4% cold worked material was made by tensile loading based on the estimated plastic strain (approximately 4%) at RV penetration using previously obtained relationship between plastic strain and hardness. Crack growth tests were performed at 360°C in simulated primary water environment using 1/2TCT specimens machined out from both non-cold worked material and cold worked material. Crack growth rates (CGRs) were measured on-line using a DC potential drop method (DCPDM) and compared each other for both materials. The effect of cold work on crack growth rate of Alloy 600 will be discussed.

4:25 PM

SCC Crack Growth Behaviour of Austenitic Alloys in PWR Primary Water Conditions: *Catherine Guerre*¹; Olivier Raquet¹; Guy Turluer²; ¹Commissariat à l'Énergie Atomique; ²Institute de Radioprotection et de Sûreté Nucléaire

Fatigue air pre-cracked Compact Tensile (CT) specimens in Alloy 600 and in cold-worked stainless steel were tested in the VENUS corrosion loop, a high temperature recirculating loop, which simulates the conditions of primary water of Pressurized Water Reactors (PWR). In order to assess the effect of cyclic loading on Stress Corrosion Cracking (SCC) crack growth and the effect of temperature, CT specimens were tested under either constant loads or under low frequency cyclic loadings at 325°C or at 288°C. Two Alloy 600 materials, with different microstructure and mechanical properties, and a cold worked 316 L stainless steel were studied. PWSCC crack growth rates were monitored in-situ by the direct current potential drop method and were validated by post-mortem observations. Fracture surfaces were characterised by macroscopic and microscopic observations. Comparison of the crack growth rates and of the fracture

features demonstrated that they depend on the wave form of the mechanical loading. The results will be compiled in a database and will be compared to international results. Support by the Directorate for Reactor Safety of the French Institute for Radiological Protection and Nuclear Safety (IRSN) is gratefully acknowledged.

4:50 PM

Environmentally Assisted Crack Growth of Cold-Worked Type 304 Stainless Steel in PWR Environments: *David R. Tice*¹; Norman Platts¹; Keith Rigby¹; John Stairmand¹; Howard Fairbrother¹; ¹Serco Assurance

Austenitic stainless steels used in light water reactor plant may be present in a hardened condition, either intentionally (to increase strength as in some bolting applications) or as a result of fabrication, such as bending, surface grinding, machining or shrinkage adjacent to welds. Additionally, irradiated components undergo hardening due to neutron damage. The service experience of austenitic stainless steels in pressurized water reactor (PWR) environments is generally very good and there is no evidence for susceptibility to stress corrosion cracking (SCC) in good quality PWR primary coolant for either annealed or sensitized Types 304 and 316 steels. However, intergranular (IG) SCC has been observed for material subjected to high levels of neutron irradiation, both in plant (core baffle bolts) and in laboratory tests. Irradiation results in several material changes and the cause of SCC of irradiated material in PWRs has not been clearly established. The work described in this paper is aimed at examining whether hardening alone can produce susceptibility to SCC in PWR conditions. Crack growth testing has been performed on cold-(and warm-) worked Type 304 stainless steel in PWR primary coolant chemistry over a range of temperatures and loading conditions. Tests were performed both on standard compact tension specimens containing through-thickness cracks and on specimens containing surface-breaking (semi-elliptical) defects more representative of cracks which might occur in a real component. It was found that, for moderate levels of cold work (0.2% proof stress <700 MPa), IGSCC did not propagate from fatigue pre-cracks in PWR primary coolant chemistry conditions. However, if an intergranular defect was first produced by oxygenating the test environment, continued crack propagation could occur even in well controlled PWR primary chemistry. Testing was also carried out on cold-worked Type 304 stainless steel under cyclic loading. Fatigue crack growth rates in the PWR primary environment were enhanced by up to 20 times compared to growth rates in air, with the cyclic crack growth rate in water increasing with decreasing loading frequency. Comparison with data on annealed 304 stainless steel indicated that the degree of enhancement of fatigue crack growth for 20% cold worked material was no greater than that for annealed material.

5:15 PM

SCC of Cold-Worked Austenitic Stainless Steels in Primary Water of PWRs: Olivier Raquet¹; *Emmanuel Herms*¹; Thierry Couvant²; François Vaillant²; Jean-Marie Boursier²; ¹Commissariat à l'Énergie Atomique Saclay; ²Electricité de France Les Renardières

The detrimental role of cold-work on Stress Corrosion Cracking (SCC) susceptibility of Austenitic Stainless Steels (ASSs) is examined in the case of Pressurized Water Reactors (PWRs) conditions. The main focus of this study is to identify the associated mechanical and cold-working conditions leading to a SCC susceptibility of ASSs in PWRs primary water. Several modes of cold-working procedures (fatigue, cold rolling, counter sinking, shot-peening, tensile loading) were applied to ASSs before standards Constant Extension Rate Tests (CERTs) or long-term constant load tests and constant deformation tests in PWR primary water at 360°C. High cold-worked ASSs were demonstrated to be strongly susceptible of cracking under dynamic mechanical conditions (CERTs). For constant loadings and constant deformations, crack initiation occurs but propagation seems impossible. The role of the initial loading history associated with cold-working procedures and the importance of dynamic strain on the SCC susceptibility of ASSs in hydrogenated PWR water must be particularly emphasized. Interstitial hydrogen associated with natural electrochemical charging in PWRs primary water at 360°C appears to have a noticeable embrittling effect on cold-worked 304L ASS at room temperature.

LAS and RPV Steel

Tuesday AM
August 16, 2005

Room: Ballroom I
Location: Cliff Lodge

Session Chairs: Armin Roth, Framatome ANP GmbH; Mikhail A. Sokolov, Oak Ridge National Laboratory

8:00 AM

Effect of Radiation on Embrittlement and Matrix Cu Content of a RPV Weld with Different PWHT Conditions: *Mikhail A. Sokolov*¹; Randy K. Nanstad¹; Michael K. Miller¹; ¹Oak Ridge National Laboratory

The influence of temperature, hold time, and cooling rate on the Charpy impact properties and the copper level in the matrix has been investigated on a weld fabricated from the same weld wire used for HSSI Weld 73W and a Linde 80 flux before and after irradiation to 0.8×10^{19} n/cm². This weld has a relatively high bulk copper content, 0.32% wt, in as-welded condition. The heat treatment consisted of heating material to desired temperature, holding at the post-weld heat treatment (PWHT) temperature, and then cooling down to room temperature. Except for special cases, all PWHTs were performed with heating and cooling rate of 15F/h (8°C/h) to simulate heating/cooling rate of a real vessel. In two special cases, material was heated with 15F/h (8°C/h) rate but water quenched after holding at the PWHT temperature. The highest PWHT temperature was 650°C/24h. Next PWHT was 610°C/24h that was typical PWHT of reactor pressure vessels (RPV). Third PWHT was 580°C/100h. In addition, a part of material after 610°C/24h PWHT was heat treated at 454°C/168h to simulate a post-irradiation annealing. Charpy properties were measured using sub-size 3×4 mm specimens and matrix Cu content was measured by atom probe tomography before and after irradiation. Charpy specimens were irradiated in Ford Reactor at 288°C. It was found that the higher PWHT temperature resulted in higher Charpy upper-shelf energy (USE) with little effect on ductile-to-brittle transition temperature (DBTT). At the same time, lower PWHT temperature and slower cooling rate are beneficial in reducing the matrix Cu content. Matrix Cu content after irradiation to 0.8×10^{19} n/cm² was about the same for all three welds measured regardless of their different matrix Cu contents in the unirradiated condition. Consequently, weld with lowest PWHT temperature (lowest matrix Cu) exhibited the lowest shift of DBTT and drop in USE. These results are proving the postulate about impotence of copper in solution (matrix Cu) rather than bulk Cu content in radiation embrittlement of RPV materials. Additional annealing at 454°C/168h after 610°C/24h PWHT did not show any additional effects on subsequent radiation embrittlement.

8:25 AM

Boric Acid Corrosion of Light Water Reactor Pressure Vessel Head Materials: *Jong Hee Park*¹; Omesh Chopra¹; Ken Natesan¹; William J. Shack¹; William Cullen²; ¹Argonne National Laboratory; ²U.S. Nuclear Regulatory Commission

An experimental program was conducted at Argonne National Laboratory to develop electrochemical potential data and corrosion rates of the materials found in the reactor pressure vessel head and control rod drive mechanism (CRDM) nozzles in boric acid solutions of varying concentrations at temperatures of 95–316 °C (203–600°F). Tests were conducted in postulated environmental conditions in the nozzle/head crevice, e.g., (a) high-temperature, high-pressure aqueous environment with a range of boric acid solution concentrations, (b) high-temperature (235–320°C) molten salt solutions, and (c) low-temperature (95°C) saturated boric acid solutions. These correspond to the following situations: (a) low leakage through the nozzle and nozzle/head annulus plugged, (b) low leakage through the nozzle and nozzle/head gap open, and (c) significant cooling due to high leakage and nozzle/head gap open. The results indicate significant corrosion only for the low-alloy steel and no corrosion for Alloy 600 or 308 stainless steel cladding. Also, corrosion rates were significant in saturated boric acid solutions whereas no material loss was observed in boric acid melts or deposits in the absence of moisture. Tests were also conducted with alloys of various Cr contents in the range of 0.2–25 wt.% to evaluate the effect of Cr loss from Type 308SS weldment on the corrosion rate in a room-temperature-saturated boric acid solution at temperatures between 150 and 316°C and 12.4 MPa. The corrosion test results from this study are compared with the existing corrosion/wastage data in the literature.

8:50 AM

The Effect of Transients on the Crack Growth Behaviour of Low Alloy Steels for Pressure Boundary Components under Light Water Reactor Operating Conditions: *Armin Roth*¹; Bastian Devrient¹; Dolores Gómez-Briceño²; Jesús Lapeña²; Miroslava Ernestová³; Miroslav Zamboch³; Ulla Ehrnsten⁴; Jürgen Föhl⁵; Thomas Weissenberg⁵; Hans-Peter Seifert⁶; Stefan Ritter⁶; ¹Framatome ANP GmbH; ²Centro de Investigaciones Energéticas Medioambientales y Tecnológicas; ³Nuclear Research Institute; ⁴Technical Research Centre of Finland; ⁵Materialprüfungsanstalt Universität Stuttgart; ⁶Paul Scherrer Institut

A European research project (CASTOC) was launched to investigate some of the remaining open issues regarding the environmentally assisted cracking of low alloy steels in high-temperature water. The materials of concern comprised low alloy steels for pressure boundaries of both Western type boiling water reactors (BWR) and Russian type pressurised water reactors (VVER). The environments were based on BWR normal water chemistry and VVER primary water chemistry. Besides studies under constant conditions (purely static or cyclic load and constant chemistry), a special emphasis was put on mechanical transients (e.g. periodic partial unloading) and chemical transients (e.g. Sulphate, Chloride). At relevant stress intensity factors it could be shown that immediate cessation of growing cracks occurs after changing from cyclic to static load in high purity oxygenated BWR water and oxygen-free VVER water corresponding to steady state operation conditions. Susceptibility to environmentally assisted cracking under static load was observed for a heat affected zone material in oxygenated high purity water and also in base materials during a chloride transient representing BWR water condition below Action Level 1 of the EPRI Water Chemistry Guidelines according to the electrical conductivity of the water but in the range of Action Level 2 according to the content of chlorides. Time based crack growth was also observed in one Russian type base material in oxygenated VVER water and in one Western type base material in oxygenated high purity BWR water at stress intensity factors above the limit for linear elastic fracture mechanics. The results provide an important contribution to the mechanistic understanding of the crack growth behaviour in the regarded corrosion system. This is an important key for the evaluation of transient events, which may occur in a plant during service.

9:15 AM

Mitigation Effect of Hydrogen Water Chemistry on SCC and Low-Frequency Corrosion Fatigue Crack Growth in Low-Alloy Steels: *Hans-Peter Seifert*¹; Stefan Ritter¹; ¹Paul Scherrer Institute

The mitigation effect of hydrogen water chemistry (HWC) on the SCC and low-frequency corrosion fatigue crack growth behaviour of low-alloy steels was investigated under those critical BWR system conditions, where sustained and fast SCC and corrosion fatigue crack growth significantly above the BWRVIP-60 SCC disposition lines and ASME XI reference fatigue crack growth curves was observed under normal water chemistry conditions (NWC). Application of HWC resulted in a significant drop of SCC and low-frequency corrosion fatigue crack growth rates by at least one order of magnitude with respect to NWC conditions. HWC is therefore a promising and powerful mitigation method under these critical system conditions.

9:40 AM

Corrosion of SA 508 Low Alloy Steel in Primary Water of PWR: *Hong Pyo Kim*¹; Jin Ki Hong¹; Dong Jin Kim¹; Seong Sik Hwang¹; Bong Sang Lee¹; Jun Hwa Hong¹; ¹Korea Atomic Energy Research Institute

SA508 low alloy steel of reactor vessel may be exposed to the primary coolant due to damage of the cladding on the SA 508. For integrity concern with regard to corrosion of the SA508 in reactor vessel, the corrosion tests such as general corrosion, galvanic corrosion, crevice corrosion and flow accelerated corrosion (FAC) were performed in a typical primary water. Corrosion rate was evaluated by weight loss measurement, profilometry and polarization curve. Primary coolant environment of PWR was divided into four stages depending on operation: start-up operation, normal power operation, shut down operation and overhaul. For power operation and shut-down steps, FAC rate was higher than any other form of corrosion and maximum corrosion rate was 0.09mm/year. For overhaul step, the galvanic corrosion rate was higher than corrosion rate of any other form of corrosion, and maximum galvanic corrosion rate was 0.43mm/year.

10:05 AM Break

Operational Experience - I

Tuesday AM
August 16, 2005

Room: Ballroom I
Location: Cliff Lodge

Session Chairs: Christer Jansson, SwedPower AB; C. E. (Gene) Carpenter, U.S. Nuclear Regulatory Commission

10:30 AM

Flow Accelerated Corrosion of Tube Support Plates at Bruce NGS Unit 8: *Peter J. King*¹; ¹Babcock & Wilcox Canada

During the Fall 2003 planned outage of Bruce Unit 8, significant degradation of tube support plates (TSPs) was found in three of the unit's eight steam generators (SGs). A combination of visual and eddy current inspections revealed that ligaments of the broach plates were being thinned from the underside, and that degradation was more severe on upper plates in the hot leg side. Inspection

evidence suggests that TSPs in the other SGs are much less degraded. Flow accelerated corrosion (FAC) was identified as the most probable degradation mechanism. FAC had not previously been observed by Bruce Power on the TSPs, although other components, such as scallop bars (U-bend support bars), primary separator cyclones, and secondary separator cyclones were known to be affected by this damage mechanism. This paper discusses the nature of the observed degradation, associated investigations into the controlling factors, and steps being taken at the plant to mitigate the problem.

10:55 AM

Flow Accelerated Corrosion and Cracking of Carbon Steel Piping in Primary Water - Operating Experience at the Point Lepreau Generating Station: John P. Slade¹; Tracy S. Gendron²; ¹NB Power Nuclear; ²Atomic Energy of Canada Ltd

This paper reports operating experience where both flow accelerated corrosion (FAC) and initiated environmental cracking have occurred in type SA-106 Gr. B carbon steel piping in a CANDU® reactor. At the Point Lepreau Generating Station (PLGS), both types of degradation were observed at the same location in piping that transports ~310°C (590°F) primary coolant away from the reactor core. Cracks were initiated from both inside and outside surfaces. Cracking and FAC have been life limiting for small number of pipes at PLGS. This paper provides an overview of the PLGS degradation history, characteristics of the observed corrosion and cracking, plausible mechanisms, primary causal factors, and failure rates.

11:20 AM

Risk-Reduction Strategies Used to Manage Cracking of Carbon Steel Primary Coolant Piping at the Point Lepreau Generating Station: John P. Slade¹; Tracy S. Gendron²; ¹NB Power Nuclear; ²Atomic Energy of Canada Ltd

Since 1997, sections of nine ASME SA 106 Grade B carbon steel primary coolant system piping at the Point Lepreau Generating Station (PLGS) have been replaced because of intergranular cracking. This cracking at PLGS is unique among the world's CANDU® reactors and has potential to have a significant negative impact on the safe and reliable operation of the Station. Although the mechanism(s) of cracking initiated from both inside and outside surfaces has not been confirmed, several primary causal or proximate factors have been identified that form the basis for cost-effective risk management strategies. New Brunswick Power Nuclear (NBPN) uses a combination of three strategies to manage the observed cracking, depending on the probability of cracking at that location in the piping system, the potential for risk reduction in applying the strategy, and the time in the reactor life cycle. The strategies are: Inspection and Repair, Demonstration of Low Risk, and Prevention of Cracking. This paper describes the methods used to select appropriate management activities based on economic analysis and risk reduction.

11:45 AM

Recent In-Service Experience with Degradation of Low Alloy Steel Components Due to Localized Corrosion and Environmentally Assisted Cracking in German PWR Plants: Armin Roth¹; Erika Nowak²; Martin Widera³; Ulf Ilg⁴; Ulrich Wesseling¹; Ronald Zimmer¹; ¹Framatome ANP GmbH; ²E.ON Kernkraft GmbH; ³RWE Power AG; ⁴EnBW Kraftwerke AG

Recent in-service experience in commercially operating German PWR type plants revealed minor degradation of low alloy steel components by localized corrosion and, in some cases, by environmentally assisted cracking (EAC). All indications were detected by regular inspection techniques such as leak detection systems, visual inspection or non-destructive testing. The plant safety was not affected in any of the cases. Subsequent failure analyses exhibited the existence of shallow pitting caused by oxygenated water during shut-down periods, where dissolved oxygen can occur in both BWRs and even PWRs under certain conditions. In some cases cracks with typical features of Strain-Induced Corrosion Cracking (SICC), a special case of EAC, were also present. It was concluded that pitting was a necessary precondition for the initiation of cracks due to slow plastic deformation rates during start-up periods. Appropriate remedial actions were identified and defined for application in order to avoid future incidents.

PWR Primary - V

Tuesday AM
August 16, 2005

Room: Ballroom II
Location: Cliff Lodge

Session Chairs: Il Soon Hwang, Seoul National University; John Hickling, Electric Power Research Institute

8:00 AM

Influence of Orientation of Cold Work and Carbide Precipitation on IGSCC Behaviors of SUS 316 in Hydrogenated High Temperature Water: Koji

Arioka¹; Goro Chiba¹; Takuyo Yamada¹; Takumi Terachi¹; ¹Institute of Nuclear Safety System, Incorporated

IGSCC susceptibility of 316 austenitic stainless steel (SUS 316) in PWR primary water was studied to study the influence of cold work and temperature by compact type specimens (0.5T for cold worked materials) and CERT (1x10⁻⁷/s) using specimens with cold deformed hump. Simple monotonic temperature dependence was recognized on IGSCC susceptibility by crack growth measurement as same as that by CERT tests, and the obtained activation energy was 107KJ/mol. Regarding to the influence of cold work on IGSCC behaviors, remarkable effect of the orientation of CT specimens to the rolling direction was recognized on 20%CW316. Then, to examine the effect of cold work and temperature on IGSCC behaviors, the role of grain boundary sliding was studied in high temperature air using CT specimens. From the correlation between the IGSCC behaviors in water and grain boundary sliding in air, the role of grain boundary sliding on IGSCC mechanism will be discussed.

8:25 AM

Stress Corrosion Cracking of 304L Stainless Steel in PWR Environment: Thierry Couvant¹; Francois Vaillant¹; Jean-Marie Boursier¹; Yves Rouillon²; ¹Electricité de France R&D; ²Electricité de France/DIN/CEIDRE

Austenitic stainless steels are widespread in primary and auxiliary circuits of Pressurized Water Reactors (PWRs). Moreover, some components suffer stress corrosion cracking (SCC) under neutron irradiation. This degradation could be the result of the increase of hardness and/or the modification of chemical composition at the grain boundary by irradiation. In order to avoid complex and costly corrosion facilities, the effects of irradiation on the material are commonly simulated by applying a pre-strain on non-irradiated material prior to stress corrosion cracking tests. Stress corrosion tests were conducted on an austenitic stainless steel AISI 304L in PWR environment. Particular attention was directed towards strain localization effects. Results have demonstrated that crack growth rate and crack growth path in high-temperature hydrogenated water were dependent of deformation mechanisms at the crack tip (strain incompatibilities). Interpretation of strain hardening effect was essentially based on SEM and TEM examinations.

8:50 AM

Comparison of the Fatigue Life of 304L SS as Measured in Load and Strain Controlled Tests: Harvey D. Solomon¹; Claude Amzallag²; Ron De Lair³; Alexander J. Vallee¹; ¹GE-GRC; ²Electricité de France; ³GE-Retired

Load-controlled and strain-controlled tests run at 150°C and 300°C, in air and PWR water on the same heat of 304L, are contrasted for tests run to as long as ten million cycles. Cyclic stress-strain curves were developed to enable the comparison of these tests on a common basis of stresses or strains. The data was considered in terms of the stress amplitude, the total strain amplitude and in terms of just the non-elastic component of the strain. When the data was converted to a common stress or strain basis there was good agreement for the data obtained at lives of one million cycles or less, but there were still some differences in the ten million-cycle endurance limit stress/strain regime.

9:15 AM

Statistical Analysis of the LCF Behavior of 304L SS Tested at 150°C and 300°C in Air and PWR Water: Harvey D. Solomon¹; Claude Amzallag²; ¹GE-GRC; ²Electricité de France

A statistical analysis of the fatigue life was performed on the results of strain-controlled tests on 304L specimens, tested in PWR water and air at 150°C and 300°C. This analysis used the fatigue life defined by Coffin-Manson and Basquin relations. With these correlations, the individual data points could be translated to a common total strain amplitude or fatigue life. The resulting distribution was then analyzed using Weibull statistics. The tests run in PWR water had Weibull modulus values of 6.5-7.0, whereas the modulus was in the range of 4.1-4.3 for the tests run in air. The higher modulus denotes a tighter distribution, perhaps owing to the effect of the environment overweighing the specimen-to-specimen metallurgical differences.

9:40 AM Break

Zircaloy

Tuesday AM
August 16, 2005

Room: Ballroom II
Location: Cliff Lodge

Session Chairs: Arthur T. Motta, Pennsylvania State University; Gary S. Was, University of Michigan

10:30 AM

Characterization of Oxides Formed on Model Zirconium Alloys in 360°C Water Using Micro-Beam Synchrotron Radiation: Aylin Yilmazbayhan¹; Arthur T. Motta¹; H. G. Kim²; Yong Hwan Jeong²; Jeong Yong Park²; Robert J.

Comstock³; Barry Lai⁴; Zhonghou Cai⁴; ¹Pennsylvania State University; ²Korean Atomic Energy Research Institute; ³Westinghouse Electric Company; ⁴Argonne National Laboratory

Uniform oxidation by the primary circuit water may limit the service of Zr alloy fuel cladding in Light Water Reactors, especially under more severe fuel duty cycles. Understanding the impact of chemistry and microstructure on corrosion performance may allow us to design better alloys for severe duty cycle applications. To undertake such research, model zirconium alloys (Zr-xCr-yFe, Zr-xCu-yMo, Zr-xSn and Zr-xNb, with various values of x and y) were corroded at 360°C in pure water and lithiated water to help isolate the role of individual alloying elements on the oxide formation process. The structure of the protective oxide, believed to be the cause for the different corrosion behavior of different zirconium alloys, was investigated using microbeam synchrotron radiation diffraction. Experiments were conducted at both the Advanced Photon Source, in the USA using a 0.25 micron beam, and in the Pusan Light Source, Korea, using a 1 micron beam. Such micro-diffraction experiments allow the determination of phases present, oxide texture, grain size and accumulated stress, as a function of distance from the oxide-metal interface. The results of this examination show heretofore unobserved details of the oxide-metal interface and of the variation of phase content with distance from oxide-metal interface and overall oxide thickness. We focus on this paper on the evolution of texture and phase content, and compare these between the different model alloys to help elucidate the role of individual alloying elements in the oxide formation process.

10:55 AM

Effect of Pre-Deposited Magnetite on Deposition of Nickel Oxides at Zr Surface in 573K Pressured Water: *Jei-Won Yeon*¹; Yongju Jung¹; Hansook Lee¹; Myung-Hee Yun¹; Won-Ho Kim¹; ¹Korea Atomic Energy Research Institute

Metal oxides released from the surfaces of PWR primary circuit are transported to the reactor core, where they are activated to form radioactive CRUD. Recently the operation programs of many PWR plants have been changed to use a long-term fuel cycle and higher thermal duties. As a result, the amount of fuel CRUD of which the major component is known to be nickel ferrite, has increased considerably. It has been reported that the fuel CRUD attributes to the occurrence of axial offset anomaly and an increase of the dose rate in the coolant system. The impact of the fuel CRUD could be reduced by various filtering systems installed in the chemistry and volume control system and the ultrasonic fuel cleaning system which has been recently developed. Nevertheless, it is generally accepted that the most effective solution is to find an optimal coolant chemistry condition to mitigate the deposition process of the corrosion products on the fuel cladding. In this study, the deposition tests of nickel ion were carried out on Zr cladding covered with magnetite in order to elucidate the formation process of nickel ferrite using a high-temperature loop system. The content of nickel in deposits on the Zr cladding increased with the amount of magnetite. This is an evidence that pre-deposited magnetite on Zr surface expedites the deposition of nickel oxides in high temperature coolant.

11:20 AM

Effect of Zinc Injection on Crevice Corrosion Resistance of Pre-Filmed Zircaloy-2 Tube under Heat Transfer Condition: *Hirohisa Kawamura*¹; Hiromi Kanbe¹; Ryo Morita¹; Fumio Inada¹; ¹Central Research Institute of Electric Power Industry

The effect of zinc injection to boiling water reactor (BWR) coolant on general and crevice corrosion of pre-filmed zircaloy-2 fuel cladding were examined under simulated and accelerated BWR core condition except for irradiation, using a heat transfer corrosion test facility with zircaloy spacer crevice region in which a two-phase flow condition could be simulated. The thickness and chemical compositions of zirconium oxide layer formed on zircaloy-2 tube were examined using scanning electron microscope with energy dispersive X-ray diffraction spectroscopy (SEM-EDX) and Auger electron spectroscopy (AES) techniques. Hydrogen contents in zircaloy-2 tube were also examined using hydrogen gas analysis. It was tentatively concluded that the corrosion resistance of zircaloy-2 in the free span was maintained, but the resistance in the crevice region was not maintained when zinc was injected under the two-phase flow simulated BWR core condition except for irradiation.

11:45 AM

Transient Oxide Film Growth on Zirconium in High Temperature Aqueous Solutions: Yingzi Chen¹; *Digby D. Macdonald*¹; ¹Pennsylvania State University

The growth of zirconium oxide films on Zircaloy is a subject of continuing interest in the nuclear power industry, particularly as operators strive for higher burn-up with the concomitant increase in risk of fuel failure. In the past, the growth of the oxide has been modeled as a diffusion (of oxygen) problem, leading to an initial parabolic or cubic rate law followed by transition to a linear law. These rate laws were established by using weight gain measurements that took little account of the electrochemistry of the system. We have recently re-examined the growth of the anodic oxide film on zirconium, with the goal of providing a more accurate account of the initial growth kinetics and of relating the kinetics of the process to the defect structure of the film and the electrochemis-

try of the system. This goal is being achieved by using the Point Defect Model (PDM),¹ which has been developed by one of the authors and his colleagues over the past two decades, to describe the growth and breakdown of passive films on the metal surface. This paper is concerned with the measurement of transients in passive current and oxide film thickness on zirconium in B(OH)₃/LiOH solutions at 250°C under potential step polarization conditions across the passive range. These data are being analyzed in terms of a new rate law derived from the PDM,² in order to extract values for key parameters in the model. Additionally, we have measured extensive electrochemical impedance spectroscopic (EIS) data for passive zirconium in boric acid/lithium hydroxide solutions at elevated temperatures and these data, too, are being analyzed in terms of the PDM to extract values for key model parameters and to ascertain reaction mechanisms. The authors gratefully acknowledge the support of this work by DOE/NERI through Grant DE-FG07-02ID22618. ¹D. D. Macdonald, "Passivity - The Key to Our Metals-Based Civilization", *Pure Appl. Chem.*, 71, 951 (1999). ²D. D. Macdonald, M. Al-Rafaie and G. R. Engelhardt, "New Rate Laws for the Growth and Reduction of Passive Films", *J. Electrochem. Soc.*, 148(9), B343 (2001).

Super-Critical Water-Cooled Reactors I

Tuesday AM
August 16, 2005

Room: Ballroom III
Location: Cliff Lodge

Session Chairs: David Guzonas, Atomic Energy of Canada Limited; Junya Kaneda, Hitachi, Ltd.

8:00 AM Invited

Challenges and Recent Progress in Corrosion and Stress Corrosion Cracking of Alloys for Supercritical Water Reactor Corecomponents: Sebastien Teyssseyre¹; Zhijie Jiao¹; *Gary Was*¹; ¹University of Michigan

The Supercritical Water Cooled Reactor (SCWR) is one of the most promising Generation IV nuclear reactor designs. Reactor operating conditions call for a core coolant temperature between 280 and 620°C at a pressure of 25 MPa and neutron damage levels of 15 dpa (thermal reactor design) and 100 dpa (fast reactor design). In the hotter regions of the core, irradiation-induced changes in microstructure (swelling, RIS, hardening, phase stability) and mechanical properties (strength, thermal and irradiation induced creep, fatigue) are major concerns. Throughout the core, corrosion, stress corrosion cracking and the effects of irradiation on them are the most overriding issues. This paper presents a preliminary study of the effect of proton irradiation on the microstructure on two stainless steels, alloys 304L and 316L, and one nickel-base alloy, Inconel 690 and its effect on stress corrosion cracking in 500°C supercritical water. Results show a significant increase of the cracking susceptibility of those alloys and a cracking morphology, slightly different than that observed in BWR and PWR environment.

8:50 AM

Effect of Proton Irradiation and Grain Boundary Engineering on Stress Corrosion Cracking of Ferritic-Martensitic Alloys in Supercritical Water: *Gaurav Gupta*¹; Gary S. Was¹; ¹University of Michigan

Ferritic-Martensitic alloys have been identified as candidate core structural alloys for supercritical water cooled reactor (SCWR). Preliminary studies show that F-M alloys experience high oxidation rates in 500°C SCW. However, the effect of irradiation on SCC is unknown. Grain Boundary Engineering (GBE) is being explored as a means of reducing the susceptibility to IGSCC in SCW. This paper focusses on the influence of irradiation and GBE on SCC of F-M alloys T91, HT9 and HCM12A in SCW. CERT experiments were conducted in supercritical water at 400°C on T91, HT9 and HCM12A, irradiated with 2 MeV protons at 500°C to a dose of 7 dpa. F-M alloys T91 and T91-CSLE, in the unirradiated and irradiated conditions were also tested in SCW at 400°C. Results regarding the effect of irradiation and GBE in controlling deformation and cracking in unirradiated and irradiated F-M alloys exposed to SCW will be presented.

9:15 AM

Corrosion of Zirconium-Based Fuel Cladding G Alloys in Supercritical Water: *Yong Hwan Jeong*¹; Jeong Yong Park¹; H. Kim¹; Busby Jeremy²; Eric Gartner²; Michael Atzmon²; Gary Was²; Robert Comstock³; Marcelo Silva⁴; Arthur T. Motta⁴; ¹Korean Atomic Energy Research Institute; ²University of Michigan; ³Westinghouse Electric Company; ⁴Pennsylvania State University

Zirconium based claddings are candidate materials for fuel cladding and water box liners in the Gen-IV supercritical water reactor concept. The objective of this work is to evaluate the corrosion performance of Zr-based alloys in both supercritical water and high temperature steam environments. Samples of a base Zircaloy-4 alloy and twenty model alloys were exposed in both deaerated (< 5 ppb) supercritical water at 500°C/25.5 MPa and in high temperature steam at 500°C for periods between 1 and 30 days. Following exposure, oxidation was

quantified by weight gain measurements; little difference was seen between the different environments. While Zircaloy-4 specimens were highly susceptible (weight gains as high as 4,000 mg/dm²day), some model alloys were more resistant, showing weight gains that are higher than those exhibited by austenitic alloys and somewhat smaller than those exhibited by ferritic alloys. The most highly resistant model alloys were those with high volumes of second phase precipitates. We will show and review the complete corrosion results of the model alloys in supercritical water and high temperature steam, as well as preliminary characterization of the oxides layers.

9:40 AM

Corrosion-Resistant Coatings for Use in a Supercritical Water CANDU® Reactor: *David Guzonas*¹; *John Wills*¹; *Glenn McRae*¹; *S. Sullivan*²; *Karen Chu*³; *Kim Heaslip*³; *Mike Stone*³; ¹Atomic Energy of Canada Ltd; ²University of Waterloo; ³Deep River Science Academy

Advanced reactor concepts currently under investigation by Atomic Energy of Canada Limited (AECL) will operate under supercritical water (SCW) conditions to increase thermal efficiency. However, corrosion of system materials can be significant under SCW conditions. Work has been carried out at AECL Chalk River Laboratories to develop corrosion resistant coatings for critical applications in a SCW reactor. In the initial phase of this work, a number of routes to coatings are being explored, including deposition using an atmospheric-pressure plasma jet and deposition of zirconium dioxide (ZrO₂) using several chemical processes. Preliminary tests have been carried out on coatings deposited on zirconium and several types of steel. Coated coupons were exposed to SCW conditions in a static autoclave, and their corrosion rates determined and compared to those of uncoated coupons. The films and underlying substrates were characterized before and after SCW exposure using a number of surface analytical techniques including scanning electron microscopy, atomic force microscopy, and Raman spectroscopy. The paper discusses the recent results and the strategy for further coating development.

10:05 AM Break

Super-Critical Water-Cooled Reactors II

Tuesday AM
August 16, 2005

Room: Ballroom III
Location: Cliff Lodge

Session Chairs: David Guzonas, Atomic Energy of Canada Limited; Junya Kaneda, Hitachi, Ltd.

10:30 AM

Corrosion and Stress Corrosion Cracking of Ferritic-Martensitic Alloys in Supercritical Water: *Pantip Ampornrat*¹; *Chi Bum Bahn*¹; *Gary S. Was*¹; ¹University of Michigan

Ferritic-Martensitic (F-M) alloys have been selected as potential candidate materials for the Generation IV supercritical water reactor (SCWR) concept. While F-M alloys have low susceptibility to stress corrosion cracking (SCC), they can experience high corrosion rate in high temperature water. In this work, SCC and corrosion behavior of HT-9, T91, and HCM12A in pure supercritical water (SCW) was studied over a range of temperatures and oxygen contents. Experiments were conducted at a pressure 25 MPa and over a temperature range of 400°C to 500°C and in either deaerated or controlled oxygen environments. Constant extension rate tensile (CERT) experiments were performed at a strain rate of 3x10⁻⁷ s⁻¹ in a multi-sample SCW system. Corrosion coupons of each alloy were loaded in the same experiments. Results show that of the three alloys strained at 500°C, only HT-9 shows evidence of IGSCC. Oxides on corrosion coupons were characterized using weight gain measurements, SEM, EDX, XPS and XRD. The oxide formed on T91 and HCM12A consists of an iron-rich outer layer of magnetite (Fe₃O₄) and an inner layer that is iron rich but with a significant amount of chromium and with a higher oxygen content. The inner layer also contains a small amount of Mo in T91 and a small amount of W in HCM12A. The addition of 100 ppb oxygen to the water reduced the oxide thickness by about 10% and increased the stoichiometry of the oxides in both layers. The corrosion and stress corrosion cracking behaviors of these alloys as a function of temperature and oxygen content will be presented and the mechanisms governing the processes will be discussed.

10:55 AM

Stress Corrosion Cracking and Corrosion Fatigue in 12% Cr Martensitic Stainless Steels: Role of Microstructure and Hydrogen Ingress: *Gajanana Vithal Prabhugaunkar*¹; *Chandrashekhar Kerkar*¹; *Raju Chintaman Kadam*¹; ¹Indian Institute of Technology, Bombay

Martensitic stainless steels are used in nuclear reactor environment in Primary coolant circuit. These steels have good corrosion resistance and toughness combined with high strength are used in applications involving exposure to aque-

ous environment containing chlorides. The properties as well as corrosion behavior of these steels depend on their processing, microstructure and presence of certain trace elements. Toughness levels and crack growth resistance are found to drop significantly as a result of temper embrittlement and ingress of hydrogen. Observations carried out during a systematic evaluation of mechanical properties, corrosion behavior and crack growth rate measurements show that temper embrittlement. Phenomena act synergistically with hydrogen ingress leading to lowering of toughness and crack growth resistance of the material. The steels also show susceptibility to sensitization under certain processing conditions. The results of a systematic study on low carbon martensitic steel material will be presented in this paper.

11:20 AM

Corrosion of Candidate Materials for Supercritical Water-Cooled Reactors: *Todd R. Allen*¹; *Yun Chen*¹; *Lizhen Tan*¹; *Kumar Sridharan*¹; ¹University of Wisconsin

Advanced nuclear energy systems have been proposed that will use supercritical water as a coolant. Because of the limited experience with candidate alloys exposed to supercritical water, a test program has been initiated to understand oxidation behavior in these candidate alloys. This work will report on the corrosion response of two austenitic and two ferritic-martensitic alloys exposed to supercritical water at a temperature of 500°C at either 25 ppb or 2 ppm dissolved oxygen to times of 1000 hours. The alloys tested and examined in detail are 800H, D9, NF616, and HCM12A. In addition to polished coupons, HCM12A was tested after implanting oxygen into the surface. Following exposure, weight change was measured and for selected alloys, the oxide was examined. This paper will report on trends in weight gain as well as oxide development in candidate materials.

11:45 AM

General Corrosion Properties of Titanium Based Alloys for the Fuel Claddings in the Supercritical Water-Cooled Reactor: *Junya Kaneda*¹; *Shigeki Kasahara*¹; *Jiro Kuniya*¹; *Kumiaki Moriya*¹; *Fumihisa Kano*²; *Norihisa Saito*²; *Akio Shioiri*²; *Tamaki Shibayama*³; *Heishichiro Takahashi*³; ¹Hitachi, Ltd.; ²Toshiba Corporation; ³Hokkaido University

Supercritical water-cooled reactors (SCWRs) are expected to achieve more than 40% thermal efficiency, compared to about 34% for the latest BWRs. However, there are important technology gaps for safety and stability of the SCWRs. One of the critical technology issues is the materials for fuel claddings and core components which must be used in high-pressure (25MPa) and high-temperature (300°C - 550°C) water under neutron irradiation. Good mechanical properties, corrosion resistance and microstructural stability under these severe conditions are required. Primary candidate materials were selected among commercial materials used in commercial power plants such as supercritical pressure fossil-fired power plants; these are austenitic and ferritic stainless steels, Ni-based alloys and Ti-based alloys. In the present research, we analyzed corrosion performance of Ti-based alloys from the viewpoint of composition and structure of the oxide films. From the results, we discuss the most promising materials for the SCWR fuel claddings.

Operational Experience - II

Tuesday PM
August 16, 2005

Room: Ballroom I
Location: Cliff Lodge

Session Chairs: Christer Jansson, SwedPower AB; C. E. (Gene) Carpenter, U.S. Nuclear Regulatory Commission

6:00 PM

German Experience with Intergranular Cracking in Austenitic Piping in BWRs and Assessment of Parameters Affecting the In-Service IGSCC Behavior Using an Artificial Neural Network: *Renate Kilian*¹; Ulrich Wesseling¹; Karin Kuester²; Harald Hoffmann³; Ulf Ilg⁴; Erika Nowak⁵; Martin Widera⁶; ¹Framatome ANP; ²Vattenfall Europe; ³VGB PowerTech e. V.; ⁴EnBW Kraftwerke AG; ⁵E.ON Kernkraft GmbH; ⁶RWE Power AG

A new database, named DISAS, has been built up, populated and evaluated. The database includes 141 metallographically examined welds from German BWR austenitic piping and consequently 282 half welds (HAZs). 203 of them are without cracking and 79 with cracking. In parallel the results of the random non-destructive examinations from all German BWRs have been collected. This database has been used to perform an assessment of parameters affecting the in-service IGSCC behavior of austenitic BWR piping welds. The results of a common statistical evaluation are also shown, but the main focus of the assessment is the use of an artificial neural network (ANN) for sorting and interpreting the impact of material related variables and environmental parameters on the IGSCC behavior in the HAZ of austenitic BWR pipe welds.

6:25 PM

Root Cause Failure Analysis of Defected J-Groove Welds in Steam Generator Drainage Nozzles: *Paul Efsing*¹; Björn Forssgren¹; Renate Kilian²; ¹Ringhals AB; ²Framatome ANP GmbH

During the refuelling outage of Ringhals 2 in 2004, visual examinations of the outer parts of the bottom dome of the Steam Generators, SG, before the scheduled SG-pipe inspections, revealed a boron deposit outside drainage pipes from the manhole covers in two positions. The drainage pipes are made from stabilized stainless steel and are connected to the Low Alloy Steel lower dome by a nickel based dissimilar J-groove weld of alloy 82 equivalent weld metal. Dye penetrant and replica-moulding examinations of the surfaces of the J-groove welds inside the manhole both showed similar results. Two radially oriented defects were indicated in the 12 o'clock position in one of the nozzle welds on the hot side on one of the steam generators, and one similarly oriented and positioned defect in one of the cold side manhole cover nozzles in another steam generator. These defects comply well with the observations made from the external examinations during the initial stages of the Refuelling outage. Two boat samples were removed by EDM, one from each of the defected areas of the J-groove welds. Metallographic examination of the boat samples showed not only an extensive, most likely service induced, degradation of the Alloy 82 weld material, but also the presence of a manufacturing induced circumferential defect in the root pass of the J-groove weld not exposed to primary water. Given the manufacturing situation, this defect is not a complete surprise, and it was also seen when investigating the weld mock-ups that were manufactured in order to train the personnel before the weld repair that was conducted as part of the program.

6:50 PM

Laboratory Investigation of the Stainless Steel Cladding on the Davis-Besse Reactor Vessel Head: *Hongqing Xu*¹; *Steve Fyfitch*¹; *James W. Hyres*²; ¹Framatome ANP, Inc.; ²BWXT Services, Inc.

Laboratory analyses conducted on the welded stainless steel cladding on the Davis-Besse low alloy steel reactor pressure vessel (RPV) closure head are described. These examinations focused primarily on the cladding located at the base of the corroded cavity in the head, which included approximately 110 sq. cm (17 sq. in) of exposed stainless steel cladding having an average thickness of 0.65 cm (0.256 in). In this area, the cladding exhibited an upward bulge and a network of cracks. Several laboratory samples were prepared through the cladding to characterize the crack depth and morphology by light optical microscopy (LOM), scanning electron microscopy (SEM), and energy dispersive spectroscopy (EDS). Other laboratory characterizations included elevated temperature tensile testing on the cladding material, visual examinations of the interface between the cladding and the low alloy steel RPV closure head, and microstructural/microchemical characterization through the stainless steel cladding cross section. The presentation will include the results and conclusions of the laboratory investigative efforts.

7:15 PM

Laboratory Investigation of PWSCC of CRDM Nozzle 3 and Its J-Groove Weld on the Davis-Besse Reactor Vessel Head: *Hongqing Xu*¹; *Steve Fyfitch*¹; *James W. Hyres*²; ¹Framatome ANP, Inc.; ²BWXT Services, Inc.

In February 2002, significant boric acid corrosion of the Davis-Besse low alloy steel reactor pressure vessel (RPV) closure head was uncovered around control rod drive mechanism (CRDM) nozzle No. 3. Subsequent on-site non-destructive examinations (NDE) found that nozzle No. 3 had developed through-wall cracks due to primary water stress corrosion cracking (PWSCC) next to the J-groove weld. The CRDM nozzle 3 and its J-weld were carefully examined in the laboratory by fluorescent penetrant testing and stereomicroscopy that identified the remnant of the axial cracks in the Alloy 600 nozzle as well as the circumferential and axial cracks in the Alloy 182 J-groove weld. These cracks were subsequently sectioned for light optical metallography (LOM) and scanning electron microscopy (SEM) for characterization. The presentation will include the results and conclusions of the laboratory investigative efforts on the PWSCC of Alloy 600 CRDM nozzle No. 3 and its Alloy 182 J-groove weld.

7:40 PM

Laboratory Investigation of the Alloy 600 Bottom Mounted Instrumentation Nozzle Samples and Weld Boat Sample from South Texas Project Unit 1: *Hongqing Xu*¹; *Steve Fyfitch*¹; *James W. Hyres*²; *Francois Cattant*³; *Al McIlree*³; ¹Framatome ANP, Inc.; ²BWXT Services, Inc.; ³Electric Power Research Institute

In April 2003, evidence of primary water leakage was observed near two Alloy 600 bottom mounted instrumentation (BMI) nozzles at South Texas Project (STP) Unit 1. Subsequent non-destructive examination (NDE) indicated cracking in the two BMI nozzles near the J-groove weld. As a result, two segments of the BMI nozzles and one J-groove weld boat sample were removed and submitted for laboratory destructive examination. The laboratory investigation was led by a panel of failure analysis experts from EdF, DEI, BWXT, Exponent, EPRI, and Framatome ANP. The laboratory examinations included visual and stereo visual inspections, dimensional inspections, fluorescent penetrant testing (PT), replication, X-ray radiography, chemical composition analysis, modified Huey testing, microhardness testing, optical metallography with progressive sectioning, scanning electron microscopy (SEM), and energy dispersive spectroscopy (EDS). Metallurgical analyses confirmed that an extensive axial crack existed in the Alloy 600 nozzle and connected through a lack of fusion defect to penetrate the weld deposit. The presentation will discuss these major observations and their interpretation relative to NDE results.

8:05 PM

Boric Acid Corrosion of the Davis-Besse Reactor Pressure Vessel Head: *Hongqing Xu*¹; *Steve Fyfitch*¹; *James W. Hyres*²; ¹Framatome ANP, Inc.; ²BWXT Services, Inc.

In February 2002, significant corrosion was discovered on the Davis-Besse low alloy steel reactor pressure vessel (RPV) closure head. Subsequent investigations determined that this had resulted from primary water leakage allowing boric acid corrosion to occur. An approximately 17-inch diameter section of the RPV head was removed for laboratory non-destructive and destructive examinations. Detailed visual inspections were performed to characterize salient features. A non-shrink-molding compound was used to create impressions of the corroded cavity of the head and the underside of the stainless steel cladding beneath the cavity (RCS side). The resulting molds were used to obtain accurate area measurement of the exposed cladding and preserve the dimensional and surface characteristics of the corroded area. Samples from selected areas of low alloy steel and stainless steel cladding were removed for light optical metallography (LOM) and for Scanning Electron Microscopy (SEM) to characterize the corrosion surface due to boric acid attack. The presentation will include the results and conclusions of these efforts.

8:30 PM

Measurements of Carbon Steel ECP and Critical Deuterium Concentration under CANDU Conditions in the Halden Reactor: *Peter Bennett*¹; *Margaret McGrath*¹; *Khush Bagli*²; *Michael Dymarski*²; ¹OECD Halden Reactor Project; ²Ontario Power Generation Inc.

Injection of titanium dioxide (TiO₂) into CANDU primary coolant circuit is being considered as a method to mitigate flow-accelerated corrosion of the carbon steel outlet feeder pipes. A test has been conducted in a loop in the Halden reactor to investigate whether TiO₂ injections will affect the corrosion behaviour of the fuel cladding, pressure tube material and other critical materials of construction of the Primary Heat Transport System. During the test, measurements were made of the ECP of carbon steel over a period of 200 full power days. The critical deuterium concentration was determined by adding oxygenated heavy water to the loop, while simultaneous ECP measurements allowed investigation of the effect of the dissolved oxygen on the corrosion potential of carbon steel.

Noble Metal and SCC Mitigation

Tuesday PM
August 16, 2005

Room: Ballroom II
Location: Cliff Lodge

Session Chairs: Sam Hettiarachchi, General Electric; Tsung-Kuang Yeh, National Tsing-Hua University

6:00 PM

BWR SCC Mitigation Experiences with Hydrogen Water Chemistry: Sam Hettiarachchi¹; ¹General Electric

It is well accepted that once the electrochemical corrosion potential (ECP) of structural materials used in BWRs such as sensitized stainless steel, Alloy 182 and Alloy 600 are lowered to values < -230 mV(SHE) with hydrogen water chemistry (HWC) or NobleChemTM/low HWC, intergranular stress corrosion cracking of materials can be considered to be mitigated. This fact has been confirmed by numerous laboratory tests conducted by many investigators worldwide. However, the actual BWR fleet operational data confirming the benefits of hydrogen water chemistry (HWC) are limited primarily due to the limited number of ultrasonic tests (UT) performed in operating plants, infrequent UT data available before and after HWC, uncertainties associated with UT examinations, and the time and cost involved in UT examinations of plant internal components such as the recirculation piping and the core shroud. This paper is intended to summarize the available crack growth rate data from operating plants that used crack growth monitors in a variety of in-vessel locations exposed to real plant water chemistry conditions, and some of the actual plant UT data collected before and after employing HWC. The paper will also summarize a few post-HWC and post-NobleChemTM/low HWC UT data, and address the attempts that are currently in progress to collect more UT data from operating BWRs.

6:25 PM

Effect of Bulk Water Chemistry on ECP Distribution inside a Crevice: Yoichi Wada¹; Kazushige Ishida¹; Masahiko Tachibana¹; Motohiro Aizawa¹; ¹Hitachi, Ltd.

Water chemistry of an occluded volume in a crack has been studied in order to consider a mechanism of an intergranular stress corrosion cracking (IGSCC) in boiling water reactor (BWR) environment. An electrochemical corrosion potential (ECP) in a crevice made of 304SS, has been measured under a BWR condition. The ECP distribution along the crevice was affected by bulk water chemistry. However, the ECP value was rather uniform and below -400 mVvsSHE at deep part of the crevice. When water flow rate was high, the ECP became higher at shallow part of the crevice. Therefore, if potential gradient is a motive force of crack growth, it is effective to reduce bulk oxidant concentrations such as oxygen and hydrogen peroxide in order to reduce the gap of ECP between inside and outside of a crevice. Reducing agent alternative to hydrogen was also studied to make the bulk oxidant concentration decrease effectively.

6:50 PM

The Impact of Oxygen and Hydrogen Recombination Efficiency on the Effectiveness of NMCA in Reducing the Corrosion Potential in Boiling Water Reactors: Tsung-Kuang Yeh¹; ¹National Tsing-Hua University

Hydrogen water chemistry (HWC) has been widely adopted as a measure for mitigating intergranular stress corrosion cracking (IGSCC) and irradiation-assisted stress corrosion cracking (IASCC) in vessel internal components of boiling water reactors (BWRs) in the past decade. For enhancing the effectiveness of HWC at a lower hydrogen level and leading to a more effective reduction in electrochemical corrosion potential (ECP), the technique of noble metal treatment (NMT) on structural materials was brought into practice 10 years ago. The application of NMT is aimed at enhancing the oxidation reaction of hydrogen occurring on metal surfaces and thus reducing the oxidation reaction of metals. In a recent study, the effectiveness of NMT in combination with a low HWC was evaluated by predicting the hydrogen to oxygen (plus hydrogen peroxide) molar ratio ($M_{H_2/O}$) in the primary coolant circuit of a BWR. If the $M_{H_2/O}$ at a certain location is calculated to be greater than 2, it is justified that the NMT would be effective in reducing the ECP to much below the critical potential (E_{crit}) of -0.23 V_{SHE}. However, this statement is true only when the recombination efficiency of hydrogen and oxygen at this location is a perfect 100%. If not, a significant amount of oxygen and hydrogen peroxide may still be present even with an $M_{H_2/O}$ of greater than 2. Under the circumstance, the ECP may be reduced, but not to a great extent, and may remain above the E_{crit} as predicted by the DEMACE computer code. Taking the inlet of the core bypass region of a commercial BWR as an example, with a hydrogen and oxygen recombination efficiency of 100%, the ECP at this location could be reduced from 0.10 V_{SHE} to -0.28 V_{SHE} at a feedwater [H₂] of 0.2 ppm. However, if the recombination efficiency decreased to 10%, the ECP could only be reduced to -0.05 V_{SHE} instead, which was significantly higher than the E_{crit} . Based upon the results obtained from the current stage of our analysis, it would be inappropriate to use the $M_{H_2/O}$ as a sole indica-

tor at this moment for evaluating the effectiveness of NMT in mitigating IGSCC in a BWR with a low HWC. In the meantime, it is more important to clarify the recombination efficiency of hydrogen and oxygen on the noble metal treated stainless steel surfaces in order to qualify the approach of using the $M_{H_2/O}$ as an indicator for NMT effectiveness in the primary coolant circuit of a BWR.

7:15 PM

OnLine NobleChem Mitigation of SCC: Peter L. Andresen¹; Young Jin Kim¹; Sam Hettiarachchi²; Thomas P. Diaz²; ¹GE Global Research Center; ²GE Nuclear Energy

Reducing the corrosion potential is the most effective method of mitigating SCC in BWRs. Several methods exist to reduce the corrosion potential, but the most effective method uses electrocatalysis. OnLine NobleChem is a process that applies sub-monolayer quantities of Pt or other catalytic species to existing, oxidizing components. Because it is performed under full operating conditions (full temperature and flow flow), it also ensures that Pt penetrates deeper into the crack that oxidants, such as O₂ and H₂O₂. Because it is an on-line process, reapplication can be performed at appropriate intervals with little effect on plant operation. This paper focuses on the extensive SCC growth rate testing that demonstrates the effectiveness of OnLine NobleChem.

7:40 PM

Corrosion Mitigation of BWR Structural Materials by the Photoelectric Method with TiO₂-Laboratory Experiments of TiO₂ Effect on ECP Behavior and Material Integrity: Masato Okamura¹; Tetsuo Osato¹; Nagayoshi Ichikawa¹; Tadasu Yotsuyanagi¹; Kenro Takamori²; Shunichi Suzuki²; Junichi Suzuki²; ¹Toshiba Corporation; ²Tokyo Electric Power Company

Hydrogen water chemistry and noble metal chemical addition have been applied to actual BWR plants to mitigate the corrosion environment of structural materials. An electrochemical corrosion potential (ECP) of stainless steel (SS) is one of the most important indicators of intergranular stress corrosion cracking (IGSCC) susceptibility of the materials. We tried to lower the ECP of SS by using n-type semiconductor which is excited by photon irradiation and supply electrons to electrochemical reactions on the surface. Excited electrons will participate in anodic current increasing on the metal surface, therefore SS coated with the semiconductor, called photo-catalyst, has some possibility of shifting the ECP in the negative direction under the photons irradiation as Cherenkov-rays exist in the region of the nuclear reactor core. As the n-type semiconductor, TiO₂ was selected. TiO₂ is the well-known photo-catalyst and that is widely used in many fields. The effects of TiO₂ coating on the ECP of type 304 SS under UV irradiation condition simulating Cherenkov radiation in BWR circumstance were investigated. This report describes following items, (1) the ECP lowering ability, (2) photon flux, (3) material tests. ECP measurements of TiO₂ coated type 304 SS were performed under Normal Water Chemistry (NWC) and Hydrogen Water Chemistry (HWC) conditions. We controlled the water conditions by operating the high temperature and high pressure water circulating loop and simulated the water chemistry of several parts of the BWR plant. The ECP specimens were prepared from the plates of type 304 SS and were exposed to high temperature water for prefilming before TiO₂ coating on their surface. The ECP of TiO₂ coated SS shifted rapidly in the negative direction just after UV irradiation, even under high-oxygenated condition such as high concentration of hydrogen peroxide in the water. We confirmed that TiO₂ can shift the ECP of SS in the negative and lower below the recommended value under UV irradiation and can keep the potential stably. The effect of the amount of TiO₂ on the ECP of SS under UV irradiation was also investigated. Photon flux (Cherenkov radiation intensity) produced by gamma ray irradiation of water was evaluated. Some measurements of Cherenkov radiation intensity were made at the research reactor (Toshiba Training Reactor). Slow strain rate tests (SSRT) and compact tension tests (CT) were performed to study TiO₂ effect on IGSCC susceptibility of type 304 SS. It was confirmed that TiO₂ under UV irradiation prevented the IGSCC of type 304 SS.

8:05 PM

Electrochemical Behavior of Oxygen and Hydrogen on ZrO₂ Treated Type 304 Stainless Steels in High Temperature Pure Water: Tsung-Kuang Yeh¹; Chuen-Hong Tsai¹; Chang-Tong Liu¹; ¹National Tsing-Hua University

Hydrogen water chemistry (HWC) has been widely adopted as a measure for mitigating intergranular stress corrosion cracking (IGSCC) and irradiation-assisted stress corrosion cracking (IASCC) in vessel internal components of boiling water reactors (BWRs) in the past decade. For enhancing the effectiveness of HWC in the aspects of lower hydrogen consumption and of a more effective reduction in electrochemical corrosion potential (ECP), the technique of inhibitive surface treatment on structural materials was brought into consideration. The application of inhibitive treatment is aimed at deterring the reduction reactions of oxidizing species occurring on metal surfaces and the oxidation reaction of metals. In the current study, surfaces of pre-oxidized square specimens made of Type 304 stainless steels (SS) were treated with ZrO₂ by hydrothermal deposition at 150°C. Some pre-oxidized specimens remained untreated. Electrochemical polarization analyses at 288°C were conducted to characterize the electrochemical properties of the treated and untreated SS specimens in pure water with dissolved oxygen or hydrogen. The polarization results showed that the

treated specimens exhibited lower corrosion potentials, corrosion current densities, exchange current densities, and cathodic current densities than the untreated one in high temperature pure water with dissolved oxygen. For the environment with dissolved hydrogen only, reductions in anodic current density and exchange current density were observed, indicating that the ZrO₂ treatment also deterred the oxidation reaction of hydrogen. However, in comparison with the data obtained, the ZrO₂ treatment seemed to be relatively more effective in inhibiting the oxygen reduction reaction than inhibiting the hydrogen oxidation reaction. One additional beneficial outcome was that the anodic current density of the metal was also inhibited, leading to a much lower overall corrosion current density of the ZrO₂ treated specimen. Based upon the results obtained from the current stage of our experiment and consistent with our earlier crack growth experiment results, inhibitive treatments showed a distinct benefit in terms of corrosion mitigation. Currently, analyses in a pure water environment with the presence of hydrogen peroxide are being carried out to support and further confirm our present findings.

8:30 PM

Effect of Zn on SCC of 316L Stainless Steel at Low Potential: *Martin M. Morra*¹; Peter L. Andresen¹; Michael Pollick¹; ¹General Electric Global Research Center

The beneficial effects of Zn addition on oxide films in normal BWR water chemistries include reduced film thickness, greater protectiveness, less incorporation of ⁶⁰Co, and a higher strain to fracture. At high corrosion potential, however, the ability of mitigating quantities of Zn⁺² to reach a crack tip and slow SCC growth is limited. Because of this Zn may be more beneficial as a tool for blocking SCC initiation in normal water chemistries. In order to utilize Zn to reduce SCC growth rate the addition must be performed at low corrosion potential. There are two benefits to this approach. First, Zn can provide an added boost to the already demonstrated effectiveness of low corrosion potential in reducing SCC growth rates. Second, Zn may reduce SCC growth rates in high yield strength materials that exhibit moderately high growth rates at low potential. In this study the effect of adding Zn at low potential on the SCC growth rate of cold worked 316L stainless steel was investigated. The intent of these tests was to mimic possible synergistic effects of Zn and low corrosion potential achieved when using Zn in combination with NobleChem™. Replicate crack growth rate tests were performed on 0.5T CT specimens under constant K conditions in high purity water at 288°C. In these tests long-time steady state crack growth rates were first obtained at low corrosion potential by hydrogen addition after which 20 ppb Zn was injected. Results show that Zn addition produces SCC growth rates that are 3 to 5 times lower than those obtained at low potential. Replicate testing of the same material demonstrated a consistent response of crack growth rate to Zn addition.

Irradiation Assisted Stress Corrosion Cracking - I

Wednesday AM
August 17, 2005

Room: Ballroom I
Location: Cliff Lodge

Session Chairs: Stephen M. Bruemmer, Pacific Northwest National Laboratory; Bogdan Alexandreanu, Argonne National Laboratory

8:00 AM

The Effect of Oversized Solute Additions on the Irradiation-Assisted Stress Corrosion Cracking Resistance of Austenitic Stainless Steels: *Micah J. Hackett*¹; Gary S. Was¹; ¹University of Michigan

Oversized solutes have significant effects on the microstructure of irradiated alloys, including void swelling, dislocation loop microstructure and radiation-induced segregation (RIS). Solute additions, such as zirconium and hafnium, are believed to decrease RIS and dislocation density, which can reduce grain boundary sensitization and cracking. In this work, Fe-14Cr-14Ni was doped with 0.3 and 0.45 wt% Zr, and Fe-17Cr-14Ni was doped with 1.17 and 0.16 wt% Hf. These alloys were then irradiated with 3.2 MeV protons up to 10 dpa at 400°C. The irradiated microstructure was characterized by TEM and RIS quantified using STEM-EDS. Constant extension rate tensile (CERT) tests in BWR normal water chemistry were conducted to determine the effects of oversized solutes on stress corrosion cracking behavior. Previous work shows increases in IGSCC resistance due oversized solute addition. The effects of varying Zr and Hf concentrations on SCC resistance due to the irradiated microstructure and microchemistry will be discussed.

8:25 AM

Effect of Metallurgical Condition on Irradiation-Assisted Stress Corrosion Cracking of Commercial Stainless Steels: *Jeremy Todd Busby*¹; Ed A. Kenik²; Gary S. Was¹; ¹University of Michigan; ²Oak Ridge National Laboratory

Irradiation-assisted stress corrosion cracking (IASCC) is complex and sensitive to the metallurgical condition of the alloy. Here, the objective is to systematically examine the influence of the metallurgical condition on the radiation-induced changes and IASCC susceptibility in stainless steels. A 304 alloy (solution-annealed) and a 316 PWR baffle-bolt (either cold-worked, solution-annealed or a desensitized state designed to form coherent grain-boundary carbides) were irradiated with 3.2-MeV protons at 360°C to 5.5 dpa. Hardness, microstructure and RIS were quantified after irradiation. Constant extension-rate tensile tests were performed in simulated BWR (NWC) and PWR environments. Both alloys were susceptible in the solution-annealed condition in both environments. The carbide bearing state was extremely susceptible in the oxygenated environment, due to residual sensitization. In the PWR environment, cracks initiated but did not propagate, indicating a potentially beneficial influence of carbides. The cold-worked state was resistant to IG cracking in both the PWR and BWR environments.

8:50 AM

Irradiation Assisted Stress Corrosion Cracking of Heat Affected Zones of Austenitic Stainless Steel Welds: *Raluca Stoencescu*¹; Didier Gavillet¹; Bob van der Schaaf²; Armin Roth³; Carsten Ohms⁴; Steven Van Dyck⁵; Maria-Luisa Castano⁶; ¹Paul Scherrer Institute; ²NRG; ³Framatome ANP; ⁴JRC; ⁵SCK-CEN; ⁶CIEMAT

Irradiation assisted stress corrosion cracking is known to appear in the internal components of boiling water reactors such as core shrouds. Although the behaviour of austenitic stainless steel base materials has been thoroughly investigated, few studies were dedicated to the weld metal and heat affected zones (HAZ). The goal of this study is to better understand the welding and neutron irradiation induced changes in the HAZ that may promote intergranular cracking. The evolution of residual stresses, microstructure, microchemistry, mechanical properties, and the stress corrosion behaviour of two welded austenitic stainless steels have been investigated, before and after irradiation. Slow Strain Rate Tensile tests have been performed. Flat tensile samples, containing the weld and HAZ have been fabricated from AISI 304 and AISI 347. Stress corrosion tests have been performed at 290°C in low conductivity water with 200 ppb dissolved oxygen, and in inert gas.

9:15 AM

Irradiation Effects in a Highly Irradiated Cold Worked Stainless Steel Removed from a Commercial PWR: *Joyce Conermann*¹; Regis Shogan¹; Koji Fujimoto²; Toshio Yonezawa²; Yoichiro Yamaguchi³; ¹Westinghouse Electric Company; ²Mitsubishi Heavy Industries, LTD.; ³Nuclear Development Corporation

Mechanical and corrosion properties were measured on a cold worked, Type 316 stainless steel tube removed from the core of a PWR after 23 years of service. Neutron exposure levels ranged from near 0 to 65 dpa and irradiation temperatures from 290 to 320°C. As expected, the strength of the material increased

and the ductility decreased with irradiation. Slow strain rate and stressed O-ring crack initiation tests in PWR water were used to determine the susceptibility of the material to irradiation assisted stress corrosion cracking. The data indicate that IASCC susceptibility may accelerate above 20 dpa and saturate after 40 dpa. The property changes were correlated with irradiation induced microstructural changes using high resolution microscopy, chemical composition analysis near the grain boundaries and retained gas analysis. Grain boundary chemical changes did not saturate above 40 dpa as did the IASCC susceptibility. The most interesting feature observed was a coating of bubbles on the grain boundaries. Negligible swelling was observed at all material conditions.

9:40 AM

Crack Growth Behavior of Irradiated Austenitic Stainless Steel Weld Heat Affected Zone Material in High-Purity Water at 289°C: *Omesh K. Chopra*¹; Bogdan Alexandreanu¹; William J. Shack¹; ¹Argonne National Laboratory

Austenitic stainless steels (SSs) are used extensively as structural alloys in the internal components of reactor pressure vessels because of their superior fracture toughness properties. However, exposure to high levels of neutron irradiation for extended periods can exacerbate the corrosion fatigue and stress corrosion cracking behavior of these steels by affecting the material microchemistry, material microstructure, and water chemistry. Experimental data are presented on crack growth rates of austenitic SS weld heat affected zone (HAZ) specimens before and after they were irradiated to a fluence of 5.0×10^{20} n/cm² ($E > 1$ MeV) (~ 0.75 dpa) at $\sim 288^\circ\text{C}$. Crack growth tests were conducted under cycling loading and long hold time trapezoidal loading in simulated boiling water reactor environments on Type 304L SS HAZ of the H5 weld from the Grand Gulf reactor core shroud and on Type 304 SS HAZ of a laboratory-prepared weld. The effects of material composition, irradiation, and water chemistry on growth rates are discussed.

10:05 AM Break

Irradiation Assisted Stress Corrosion Cracking - II

Wednesday AM
August 17, 2005

Room: Ballroom I
Location: Cliff Lodge

Session Chairs: Stephen M. Bruemmer, Pacific Northwest National Laboratory; Bogdan Alexandreanu, Argonne National Laboratory

10:30 AM

Effect of the Accelerate Irradiation and Nuclear Transmuted Gas on IASCC Characteristics for Highly Irradiated Austenitic Stainless Steels: *Koji Fujimoto*¹; Toshio Yonezawa¹; Eiji Wachi¹; Yoichiro Yamaguchi²; Morihito Nakano³; Regis P. Shogan⁴; Jean-Paul Massoud⁵; Thomas R. Mager⁴; ¹Mitsubishi Heavy Industries, Ltd.; ²Nuclear Development Corporation; ³Kansai Electric Power Company, Inc.; ⁴Westinghouse Electric Corporation; ⁵Electricité de France

In order to clarify the IASCC characteristics of highly irradiated austenitic stainless steels over dose of 40 dpa, SCC susceptibility in simulated PWR primary water, mechanical and metallurgical properties and nuclear transmuted gas volume have been investigated for the austenitic stainless steels after irradiation in actual PWRs up to dose of 65 dpa or in a FBR (BOR60) up to dose of 40 dpa. The IASCC susceptibility of the stainless steels irradiated in FBR was extremely lower than that of the stainless steels irradiated in PWR, due to the SSRT tests in PWR environment for irradiated stainless steels. The mechanical properties and radiation induced segregation (RIS) for the stainless steels irradiated in FBR revealed the same tendency as those for the stainless steels irradiated in PWR. But the amount of nuclear transmuted gas volume for the stainless steels irradiated in FBR was extremely smaller than that for the stainless steels irradiated in PWR. Also, remarkable cavities formation was observed not only in the grain, but also near the grain boundary in the highly irradiated stainless steel. Therefore, it was suggested that the nuclear transmuted gas was as the one more important cause for IASCC in PWR, in addition to conventional proposals as RIS and radiation hardening. Also, there is the possibility that the IASCC characteristics different from the low irradiation range appear in the high irradiation range.

10:55 AM

Plastic Deformation Behavior of IGSCC on Thermally-Sensitized and Irradiated Type 316LN Stainless Steel: *Yukio Miwa*¹; Takashi Tsukada¹; ¹Japan Atomic Energy Research Institute

For IGSCC behaviors of the thermally-sensitized and the irradiated stainless steels, similar and different effects of grain boundary microchemistry, water chemistry and water temperature had been reported by many researchers. In this paper, the effects of plastic deformation behavior were examined for the thermally-sensitized and the irradiated type 316LN stainless steel. Specimens of type 316LN stainless steel were irradiated at 473 K to 1 dpa in High Flux Isotope Reactor (HFIR). Other specimens were thermally sensitized at 1033 K for 100 hours.

WEDNESDAY AM

SSRT was conducted for the specimens at 573 K in oxygenated water (DO=10ppm). Between these specimens, the comparisons of plastic deformation behavior and the %IGSCC were conducted after SSRT with some strain rates. Plastic deformation behaviors such as the work hardening coefficient and the maximum stress where IASCC initiated was similar to those of thermally-sensitized specimens in true stress-true strain relation of Swift type constitutive equation. Moreover, the effect of strain rate on %IGSCC was also same on both specimens. It was concluded from these results that initiation mechanism of IASCC was similar to that of IGSCC for specimens irradiated around 1 dpa.

11:20 AM

Development of Test Techniques for In-Pile SCC Initiation and Growth Tests and the Current Status of In-Pile Tests Using Pre-Irradiated Materials at JMTR: *Hirokazu Ugachi*¹; *Yoshiyuki Kaji*¹; *Junichi Nakano*¹; *Yoshinori Matsui*¹; *Kazuo Kawamata*¹; *Takashi Tsukada*¹; *Nobuaki Nagata*²; *Koji Dozaki*²; *Hideki Takiguchi*²; ¹Japan Atomic Energy Research Institute; ²JAPCO

Irradiation assisted stress corrosion cracking (IASCC) is one of the critical concerns when stainless steel components have been in service in light water reactors (LWRs), for a long period. In general, IASCC can be reproduced on the materials irradiated over a certain threshold fluence level of fast neutron by the post-irradiation examinations (PIEs). It is, however, considered that the reproduced IASCC by PIEs must be carefully distinguished from the actual IASCC in nuclear power plants, because the actual IASCC occurs in the core under simultaneous effects of radiation, stress and high temperature water environment. In the research field of IASCC, mainly PIEs for irradiated materials have been carried out, because there are many difficulties on SCC tests under neutron irradiation. Hence as a part of the key techniques for in-pile SCC tests, we have embarked on a development of the test technique to obtain information concerning effects of applied stress level, water chemistry, irradiation conditions, etc. A high temperature water loop facility was designed to be installed at the Japan Materials Testing Reactor (JMTR) to carry out material irradiations and in-pile testing for the study of IASCC. The water loop facility was designed to simulate boiling water reactor (BWR) environment and supply high temperature pure water into five irradiation capsules at a time. We have developed newly testing units in the core of JMTR, and in-pile SCC initiation and growth tests using pre-irradiated materials have been started since October 2004. Although it is difficult to detect the crack initiation in in-pile SCC tests, the crack initiation can be evaluated by the detection of specimen rupture if the cross section area of the specimen is small enough. Therefore, we adopted uniaxial constant load (UCL) tensile test method with small tensile specimens in in-pile SCC initiation test. In order to monitor crack length of a small compact tension (CT) specimen for long time, we adopted the six terminals direct current potential drop (DCPD) method, because it is easy to compensate the temperature of the CT specimen and the two terminals can be used for the spare of the DCPD measurement. In this paper, we describe the development of several techniques, especially control of loading on specimens, monitoring technique of crack initiation and propagation and monitoring technique of water conditions, and the current status of in-pile SCC tests using pre-irradiated materials at JMTR.

11:45 AM

Fractographic Observations on a Highly Irradiated AISI 304 Steel after Constant Load Tests in Simulated PWR Water and Argon and after Supplementary Tensile and Impact Tests: *Ulla M. Ehrnsten*¹; *Pertti Aaltonen*¹; *A. Toivonen*¹; *W. Karlsen*¹; *J.-P. Massoud*²; ¹VTT; ²Electricité de France

Intergranular cracking was observed in highly irradiated AISI 304 after constant load tests at 340°C in simulated PWR water and also in argon (but to a lesser extent). The applied stresses were in the range of 500-800 MPa in simulated PWR water and 700 MPa in argon. Supportive investigations on the mechanical behaviour of the irradiated steel were performed on small samples. These investigations consisted of manual impact testing at liquid nitrogen and room temperature and tensile testing at room temperature and at 300°C. The prevailing fracture mode for the material was intergranular in the three first tests. Tensile testing at 300°C using a fast strain rate of about $1 \times 10^{-3} \text{ s}^{-1}$ resulted in ductile dimple fracture. The investigations performed show that the irradiated stainless steel in question is susceptible to intergranular cracking without environmental assistance especially at low temperature (room temperature and below). The difference in fracture mode between tensile test in air at 300°C, resulting in ductile fracture, and constant load testing in argon gas at 340°C, resulting in intergranular fracture cannot be comprehensively explained based on the results. The fracture mode may be strain rate sensitive, with an increased susceptibility to intergranular fracture at slow strain rates. More investigations are under consideration.

PWR Secondary - I

Wednesday AM
August 17, 2005

Room: Ballroom II
Location: Cliff Lodge

Session Chairs: Jeffrey A. Gorman, Dominion Engineering, Inc.; François Vaillant, Electricité de France R&D

8:00 AM

Laboratory Examination of Pulled Steam Generator Tube with Free Span Axial ODS/SCC: *Albert Richard Vaia*¹; *Jim M. Stevens*²; *P. J. Prabhu*¹; ¹Westinghouse Electric Company; ²Texas Utility

Axial indications of outside diameter stress corrosion cracking (ODSCC) were reported in free span locations of mill annealed alloy 600 tubes in the Comanche Peak Unit 1 steam generators. One tube containing several such indications was removed from the steam generator for detailed laboratory examination. Non-destructive and destructive examination of the pulled tube specimens confirmed the existence of axial ODS/SCC. Laboratory examination using several techniques was performed at Westinghouse hot cell in Pittsburgh. The laboratory examination results are summarized in this article. The axial indications were in alignment azimuthally. A high concentration of "inclusions" was found to exist in the same azimuth along a long length of this tube. The identified inclusions were likely involved in the axial free span cracking. This observation is a first of a kind linking steam generator tubing inclusions to active degradation. In addition, ATEM examination of one specimen was performed at the Pacific Northwest Laboratories. A brief summary of the ATEM results is also included here for completion.

8:25 AM

Quantitative Morphological Characterization of Deposits Formed in Secondary Side of Comanche Peak Steam Electric Station Using Scanning Electron Microscopy: *Seifollah Nasrazadani*¹; *Haritha Namduri*¹; *Jim Stevens*²; *Robert Theimer*²; ¹University of North Texas; ²Texas Utilities

Samples collected from different components of units one and two of Comanche Peak Steam Electric Station (CPSES) during refueling shutdowns in past three years were analyzed quantitatively using Scanning Electron Microscopy (SEM). Morphological features of iron oxides (magnetite, and hematite) and oxyhydroxides (goethite, lepidocrocite) formed on samples exposed to low and high pressure feedwater heaters, main condenser, and moisture separators were analyzed. EDS 2004 software was utilized to characterize size and shape of particles along with statistical distribution of the data. This paper will provide an example of how digital images captured in modern SEMs can be analyzed quantitatively.

8:50 AM

The Effect of Residual Stress and Environment on the Initiation and Propagation of ODS/SCC Cracks in Thermally Treated Alloy 600 Steam Generator Tubing: *Ronald George Ballinger*¹; *Thomas Esselman*²; *William McBrine*²; *Thomas McKrell*³; *Alan McIlree*³; *Russell Lieder*⁴; *Robert White*⁴; ¹Massachusetts Institute of Technology; ²Altran Corporation; ³Electric Power Research Institute; ⁴FPL Energy, LLC

The first incidence of ODS/SCC in thermally treated alloy 600 tubing in a US PWR has been analyzed. Residual stresses were determined to have dominated the SCC process. This paper provides background on the tubing and an analysis of the effect of residual stress on the cracking. The tubing microstructure, corrosion tests performed on the tubing, measurement of the residual stress, and other test results will be reported. The threshold stress intensity factor for crack growth, K_{ISCC}, must be in the range 2-3 MPa√m for the observed behavior to have occurred. The implications for tubing life in other tubes are explored.

9:15 AM

Impurity Source Terms and Behavior in Nuclear Once-Through Steam Generator Cycles: *Rocky H. Thompson*¹; ¹Progress Energy Florida

Intergranular attack in the freespans of the superheat region is the dominant damage mechanism in most original once-through steam generators (OTSG) with sensitized Alloy 600 tubing. Lead was implicated in the IGA at one OTSG plant based on analytical transmission electron microscopy (ATEM) of pull tube specimens. Concentrated sodium sulfate solutions (~1.5 molal) were also implicated based on hideout return data from all of the OTSG plants. Aluminum is a major specie in OTSG hideout return which can contribute elevating the pH(t) in steam generator crevices. Streaks of aluminum containing deposits have been observed on pulled tubes in the freespans above the 7th tube support plate. Aluminum silicates have ion exchange properties. Aluminum silicate deposits may contribute to the adsorption of corrosive impurities on the steam generator tube surfaces. While not implicated in any observed OTSG corrosion phenomena, fluoride is observed to varying degrees at OTSG plants. The sources of these impurities, Al, Pb, and F, and their transport around the secondary cooling cycle were

recently investigated at Crystal River-3 and other OTSG plants. A mass balance approach was used to identify the source terms for Al, Pb, and F, as well as Na, Cl, K, SO₄, Ca, Mg, and silica based on steam generator hideout return and turbine wash data, deep bed condensate polisher resin analyses, makeup water sampling, and integrated filter sampling of various process liquid and steam streams in the secondary cycle. This paper summarizes the results of these investigations. By the end of 2005, four of the seven operating OTSG plants will have replaced steam generators with OTSGs containing thermally treated Alloy 690 tubes. While laboratory testing to date has shown thermally treated Alloy 690 to be more resistant to corrosion than sensitized Alloy 600, it is nonetheless not completely immune to corrosion. An ALARA chemistry philosophy is therefore still prudent with replacement OTSGs and requires that the source terms for all potentially corrosive impurities be identified so that efforts can be made to minimize their ingress into the secondary cycle. The investigation results summarized in this paper contribute to maintaining ALARA chemical impurities for plants with original or replacement OTSGs.

9:40 AM

Observations and Insights into Pb-Assisted Stress Corrosion Cracking of Alloy 600 Steam Generator Tubes: *Larry E. Thomas*¹; Stephen Bruemmer¹; ¹Pacific Northwest National Laboratory

High-resolution analytical transmission electron microscopy examinations of mill-annealed (MA) alloy 600 steam generator tubes from PWR service have in many cases revealed Pb incorporated in the corrosion products within intergranular cracks and deeply penetrated grain boundaries. To develop a better understanding of Pb effects on intergranular attack and stress-corrosion cracking, cracks produced under controlled environmental and material conditions in laboratory test samples were examined for comparison. The laboratory samples have included both MA and thermally treated alloy 600 tested in 320-350°C AVT water and caustic solutions. These comparisons showed that Pb alone in AVT water accurately reproduces the crack morphological and chemical signatures seen in many MA alloy 600 service tubes. Tests with caustic solutions yielded crack characteristics different from those in the pulled tubes from service. Observations indicating possible mechanisms of the Pb-assisted cracking and implications concerning the local crack environments in service will be discussed.

10:05 AM Break

PWR Secondary - II

Wednesday AM
August 17, 2005

Room: Ballroom II
Location: Cliff Lodge

Session Chairs: Jeffrey A. Gorman, Dominion Engineering, Inc.; François Vaillant, Electricité de France R&D

10:30 AM

Modeling Concentrated Solution Transport and Accumulation in Steam Generator Tube Support Plate Crevices: *Allen Baum*¹; Karoline Evans¹; ¹Bechtel Bettis, Inc

This paper describes two inter-related models that characterize how concentrated chemical solutions are transported and where they accumulate in tube support plate crevices. Solute accumulation is assumed to be governed by capillary effects, with the smallest pores filling first. A disjoining pressure model governs solute transport. The two models are inter-related by requiring the same solute pressure in the disjoining films and in the capillaries. The solute pressure then successively defines the solute boiling point elevation, the solute concentration, and the solute mass. The solute concentration and mass impact the aggressiveness of the local environment. The model addresses whether alkaline or acidic species will accumulate based on their relative solubility and volatility.

10:55 AM

Clues and Issues in the SCC of High Nickel Alloys Associated with Lead: *Roger W. Staehle*¹; ¹Staehle Consulting

Effects of Lead (Pb) on the SCC (PbSCC) of high nickel alloys are by well known to be a concern in modern steam generators including those using Alloy 690TT tubes. Pb has now been observed at the tip of SCC from four steam generators. The purpose of this discussion is to review special features associated with PbSCC and to assess what these mean to the occurrence of PbSCC in the future. Important characteristics of PbSCC seem to be the following: Occurrence in both Alloy 600 MA/TT and 690TT although the latter is less prominent than the former; greatly accelerated PbSCC in alkaline steam phases for Alloy 690TT; substantial reduction in intensity at neutral pH for Alloy 690TT and less for Alloy 600; proneness to PbSCC in acidic solutions containing chloride and negligible effect of Pb in sulfate solutions; significant migration of Pb to crack tip in alkaline solutions with largest accumulation midway in SCC; diminished Pb at crack tip in acidic solutions; generally intergranular SCC in MA heat treat-

ments and transgranular SCC in TT, SN, and SR heat treatments; high Pb concentration of Pb compounds at heat transfer surfaces both in recirculating and once through SGs; significant accumulation on hot surfaces while the Pb concentration in feed water is in the ppt range; and finally small amounts of SCC in SGs even with Alloy 600 despite significant quantities of Pb observed in deposits. To date, no SCC due to Pb has been observed in Alloy 690. This may be due to lesser concentration in deposits with line contact crevices on the secondary side of SGs or it may be due to the lower rate of PbSCC in relatively neutral solutions. Based on the trends to date together with the inherently possible PbSCC, additional research and modeling are proposed.

11:20 AM

Effect of Lead Contamination on SG Tube Degradation: *Yucheng Lu*¹; ¹Atomic Energy of Canada Ltd.

Lead is one of the most common impurities found in the steam generator (SG) secondary side chemistries. Field experience and laboratory studies have confirmed that all SG tube materials are susceptible to lead-induced stress corrosion cracking (SCC). Electrochemical measurements provide information on corrosion susceptibility and rate of SG tube materials as a function of electrochemical corrosion potential (ECP) and water chemistry. Using laboratory data in combination with chemistry monitoring and diagnostic software makes it possible to assess the impact of plant operating conditions on SG tube corrosion for SG life management. This paper discusses the results of electrochemical measurements made to elucidate the effect of lead on the corrosion susceptibility of SG tube materials. The effect of several different lead species on the electrochemical corrosion behaviors of SG tube materials was investigated. The detrimental effect of lead contamination on passive films of tube alloys was also investigated using photoelectrochemical measurements.

11:45 AM

The Effect of Metal Cations Including Pb²⁺ on Dissolution and Passivation of Nickel Base Alloys: *Harshan Radhakrishnan*¹; *Roger C. Newman*¹; Anatolie Carcea¹; ¹University of Toronto

There are similarities between the behavior of nickel-base alloys in the presence of Pb cations (manifested as corrosion and stress corrosion in hot water) and that of aluminum in the presence of low-melting-point alloying elements, or their dissolved cations, such as Hg, Ga or In. Even Zn, which does not have a particularly low melting point (420°C) causes activation of aluminum, at least when alloyed (we are not aware of any reports of an effect of Zn via the aqueous phase). Such effects in Al base systems are believed to involve direct contact of the metallic activator with the aluminum, and interference with passivation through continual occupation of sites where an oxide film is trying to form a protective network; this requires rapid surface diffusion of the activator atoms¹. Since this effect only requires submonolayer coverage of the activator, one can speculate that underpotential deposition would be enough to give a noticeable activation effect, and thus that the potential range where activation occurs might not correspond exactly to the range of stability of the solid (or liquid) activator metal. The situation with Ni base alloys is not quite as clear as with aluminum, and up to now the site of the action of lead has not been demonstrated. An electrochemical study has been carried out using solutions of various pHs near 100°C and a range of Ni base materials: pure Ni, Ni-10Cr, and alloys 600, 800 and 690. Lead and indium have been explored as possible activator cations. The interpretation of the results is complicated by deposition and stripping of the metal cations, but there do appear to be deleterious effects of their deposition on the passivating ability of the substrate. Whether this is truly analogous to aluminum activation remains to be demonstrated. ¹F. Sato and R.C. Newman: Mechanism of activation of aluminum by low-melting point elements: Part 2 - Effect of zinc on activation of aluminum in pitting corrosion. *Corrosion*, 55, 3-9 (1999).

12:10 PM

Effects of Pb on SCC of Alloy 600 and Alloy 690 in Prototypical Steam Generator Chemistries: *Jesse B. Lumsden*¹; Allan McIlree²; Richard Eaker³; ¹Rockwell Automation; ²Electric Power Research Institute; ³Duke Energy

Intergranular attack/stress corrosion cracking of Alloy 600 continues to be an issue in the tube/tube support plate crevices and top of tubesheet locations of recirculating steam generators and in the upper bundle of free span superheated regions of once through steam generators (OTSG). Recent examinations of degraded pulled tubes from several plants suggest possible lead involvement in the degradation. Laboratory investigations have been performed to determine the factors influencing lead cracking in Alloy 600 and Alloy 690 steam generator tubes. Test environments of pH 9 and 7, with the addition of lead oxide, were used to test highly strained reverse U-bend specimens. Specimens tested in a pH 9 environment were tested at controlled electrochemical potentials. Results demonstrated maximum susceptibility was at open circuit potential, unlike cracking of Alloy 600 in caustic and acid sulfate environments where maximum susceptibility occurs when specimens are polarized above the open circuit potential. Transgranular, intergranular and mixed mode cracking was observed and in all Alloy 600 conditions tested (mill annealed, sensitized, thermally treated) while thermally treated Alloy 690 has so far resisted cracking. Electrochemical measurements showed that the presence of Pb shifts the open circuit potential in the anodic direction and alters the polarization curve for both alloys. Testing results

suggest a film rupture/anodic dissolution model with displacement plating of Pb preceding passive film formation is consistent with the experimental observations.

Irradiation Assisted Stress Corrosion Cracking - III

Wednesday PM
August 17, 2005

Room: Ballroom I
Location: Cliff Lodge

Session Chairs: Jeremy T. Busby, Oak Ridge National Laboratory; Edward P. Simonen, Battelle

1:30 PM

In-Core Crack Growth Rate Studies on Irradiated Austenitic Stainless Steels in BWR and PWR Conditions in the Halden Reactor: *Torill Karlsen*¹; Peter Bennett¹; Nils Walther Høgberg¹; ¹OECD Halden Reactor Project

In-core crack growth rate measurements have been made on small Compact Tension (CT) specimens prepared from irradiated 304, 346 and 316 NG stainless steels with five different fluences, ranging from 0.08 to 2.5×10^{22} n/cm² (> 1MeV). The specimens were instrumented for on-line propagation monitoring with the reversing DC potential drop method and equipped with pressurised bellows that enabled on-line variation of applied stress intensity level. The tests were performed in BWR oxidizing and reducing environments at 280°C and in PWR conditions (with 2 ppm Li and 1200 ppm B), at 335°C. The microstructural and microchemical characteristics of the irradiated materials are described. Significant reductions in crack growth rate were recorded for the lower fluence materials in reducing environments while less marked changes in growth rate were observed in the high dose materials. The cracking response is examined in terms of the operating conditions, the materials' mechanical properties (e.g. yield strength) and K/size effects. Comparisons are also made with results from other crack growth studies on irradiated materials.

1:55 PM

Irradiation Assisted Stress Corrosion Cracking Susceptibility of Core Component Materials: Kazuhiro Chatani¹; Yuji Kitsunai¹; Mitsuhiro Kodama¹; Shunichi Suzuki²; *Yoshihiko Tanaka*²; Suguru Ooki²; Hiroshi Sakamoto³; Tomomi Nakamura⁴; ¹Nippon Nuclear Fuel Development Company, Ltd.; ²Tokyo Electric Power Company, Inc.; ³Toshiba Corporation; ⁴Hitachi Ltd.

In order to evaluate irradiation assisted stress corrosion cracking (IASCC) susceptibility for core components, we conducted slow strain rate tests and grain boundary analyses of irradiated Type 304 ($1.2 - 3.6 \times 10^{24}$ n/m², E>1MeV) and Type 316 ($0.23 - 1.2 \times 10^{25}$ n/m², E>1MeV) obtained from in-core components of commercial boiling water reactors. In the case of 32 ppm dissolved oxygen, all specimens showed no intergranular SCC. Although sufficient radiation-induced grain boundary chromium depletion for IASCC occurrence was observed in Type 316 irradiated to 1.2×10^{25} n/m², the radiation ductility loss was small, and IASCC did not occur. This data indicates that IASCC susceptibility might be influenced by radiation hardening rather than radiation-induced grain boundary segregation. As compared with the data obtained from the material irradiated in the reactor core region, it seemed that the amount of radiation hardening was lower and that of radiation-induced grain boundary segregation was higher in this study. These results indicate that radiation-induced phenomena depends on neutron flux. The paper will discuss the effect of radiation hardening and radiation-induced grain boundary segregation on IASCC susceptibility of austenitic stainless steels.

2:20 PM

Influence of the Neutron Spectrum on the Tensile Properties of Irradiated Austenitic Stainless Steels, in Air and in PWR Environment: *Jean-Paul Etienne Massoud*¹; Miroslav Zamboch²; Pietr Brabec²; Valentin Shamardin³; Valeriy Prokhorov³; Philippe Dubuisson⁴; ¹Electricité de France R&D; ²Nuclear Research Institute; ³RIAR; ⁴Commissariat à l'Énergie Atomique/SRMA

In order to address the issue of highly irradiated austenitic stainless steels of the core internals of PWRs, EDF has initiated a R&D program based upon the irradiation of test materials in several experimental reactors (fast breeder reactor and light water reactors) in a temperature range 300-400°C, up to the damage of the end of life (~ 80 dpa for 40 years service). However, irradiation conditions in fast breeder reactors are not those of a PWR: the neutrons flux is higher, the helium and hydrogen production rates are lower, due to lower thermal neutrons flux. Helium is responsible for high degradation of the ductility at irradiation temperature above ~ 500°C. At temperatures below 400°C, helium is believed to have no influence on strengthening or loss of ductility of austenitic stainless steels. An experiment has been designed in order to verify that conclusion. In order to assess the influence of the neutron spectrum both on the tensile characteristics in air and in PWR environment, the Samara experiment is aiming at the irradiation of tensile specimens in the SM experimental light-water reactor of the Research Institute for Atomic Reactors (RIAR, Russia), at a temperature

close to ~ 300°C. Specimens were irradiated in two positions: a position with a pure fast neutron spectrum, and a position with both fast and thermal neutron fluxes (in order to produce a high helium content). The tensile tests results obtained after irradiation in the frame of this experiment show that Helium has no influence on strengthening or loss of ductility of austenitic stainless steels (CW 316 and SA 304L) at low temperature (300°C). This experiment also allows to assess the coherence of the mechanical behaviour of these materials in the different irradiation experiments. With regard to mechanical properties, the irradiation in fast breeder reactor seems very similar to irradiation in light water reactors at low temperature. The Slow Strain Rate Tests in PWR environment results obtained after irradiation in the frame of this experiment show that higher amount of helium has no influence on strengthening, loss of ductility and fracture surface characteristics of austenitic stainless steels (CW 316 and SA 304L) at low temperature (300°C). With regard to corrosion-mechanical properties, the irradiation with fast neutron spectrum seems very similar to irradiation with mixed neutron spectrum at low temperature.

2:45 PM

Study on SCC Growth Behavior of BWR Core Shroud: *Suguru Ooki*¹; Y. Tanaka¹; K. Takamori¹; S. Suzuki¹; S. Tanaka²; Y. Saito²; T. Nakamura³; T. Kato³; K. Chatani⁴; M. Kodama⁴; ¹Tokyo Electric Power Company; ²Toshiba Corporation; ³Hitachi, Ltd.; ⁴Nippon Nuclear Fuel Development Company, Ltd.

Recent studies suggest that material hardening should cause enhancement in SCC growth rate of Stainless Steels. While the hardening of BWR core shroud of high fluence is governed mainly by neutron irradiation, the hardening of HAZ of BWR core shroud of low fluence is dominated by welding heat input. Therefore, in this study, SCC growth rates of SS irradiated up to the middle of 10^{24} n/m² and un-irradiated SS were measured in order to obtain reasonable estimation for SCC growth behavior in the core shrouds. The SCC growth rates of actual BWR core shrouds made of 304 SS were measured using 1T-CT specimens in BWR simulated environment. The cumulative neutron fluences of the specimens were $1.5-5.1 \times 10^{24}$ n/m². The stress intensity factor, K for the SCC growth tests was from 10.5 to 24.2 MPa m^{0.5}. The test results showed that the SCC growth rate of the actual core shrouds were enveloped by the current upper limit, 9.2×10^{-7} mm/s of the K-da/dt disposition curve of JSME NA1-2002 standard for Austenitic SS in NWC Reactor Water, suggesting that the limit is reasonably applicable even for SS irradiated up to those fluences. The SCC growth rates of a BWR shroud mock-up made of 316L SS, taking the simulated welding procedures, were also measured using 1/2T-CT specimens from HAZ. In spite of substantial hardness of HAZ that is apart from several mm from the fusion line, 200 HV, all SCC growth rates from the specimens were below the K-da/dt disposition curve of the JSME NA1-2002 standard for Low Carbon Austenitic SS in NWC Reactor Water. This fact suggests that the degree of hardening assumed in actual shrouds' apart from several mm from the fusion line should bring little enhancement effect in SCC growth rates.

3:10 PM Break

Crack Growth

Wednesday PM
August 17, 2005

Room: Ballroom I
Location: Cliff Lodge

Session Chairs: Gary S. Was, University of Michigan; Tetsuo Shoji, Tohoku University

4:00 PM

The Effect of Hold Time on the Crack Growth Rate of Sensitized Stainless Steel in High Temperature Water: *Anders Jenssen*¹; Christer Jansson²; Johan Sundberg¹; ¹Studsvik Nuclear AB; ²SwedPower AB

Periodic unloading with a hold time at maximum load is often applied in laboratory crack growth rate studies on environmentally assisted cracking. The purpose of the unloading/reloading cycle is normally to maintain a straight crack front, to break up unbroken ligaments behind the crack front, and to achieve stable crack growth. However, a fatigue component will be included in the total crack advance that can be difficult to assess. In order to quantify the effect of hold time on the crack growth rate, eight 1TCT specimens of sensitized Type 304 stainless steel were simultaneously tested in an autoclave under BWR normal water chemistry (288°C and 500 ppb O₂) conditions. The specimens were individually loaded and the crack advance was measured in each specimen by DCPD. Each specimen was tested at one hold time (single variable test) and the following hold times were investigated: 1,000 s, 3,600 s, 6,000 s, 10,000 s, 36,000 s and 100,000 s. The hold times of 3,600 and 10,000 s were investigated with duplicate specimens. This paper will present and discuss the effect of hold time on the crack growth rate.

4:25 PM

Effects of Positive and Negative dK/da on SCC Growth Rates: Peter L. Andresen¹; Martin M. Morra¹; Ron M. Horn²; ¹GE Global Research Center; ²GE Nuclear Energy

The effect of rising or falling stress intensity factor (K) on the SCC growth rates of stainless steel and nickel alloys has been studied in high temperature water. This is done using sophisticated test control software that changes loading (P) based on crack length (a) by controlling dK/da, not simply dP/dt. The majority of SCC problems develop adjacent to welds, which have a complex residual stress profile vs. wall thickness. This, coupled with the dependence of K on crack length, causes K to change as the crack grows, not per se with time (t). The effect of "K-dot" on crack tip strain rate and the associated crack growth rate is discussed.

4:50 PM

Application Specific Evaluation of Stress Corrosion Crack Growth Rate Based on Inspection Data on Alloy 600 Tubing: Yogen Garud¹; Brian Woodman¹; Gary Boyers²; ¹APTECH Engineering Services, Inc.; ²Florida Power & Light Company

Stress corrosion cracking (SCC) of Ni-Cr-Fe Alloy 600 in the light-water reactor service conditions (high purity, near-neutral aqueous environment) is now a well-recognized mechanism of active degradation. The common practice to address this SCC, until replacement with a more resistant material, is to manage the degradation through an active inspection and a critical assessment for remaining useful life of the subject components. A key factor influencing the assessment is the degradation rate or the crack growth rate (cgr) of SCC for the service applications of interest. Both the life prediction and the justification of inspection interval are affected. Although the related laboratory data on cgr can be used as a reference, the difference or unknowns in service conditions lead to consideration of a preferred alternative of inferring the application (service) specific cgr. In this way, interpretation of the inspection results becomes a critical and integral part of the life assessment. The above aspects of SCC growth rate evaluation and its practical application are explored in this paper. This is illustrated with respect to the high-temperature mill-annealed Alloy 600 tubing in steam generator application. The paper presents a refined analysis of inspection data leading to a better definition of plant-specific cgr that is suitable for probabilistic life assessment or structural performance estimation. A new optimization scheme is discussed that minimizes the impact of uncertainty in short-term rate of degradation and leads to a more realistic, representative cgr distribution while maintaining the random variation in the resulting distribution. The impact of this alternative cgr interpretation is discussed with plant-specific data on SCC, in terms of the estimated structural integrity margins and useful remaining life of the steam generator.

5:15 PM

High-Resolution Characterizations of Stress-Corrosion Cracks in Austenitic Stainless Steel from Crack Growth Tests in LWR-Simulated Environments: Larry E. Thomas¹; Peter L. Andresen²; Stephen Bruemmer¹; ¹Pacific Northwest National Laboratory; ²General Electric Global Research

Stress-corrosion cracks and crack tips are observed by high-resolution analytical transmission electron microscopy in austenitic stainless steel crack-growth test samples. The crack-growth tests were performed on warm-worked or sensitized 300-series stainless steels in simulated BWR and PWR environments. Final crack growth was produced under constant K conditions and samples were removed from solution under load to maintain crack openings until samples could be backfilled. The corrosion products, reaction interfaces and local metallurgy at crack tips are assessed to investigate processes occurring during SCC crack propagation. Highly branched intergranular cracks are found all the way to tip regions in each cross-section with narrow Cr-rich spinel oxide films on the crack walls. Comparisons will be made to prior examinations of irradiation-assisted stress-corrosion cracks in BWR and PWR components. Signatures of the stress-corrosion cracking in irradiated material include Ni enrichment of the metal leading the crack tips and formation of bi-layered spinel oxide films along the crack walls. General similarities between the crack corrosion microstructures in these samples support the effective use of laboratory testing to simulate and reveal service cracking behavior. The implications of specific differences among the various samples including impurities in the crack oxides, the presence of oxide-plugged cracks, deformation structures and composition changes ahead of the crack tips will be discussed.

PWR Secondary - III

Wednesday PM
August 17, 2005

Room: Ballroom II
Location: Cliff Lodge

Session Chairs: Allan R. McIlree, Electric Power Research Institute; Jesse B. Lumsden, Rockwell Automation

1:30 PM

Evaluation of Crack Growth Rate for Alloy 600TT SG Tubing in Primary and Faulted Secondary Water Environments: Yutaka Yamamoto¹; Masayoshi Ozawa¹; Kiyotomo Nakata¹; Takao Tsuruta²; Masafumi Sato²; Taketoshi Okabe²; ¹Japan Nuclear Energy Safety Organization; ²Mitsubishi Heavy Industries, Ltd.

The evaluation of SCC crack growth rate is one of the essential factors to assess structural integrity of degraded SG tubes. Currently, SG tubes in Japanese PWR are made of either Alloy 600TT or Alloy 690TT. Crack growth rate was measured for these Alloys both in primary water and faulted secondary water environments. The test specimen was an actual size tube that has an axial ID EDM (Electro Discharge Machining) slit, and fatigue pre-crack introduced at the crack tip. Hoop stress was applied under constant load condition by the internal pressure of the test loop. Crack growth rate toward the tube wall thickness direction was monitored by AC (alternating current) potential drop method, developed by joint research of MHI and Japanese PWR utilities. Main conditions for these tests are as follows: 1) primary water environment, materials: 600TT, degree of cold work: 0, 2, 5, 8, and 18%, temperature: 360 and 320°C; 2) faulted secondary water environments, materials: 600TT, 690TT and 600MACold work: 2% pH320°C: 3.5 / 5.5 / 8.5 / 10.5; temperature: 320°C; 3) crack growth rate in primary water was not affected by the cold work of 2%, but greatly enhanced above 5%. The effect of pH320°C in faulted secondary water was clearly observed, acidic pH of 3.5 and alkaline pH of 10.5 greatly enhanced IGSCC growth rate. These results will be discussed in this paper.

1:55 PM

Stress Corrosion Cracking of Nickel Alloys in the "Complex" Environment in the Liquid Phase and in the Vapor Phase: Ellen-Mary Pavageau¹; Olivier Horner¹; Francois Vaillant¹; Odile de Bouvier¹; Frederic Delabrouille¹; ¹Electricité de France

Secondary side corrosion cracking of Mill Annealed Alloy 600 steam generator tubes occurs in flow restricted areas where impurities get concentrated under heat flux. A typical environment, called the "complex" environment, was determined a few years ago as the laboratory environment best reproducing deposits, films and cracks observed on pulled tubes. It is an All Volatile Treatment environment containing alumina, silica, acetic acid and phosphates. The purpose of this paper is to present the stress corrosion tests that have been done since then in order to model secondary side corrosion cracking of steam generator tubes in this typical environment. The influence of temperature, chemical, mechanical and material factors on the initiation and propagation stages of stress corrosion cracking are examined. Moreover, results in the liquid phase and in the vapor phase are compared. Finally, the examination of surfaces and crack tips in both phases is presented.

2:20 PM

Effect of Water Chemistries on Stress Corrosion Resistance in Alloy 600 SG Tube under Acidic Conditions: Shinichi Fukuchi¹; Kimihiro Koba¹; Hiroyuki Anada²; Manabu Kanzaki²; ¹Kyushu Electric Power Co., Inc.; ²Sumitomo Metal Industries Ltd

Environment of crevices between Alloy 600 (75Ni-15Cr-9Fe) Steam Generator (SG) tubes and support sheets in secondary coolant side is assumed to be an acidic condition, due to the concentration of SO₄²⁻. Therefore, the influence of water chemistries in acidic conditions on Stress Corrosion Cracking (SCC) and general corrosion was systematically studied, in addition to the influence of applied stresses and heat treatments of Alloy 600. C-ring tests were conducted in sulfuric acid solution with sodium sulfate and magnetite at 325°C. The pH of the test solution, from closely neutral condition to acidic condition, was controlled by the concentration of sulfuric acid and sodium sulfate. For comparison of applied stresses, Two Legs Touched (TLT) specimen and notched specimen in which applied stress was calculated to be a yield stress were tested. Influence of heat treatment was studied by mill annealing (MA) and thermal treatment (TT). As a result of the C-ring tests, SCC crack apparently appeared below pH 3 (measured value at room temperature), which suggested a threshold of SCC susceptibility under the acidic condition. Crack depth in the notched specimen was longer than that in the TLT specimen. Crack depth was almost the same between MA-600 and TT-600. Therefore the SCC susceptibility under the acidic condition increased with increasing the applied stress. The heat treatments of Alloy 600 did not affect the susceptibility of SCC. General corrosion of Alloy 600 also increased below pH 3. Both applied stresses and heat treatments did not affect the general corrosion of Alloy 600. The SCC mechanism of Alloy 600 in acidic

condition was studied by electrochemical measurements and observation of corrosion products at the crack tip by Auger Electron Spectrometry (AES). In the electrochemical measurements on the Alloy 600 in the acidic solutions, the pH dependence of corrosion potential, anodic dissolution and passivation behavior were studied at 280°C. As the results of electrochemical measurement, Alloy 600 was passivated in the closely neutral solution, but in the acidic conditions the active dissolution accelerated with decreasing pH. Active dissolution was considered to be caused by dissolving nickel. AES was used to analyze the corrosion products at the crack tip with the beam diameter in sub micro-meters. C-ring test specimen was stretched in a direction perpendicular to a surface crack and torn apart in liquid nitrogen. Then the propagation front of SCC crack was decided as the boundary between intergranular fracture surface (IG surface), which came from SCC propagation, and transgranular fracture surface (TG surface), which was extrinsically produced by tearing in liquid nitrogen. Crack tip was verified by detecting little oxide at the area of TG surface close to the boundary between IG surface and TG surface. Depth profile of chemical composition was measured at the crack tip and the crack near the free surface. As results of AES examination, oxide film at the crack tip mainly consisted of nickel and chromium. At the crack near the free surface, chemical composition of oxide film was equal to that at the crack tip. The thickness of the film at the crack near the free surface was a little thicker than that at the crack tip. The AES examination revealed that a chromium-rich oxide film was formed on the crack tip and the crack near the free surface of the specimens, which was affected by the water chemistries. Based on these results, it is assumed that SCC susceptibility would be influenced by dissolving Nickel from the Alloy 600 matrix. The stability of the chromium-rich oxide film is important for understanding the effect of the various acidic conditions.

2:45 PM

SCC Behavior of Model Alloy 600 Containing Minor Element Ce in a Caustic Solution: *Joung Soo Kim*¹; *Yong-Sun Yi*¹; *Oh-Chul Kwon*¹; *Yunsoo Lim*¹; *Mahnkyo Jung*¹; ¹Korea Atomic Energy Research Institute

High purity model alloys with major composition Ni-15Cr-9Fe-0.03C (600CE0) and Ni-15Cr-9Fe-0.03C-0.04Ce (600CE4) were produced. Using these model alloys the effect of alloying element Ce on the SCC behavior of Alloy 600 was evaluated. To obtain carbides precipitated on grain boundaries, the thermal treatment (TT) was performed on both the solution annealed alloys. Microstructural examinations using SEM and TEM EDX showed that the same structural carbides, Cr₇C₃, were precipitated on both the alloys and no significant difference in the amount of Cr depletion along grain boundaries was observed between the two model alloys. However, it was found that the coverage of grain boundary carbides was higher in the Ce-bearing alloy (600CE4). The SCC susceptibility of the alloys was investigated in 40%NaOH solution at 315°C. Being evaluated in terms of maximum crack depth, the SCC susceptibility of the alloy turned out to be reduced by the addition of Ce. The increased resistance to the SCC in the alloy 600CE4 was considered to be attributable to the increased coverage of grain boundary carbides.

3:10 PM

A New Technique for Intergranular Crack Formation on Alloy 600 Steam Generator Tubing: *Tae-Hyun Lee*¹; *Il Soon Hwang*¹; *Han Sub Chung*²; *Jang Yul Park*³; ¹Seoul National University; ²Korea Electric Power Research Institute; ³Argonne National Laboratory

For the integrity management of SG tubes, non-destructive-evaluation performed using eddy-current-test (ECT) is necessary in the assessment. The reliability of ECT evaluation is dependent on accuracy of ECT on various kinds of defects. For basic calibration and qualification of these techniques, cracked SG tube specimens having mechanical and micro-structural characteristics of intergranular cracks in the field, were needed. To produce libraries of Laboratory-Degraded-SG-tubes (LDT) with intergranular cracks, a radial denting method was explored for generating ID and OD axial crack by three-dimensional finite-element-analysis and experimental demonstration. The technique is proven to be applicable for generating axial cracks with long and shallow geometry as opposed to semi-circular crack typically obtained by internal-pressurization method. In addition, DCPD method applied with array probes was developed for accurate monitoring and controlling of crack size and shape. By these methods, long and shallow intergranular axial cracks being more typical of actual degraded SG tubes were successfully produced.

3:35 PM Break

PWR Secondary - IV

Wednesday PM
August 17, 2005

Room: Ballroom II
Location: Cliff Lodge

Session Chairs: Allan R. McIlree, Electric Power Research Institute; Jesse B. Lumsden, Rockwell Automation

4:00 PM

Experimental Investigation of the Erosion-Corrosion of UNS N044000 Steam Generator Tubing: *Amy C. Lloyd*¹; *Sandra Pagan*²; *Gabriel Ogundele*; ¹Kinectrics Inc.; ²Ontario Power Generation

In power plant operation, tubing, piping and steam generator internals have experienced degradation due to flow-assisted corrosion (FAC). FAC or erosion-corrosion is frequently observed in regions of high fluid flow during plant operation. The occurrence of this mode of failure suggests that a critical combination of environmental and hydrodynamic conditions is required in order for this form of degradation to initiate and propagate. In steam generators at the Pickering B nuclear station, erosion corrosion degradation has been observed on the UNS N044000 tubing in the vicinity of tube support plate intersections. A novel test facility was designed and constructed to investigate the conditions (thermal hydraulic and chemistry) influencing the erosion corrosion degradation of UNS N044000. A Rotating Cylinder Electrode (RCE) assembly equipped with a high temperature autoclave that has been integrated with a re-circulating flow loop system. The test facility was constructed with the capability of high temperature, high pressure and variable fluid velocity conditions, coupled with electrochemical measurement instrumentation to provide *in-situ* corrosion monitoring and determination of the corrosion rate of the sample. Static and rotating samples of Ni-Cu Alloy UNS N044000 were exposed to different chemistries of varying hydrazine and oxygen concentrations to determine the rate of material loss under different test conditions. Tests were performed at a constant temperature of 256°C and three different levels of hydrazine, dissolved oxygen and rotational speeds. The corrosion rates were found to range from 5.28 $\mu\text{A}/\text{cm}^2$ to 10.32 $\mu\text{A}/\text{cm}^2$ (2.32 mpy to 4.53 mpy). Statistical analysis of the data indicated that hydrazine concentration and flow (rotation) rate are significant variables influencing the measured corrosion rates. An empirical model developed from the test matrix suggested the predicted corrosion rate increases as the hydrazine concentration increases.

4:25 PM

Assessment of Amine Specific Effects on the Flow Accelerated Corrosion Rate of Carbon and Low Alloy Steels: *John M. Jevic*¹; *Peter King*¹; *Cindy Pearce*²; *Keith Fruzzetti*³; ¹Babcock & Wilcox Company; ²Babcock & Wilcox Canada, Ltd; ³Electric Power Research Institute

Considerable plant and laboratory data on flow-accelerated corrosion (FAC) exists for temperatures below 225°C, but there is little relevant data for the higher temperatures experienced in steam generators. In addition, recent testing has suggested that the FAC rate may be a function of the specific amine used for pH control beyond that predicted based on the pH alone. This paper presents results from a series of tests on carbon and low alloy steels at temperatures above and below 225°C further investigating amine specific effects on the FAC rate. Limited data is also presented on the effects of hydrazine concentration on the FAC rate at 256°C.

4:50 PM

Oxidation Behavior of Austenitic Materials Exposed to Secondary Side Water at 282°C: *Jeff Sarver*¹; *Peter King*²; ¹Babcock & Wilcox; ²Babcock & Wilcox Canada, Ltd.

The stress corrosion cracking (SCC) susceptibility of Alloy 600 in secondary side environments has been well documented over many years. Compared to Alloy 600, Alloy 800 and Alloy 690 have, thus far, displayed a greatly reduced SCC susceptibility in these environments. The thin oxide that forms during steam generator operation provides the sole barrier between the environment and the material; thus, it is likely that the characteristics of this oxide play an important role in determining the SCC behavior of steam generator materials. To elucidate the differences in the oxidation behavior of steam generator materials, testing was performed on specimens prepared from Alloys 600, 690, 800 and 304L stainless steel. Materials were tested in the as-received condition, and after pre-oxidation in a partial vacuum and in air. The specimens were dimensioned and weighed, then exposed in secondary side water environments at 282°C for times up to 6,000 hours. Following the exposures, specimens were removed and re-weighed. The exposed specimens were then submitted for microanalytical evaluation to examine chemical and morphological differences between the oxides. The results of the microanalytical evaluations are presented in a separate paper. The results from this program indicate that the oxide growth (based on weight gain) on Alloys 600, 690 and 800 followed parabolic kinetics. Of these three materials, Alloy 600 experienced greater weight gain than Alloy 690 or Alloy

800. It was also observed that Alloy 690 in the mill annealed (MA) condition experienced greater weight gain than Alloy 690 in the thermally treated (TT) condition. The 304L stainless steel experienced little to no weight gain, suggesting that the oxide formed during the exposures was less stable or protective than the oxide that was formed on the other materials. The results from this program suggest that Alloys 600, 690, 800 and 304L stainless steel, when exposed to secondary side environmental conditions, exhibit different oxidation behavior. Detailed evaluation of the oxides formed on these materials may illuminate what characteristics of the oxides impact the SCC behavior of steam generator materials, and may provide important clues as to how oxides influence SCC initiation mechanisms.

5:15 PM

Characterization of Austenitic Materials Exposed to Secondary Side Water at 282°C: *Sridhar Ramamurthy*¹; Ross D. Davidson¹; N. Stewart McIntyre¹; Peter J. King²; Jeff M. Sarver³; ¹Surface Science Western; ²Babcock & Wilcox Canada, Ltd; ³Babcock & Wilcox Research Center

This paper presents the results from the surface analytical measurements performed on a number of Alloy 600, 690 and 800 and 304L stainless steel coupons exposed to secondary side water chemistry at 282°C. Some of these coupons were in the form of tube samples, while others were flat polished (1 mm surface finish) coupons that contained two 100 mm wide scratches. Some c-ring samples exposed to the secondary water chemistry were also examined in this study. Some of these samples were exposed in the as-received (mill annealed or thermally treated) condition, while others were subjected to a pre-oxidation treatment either in air or in partial vacuum. Detailed SEM/EDX, XPS, ToF-SIMS, Auger, and micro-XRD analyses were performed on these samples to determine the evolution of oxide film (morphology and composition) as a function of the autoclave exposure time. In general, prior oxidation tends to produce fine crystallites on the sample surface, which subsequently influences the extent of oxide growth during the autoclave exposure. In addition, on flat polished coupons, prior oxidation also results in the oxide growth on certain selected grains during the autoclave exposure. However, this selective oxidation tends to disappear in the presence of stress/strain, such as those found at the scratched regions. On the samples exposed in the as-received condition, wide variations in the oxide morphology and chemistry were observed between the scratched and non-scratched regions. Finally, the alloy composition appears to exhibit a significant influence on the oxide morphology and its composition during the autoclave exposure. The significance of these results and their relevance to the relative stress corrosion cracking behaviour of these materials will also be discussed in this paper.

5:40 PM

The Use of Advanced Secondary Ion Mass Spectrometry Imaging Technique for the Characterization of Materials Employed in Nuclear Applications: *Sridhar Ramamurthy*¹; Gary M. Good¹; N. Stewart McIntyre¹; Alex M. Brennenstuhl²; Gino Palumbo³; Peter Lin³; ¹Surface Science Western; ²Ontario Power Generation; ³Integran Technologies Inc.

Secondary ion spectrometry (SIMS) is being increasingly used for the characterization of materials employed for nuclear applications. The reasons for this are its large dynamic range, high sensitivity (ppm or less), and the ability to detect all elements from hydrogen to uranium and their isotopes. These can be achieved with minimal sample preparation. SIMS can be used in the static or dynamic modes. Recently, the combination of dynamic profiling and imaging capability have been combined to produce three dimensional images that are capable of providing information about bulk structures in a fraction of the time compared to some of the alternative techniques that are currently available. The technique relies on the generation of a plurality of two dimensional intensity distribution images through the thickness of the structure under investigation and the recombination of these images to produce a true three-dimensional image. This paper provides details of the three dimensional SIMS imaging technique and gives an example of its use in determining why intergranular corrosion attack (IGA) was observed in some Monel 400 steam generator (SG) tubes from pressurized heavy water reactors and not others that were exposed to the same operating chemistry. The application of SIMS in the characterization of the grain boundary chemistry of Alloy 600 steam generator tube material will also be discussed. Alloy 600 samples exhibiting varying degrees of grain boundary misorientation were examined using this technique to demonstrate the usefulness of this technique in identifying the extent and the nature of grain boundary segregation. The results from these measurements indicate that grain boundary segregation appears to be widespread and variable in those materials that had low special boundary fractions versus the sample that was prepared to maximize the special boundary fraction in which essentially no segregation was observed. The significance of these observations relating to the corrosion behaviour of these materials in service will be discussed.

Irradiation Effects - I

Thursday AM Room: Ballroom I
August 18, 2005 Location: Cliff Lodge

Session Chairs: Todd R. Allen, University of Wisconsin; Danny J. Edwards, Battelle

8:00 AM

Influence of Deformation Mode on Irradiation-Assisted Stress Corrosion Cracking of Proton-Irradiated Austenitic Alloys: Jeremy Todd Busby¹; Ryoji Obata¹; Gary S. Was¹; *Zhijie Jiao*¹; ¹University of Michigan

Localized deformation (induced by low stacking fault energy (SFE) and/or irradiation damage) may play a key role in IASCC susceptibility of stainless steels. Four model alloys (UHP-304, 304+Si, 304+Ni and Fe-22Cr-15Ni) having a spread in SFE were irradiated with 3.2-MeV protons at 360°C to 0.9 and 5.5 dpa and then incrementally strained in 288°C Ar atmosphere to 3%, 7% and 12%. After each strain level, channel height, width and spacing were quantified. After 1.0 dpa and 12% strain, the degree of localized deformation in the 0.9 dpa samples was considerably higher in the base-304 alloy than the high-Ni alloy, consistent with the cracking at 5.5 dpa where the 304 failed via IG cracking while the 304+Ni alloy was resistant to cracking. The degree of localized deformation (as a function of strain, dose, and alloy) is compared to the observed IGSCC behavior to understand the role of localized deformation in IGSCC.

8:25 AM

Deformation Structures in 316 Stainless Steel Irradiated in a PWR: *Koji Fukaya*¹; Katsuhiko Fujii¹; Yuji Kitsunai²; ¹Institute of Nuclear Safety System; ²Nippon Nuclear Fuel Development

Localized deformation in irradiated materials is known to be one of the key radiation-induced property changes for occurrence of irradiation assisted stress corrosion cracking (IASCC). However, details of deformation mode and dose-dependent change in heterogeneity are still unclear in stainless steels irradiated to high doses in light water reactors (LWRs). In the present study, we intended to clarify deformation characteristics in LWR-irradiated stainless steels. The material examined was a cold-worked 316 stainless steel used as thimble tubes in a commercial pressurized water reactor irradiated to 4-35 dpa at near 300°C. Tensile specimens were loaded to 60% of yield strength, 100% of yield strength and stained to several percents by 320°C slow strain rate tensile testing. Surface steps and microstructures were examined by scanning electron microscopy and transmission electron microscopy (TEM), respectively. Surface steps were detected locally near the edge of the specimens at 100% of yield strength. TEM observations revealed that twin deformation was the major mode in the present materials. In high-dose specimens, void formation was detected at the intersection of grain boundaries and twins at a strain of several percents. Influence of dose and relation between microstructure and deformation will be presented in the conference.

8:50 AM

Irradiation-Induced Microstructure, Swelling and Post-Irradiation Deformation of 18Cr-10Ni-Ti Irradiated with Ions to 1-100dpa at 300-635°C: Oleg V. Borodin¹; Victor V. Bryk¹; Alexander S. Kalchenko¹; A. A. Parkhomenko¹; Victor N. Voyevodin¹; *Frank Albert Garner*²; ¹Kharkov Institute of Physics and Technology; ²Pacific Northwest National Laboratory

Most of the austenitic steel comprising the internals in Russian VVERs or Western LWRs resides at temperatures in the range 280-400°C and can be subjected to 1-100 dpa over the reactor lifetime. Chromium ion (1 MeV) irradiation at 10-2 dpa/sec was used to simulate the radiation response of both annealed and 5% cold-worked 18Cr-10Ni-Ti (AISI 321 analog used in Russian reactors) over the temperature range 300-635°C to doses of 1-100 dpa. The range of higher than LWR-relevant temperatures was chosen to incorporate rate-dependent temperature shifts. Post-irradiation electron-microscopic and micro-electron diffraction investigations were carried out to determine temperature distribution and dose dependence of dislocation, void structure, phase distribution and composition. Post-irradiation deformation was performed to determine the microstructural modes of deformation, showing a transition from twinning to dislocation channeling as the test temperature increases. Trends of microstructure, void swelling and deformation vs. dose, dose rate and irradiation temperature are presented.

9:15 AM

Microstructural Study and In Situ Investigation of Strain Localization in Ions Irradiated Austenitic Stainless Steels: *Cédric Pokor*¹; Philippe Pareige²; Jean-Paul Massoud³; Philippe Dubuisson⁴; Yves Brechet⁵; ¹Electricité de France; ²Université de Rouen; ³Electricité de France-R&D-MMC; ⁴Commissariat à l'Énergie Atomique; ⁵Laboratory of Thermodynamics & Metallurgical Physico-Chemistry

The microstructure of two austenitic stainless steels (SA 304L and CW 316) irradiated by Ni ions at 350°C up to an irradiation dose of 10 dpa is investigated by Transmission Electron Microscopy and atom probe. This microstructure is compared to the one of steels irradiated with neutrons in experimental reactors and of steels coming from the internal structures of Pressurized Water Reactors. The behavior of the defects due to Ni ions irradiation (Frank loops) during in situ deformation at 350°C is investigated by TEM. The principal deformation mode of these steels appeared to be "dislocation channeling": under appliance of stress, the Frank loops are destabilized and annihilated by sweeping by dislocations, leading to the formation of defect free channel. This mechanism must play a role in the loss of ductility and in the modification of the work hardening behavior noticed after irradiation for these steels.

9:40 AM

Hydrogen Trapping in 18Cr10NiTi Steel under Conditions of Double or Triple Ion Irradiation: Victor V. Bryk¹; Victor N. Voyevodin¹; Galina D. Tolstolutskaia¹; *Frank A. Garner*²; ¹Kharkov Institute of Physics and Technology; ²Pacific Northwest National Laboratory

Evidence is accumulating to show that hydrogen can be stored in metals (nickel and stainless steels) when cavities are created by particle irradiation, with synergisms between helium and hydrogen in creating cavities and storing hydrogen. Self-ions were used to create displacement damage with co-implanted hydrogen, helium and/or neon. Deuterium was used instead of protium, allowing determination of its concentration and location via (He3,D)-(He4,p) reaction. Deuterium implanted to 3000-10,000 appm at R.T. was retained in X18H10T (AISI 321) steel to 300°C. The desorption maximum at T~100°C is related to deuterium release from traps with binding energy of 0.21eV (dislocations) and 0.36eV (vacancies). Irradiations at higher temperatures with helium, chromium and neon ions result in ~100% capture of the introduced deuterium, with subsequent retention in the specimen up to temperatures of 600-800°C. Comparison of various microstructural components shows that the most efficient traps for deuterium are gas (He, Ne) bubbles.

10:05 AM Break

Irradiation Effects - II

Thursday AM Room: Ballroom I
August 18, 2005 Location: Cliff Lodge

Session Chairs: Todd R. Allen, University of Wisconsin; Danny J. Edwards, Battelle

10:30 AM

Microstructural and Microchemical Evolution in Neutron-Irradiated Stainless Steels: Comparison of LWR and Fast-Reactor Irradiations: *Danny J. Edwards*¹; Stephen Bruemmer¹; Edward P. Simonen¹; ¹Battelle

A series of Bor-60 fast-reactor irradiations have been completed on commercial and laboratory heats of 304SS and 316SS irradiated at 330°C to doses from 5 to 20 dpa. Many of these heats were previously irradiated in a BWR at 275°C from ~1 to 13 dpa and extensively characterized. A quantitative comparison will be made to assess critical changes in material microstructure and microchemistry due to differences in fast reactor versus LWR irradiation environments. Comparisons will also be made between cold-worked 316SS baffle-bolt materials irradiated in Bor-60 to a similar 316SS baffle bolt removed from the PWR service. The evolution of Frank loops, precipitates and cavities will be documented and evaluated with respect to differences in irradiated spectrum, dose rate and temperature.

10:55 AM

Dose Rate Effects on Microchemistry and Microstructure Relevant to LWR Components: *Edward P. Simonen*¹; Danny J. Edwards²; Stephen M. Bruemmer²; ¹Battelle; ²Pacific Northwest National Laboratory

Radiation affects microchemistry and microstructure in austenitic stainless steels at remarkable low dose and low dose rate and at temperatures relevant to light-water reactor (LWR) conditions. Examination of LWR components reveals decrease in Cr and increase in Ni and Si concentrations at grain boundaries irradiated to doses as low as 0.07 displacements per atom (dpa) at 288°C. Loop microstructure does not appear at 0.07 dpa but is well established at doses less than 1 dpa. Damage rate effects are modeled and compared to measured loop evolution and irradiation strengthening at very low dose rates. At low dose rates, in situ annealing promotes recovery of the primary cascade damage that does not occur at high rates. This recovery affects the evolution of both microchemistry and microstructure. The potential influences on irradiation-assisted stress corrosion cracking are evaluated.

11:20 AM

Void Swelling of Austenitic Steels Irradiated with Neutrons at Low Temperatures and Very Low dpa Rates: *Frank A. Garner*¹; Sergey I. Porollo²; Yury V. Konobeev²; Oleg P. Maksimkin³; ¹Pacific Northwest National Laboratory; ²Institute of Physics and Power Engineering; ³Institute of Nuclear Physics

In the last decade the PWR community has become aware of the potential for void swelling in austenitic internal components. A number of recent studies have shown that swelling actually increases at a given dose and temperature as the dose rate decreases. Most importantly, the lower temperature limit of swelling appears to be on the order of 300°C, a temperature relevant to a large portion of most PWR internals. Several new studies are presented here that provide additional insight on void swelling, focusing on the Russian analogs of AISI 304 and 316 stainless steel that were irradiated in two different reactors. In the 316 analog voids were observed as low as 281°C and 1.3 dpa when irradiated in BN-350 at 3.9x10⁻⁹ dpa/sec. In the 304 analog swelling at 350°C of ~0.1% was observed at only 0.6 dpa when the irradiation proceeded in BR-10 at only 1.9x10⁻⁹ dpa/sec.

11:45 AM

Response of PWR Baffle-Former Bolt Loading to Swelling, Irradiation Creep and Bolt Replacement as Revealed Using Finite Element Modeling: *Edward P. Simonen*¹; Frank A. Garner¹; Nickolas Klymyshym¹; Mychailo Toloczko¹; ¹Pacific Northwest National Laboratory

Constitutive equations developed for swelling and irradiation creep of austenitic steels allow detailed calculation of stresses and strains in a PWR baffle bolt/plate assembly. The ABAQUS code was used to conduct a finite element analysis based on assumptions of irradiation response, including the calculated depth dependence of temperature, dose and dose rate. The von Mises stresses developed as a result of 10 to 40 years of exposure were then calculated. Several key results were obtained that can be related to postulated bolt cracking behavior. The stress developed at the bolt/plate interface influences the unbolting torque measured when bolts are removed. The imprint of the bolt force on the plate is calculated to be elastic. Therefore a permanent plastically-induced imprint should not be seen when a bolt is removed. The stress concentration is high at the corner of the bolt head and bolt shaft. In particular, a high stress location is immediately below the bolt head corner and is the same location at which irradiation-assisted stress corrosion cracks are observed. The calculated bolt tension with increasing irradiation exposure was calculated. Radiation-enhanced creep initially relaxes the bolt. Differential swelling between bolt and plate increase the bolt tension over the long term, however, eventually overwhelming the creep-induced relaxation. The engineering implication of these mechanistic calculations is that the bolts should remain in tension at high irradiation exposures whereas in the absence of swelling the bolt is effectively unloaded by 10 to 15 dpa. Replaced bolts operate at a higher average fraction of the original load, especially for replacement at higher exposures.

Nickel-Base Alloys – I

Thursday AM
August 18, 2005

Room: Ballroom II
Location: Cliff Lodge

Session Chairs: Ronald M. Horn, General Electric Co; Denise J. Paraventi, Bechtel Bettis, Inc

8:00 AM

Examination of Stress Corrosion Cracks in Alloy 182 Weld Metal after Exposure to PWR Primary Water: *Peter M. Scott*¹; Marc Foucault¹; Brigitte Brugier¹; John Hickling²; Al McIlree²; ¹Framatome ANP; ²Electric Power Research Institute

Metallurgical examinations were undertaken of a series of Primary Water Stress Corrosion Cracks (PWSCC) in Alloy 182 that were available from a prior capsule test program. The purpose of that prior program was to obtain information on the relation between stress/strain and time to failure. The objective of the detailed examinations reported here was to examine the relationship between crack initiation sites and the microstructure of the weld metal as well as identifying those microstructural features that facilitate or arrest PWSCC propagation. Optical and SEM-Energy Dispersive Spectroscopy (EDS) examinations of transverse sections of the failed capsules on a plane close to the main cracks were used to characterize the weld microstructures, to search for possible surface flaws related to crack initiation sites, and to identify the orientation of the crack path in relation to the weld microstructure. Electron Back Scattering Diffraction (EBSD) was used to determine the crystal orientations of the grains on both sides of the crack flanks (i.e. grain boundary misorientation) in order to identify the conditions necessary for crack initiation/propagation or crack arrest. Cracking occurred only in high angle, high energy grain boundaries and was apparently arrested at low energy boundaries.

8:25 AM

Development of Crack Growth Rate Disposition Curves for Primary Water Stress Corrosion Cracking (PWSCC) of Alloy 82, 182, and 132 Weldments: *Glenn A. White*¹; John Hickling²; Craig Harrington³; ¹Dominion Engineering, Inc.; ²Electric Power Research Institute; ³TXU Power

An international panel of primary water stress corrosion cracking (PWSCC) experts supported the EPRI Materials Reliability Program in its development of a new crack growth rate (CGR) equation for Alloy 82/182/132 weldments. After the key metallurgical aspects are reviewed, the data and methods used to develop the deterministic CGR equation for PWSCC of Alloy 82/182/132 weldments are described. The laboratory testing techniques that have been used to generate CGR data for these weld metals in simulated PWR primary water environments are presented. The data screening procedures and data reduction methodology used to derive separate CGR curves as a function of temperature and stress intensity factor for these weld metals, including consideration of the effects of dendrite orientation, are described. Comparisons are made with other laboratory data not used in derivation of the new CGR lines, with the limited available field data, and with other proposed CGR disposition curves.

8:50 AM

Stress Intensity and Temperature Dependence for Crack Growth Rate in Weld Metal Alloy 182 in Primary PWR Environment: *Kjell Norring*¹; Martin Konig¹; Jan Lagerstrom²; ¹Studsvik Nuclear; ²Ringhals

Nickel-base weld metals are commonly used in nuclear power plants, and IGSCC is in some cases a potential problem for these alloys. In an international perspective there is need for good crack growth rate (CGR) data for Alloy 182 in primary side PWR environments. Knowledge about crack growth rates is needed for estimating the remaining life of components, for safety analysis and to determine inspection intervals. This paper will present CGR for Alloy 182 in a simulated primary side PWR environment. The results presented will cover the influence of stress intensity factor (KI = 20–56 MPa√m) at 320°C and the influence of temperature (290–340°C) with a KI-value of 32 MPa√m. A plateau value for CGR was observed for KI-values above 28–30 MPa√m. For lower stress intensity values the CGR decreases with decreasing stress intensity. The temperature dependence is expressed in terms of an activation energy.

9:15 AM

The Effect of Cold Work and Dissolved Hydrogen in the Stress Corrosion Cracking of Alloy 82 and Alloy 182 Weld Metal: *Denise J. Paraventi*¹; William C. Moshier¹; ¹Bechtel Bettis, Inc

Alloy 182 and Alloy 82 V-groove welds were tested in a hydrogenated water environment using compact tension specimens to determine the stress corrosion cracking (SCC) growth rates of these materials. The Alloy 82 weld was also cold rolled to a 12% reduction in thickness to increase yield strength. Alloy 182 crack growth rates were found to be a factor of ~3 greater than the Alloy 82 welds. The SCC growth rates were found to depend on the yield strength/cold work, where SCC rates were higher in the cold worked welds than in the as-welded condition. The effect of orientation on crack growth was less than a factor of 2. SCC growth rates were also found to increase when the dissolved hydrogen concentration was decreased from 4 to 2 ppm at 338°C. Engagement-corrected SCC growth rates show that the stress dependence for growth in welds is similar to wrought alloys.

9:40 AM

Influence of a Cyclic Loading on the Initiation and Propagation of PWSCC in Weld Metal 182: *François Vaillant*¹; Jean-Marie Boursier¹; Thierry Couvant¹; Claude Amzallag¹; ¹Electricité de France

Since significant cracking was observed in welds of the primary circuit in some countries, questions arise about stress (strain) thresholds for initiation and PWSCC crack growth rates in weld metal 182. The stress threshold for initiation was determined at 350 MPa with constant load tests, and the strain threshold between 1 and 1.4% using interrupted SSRTs. In order to confirm the stress threshold, additional tests were performed in PWR environment at 360°C up to 14,000 hours on tensile specimens with initial SCC pre-cracks (10 μm) submitted to different constant loads and on smooth specimens submitted to a gentle cyclic loading at different s_{max}. Propagation tests provided “da/dt versus K” curves at 325°C and 360°C, which accounted for the influences of heat-treatment (as-welded/stress relieved), loading (cyclic trapezoidal/static) and orientation (TS/TL). The results were discussed with regard to available data and compared to results on alloy 600.

10:05 AM Break

Nickel-Base Alloys – II

Thursday AM Room: Ballroom II
August 18, 2005 Location: Cliff Lodge

Session Chairs: Ronald M. Horn, General Electric Co; Denise J. Paraventi, Bechtel Bettis, Inc

10:30 AM

Microstructural and Microchemical Characterization of Primary-Side Cracks in an Alloy 600 Nozzle Head Penetration and its Alloy 182 J-Weld from the Davis-Besse Reactor Vessel: *Larry E. Thomas*¹; Bradley R. Johnson¹; John Vetrano¹; Stephen Bruemmer¹; ¹Pacific Northwest National Laboratory

Recent characterizations of cracks in several alloy 182 weldments removed from PWR service will be reviewed and discussed. Comparisons will be made among crack and crack-tip structures to investigate the root cause of in-service failures. High-resolution analytical transmission electron microscopy has been used to examine nanometer-scale details of corrosion products, reaction interfaces and the local metallurgy at crack tips. Cracking occurred along high-angle grain boundaries and was accompanied by corrosion from high-temperature water. No evidence for weld-induced hot cracks was found, although strong macro-segregation of Mn, Cr and Nb was documented. Analyses of impurities in the crack oxides indicated that weld inclusions might have helped to promote stress-corrosion cracking in at least one of the weldments. Important differences identified between observed structures in primary-water, stress-corrosion cracks for alloy 182 weld metal and for alloy 600 base metal will be discussed.

10:55 AM

Alloy 182 Weld Structures and SCC Growth Behavior: *Martin M. Morra*¹; Michelle Othon¹; ¹General Electric Global Research

The variability in structures present in Ni-base alloy welds stems from many sources. On macro and microstructural levels these can include interdendritic segregation, dendrite orientation, crystallographic orientation, on-cooling phase precipitation, solidification pattern, and weld pool segregation structures. Along with structural variability are superimposed and sometimes correlated residual plastic strain fields, hot cracks, residual stresses, weld defects, and varying tensile properties and hardness. Weldment design can influence almost all these variables resulting in potentially greater scatter in SCC growth rates. As a result, crack growth rate tests performed on welds must be placed in context of the structure and property fields into which the crack is growing. In this study an alloy 182 weld joint made by shielded metal arc welding two alloy 600 plates together was mapped for plastic strain distributions using Electron Backscatter Diffraction (EBSD), macro elemental segregation using wavelength dispersive spectroscopy (WDS), dendrite orientation, microhardness, and phases present. A strong dependence of residual plastic strain profiles on the geometrical features of the weldment was found in both heat affected zones. In the weld metal itself the highest residual plastic strains were found in the weld root region. Longitudinal EBSD scans of the weld metal showed regions of low residual plastic strain. The measured residual plastic strain in the weld metal was found to range from 10 to 18%. Interdendritic elemental segregation was not found to be as significant as the macro elemental segregation found in the individual weld pools formed with each weld pass. The elements Mn, Nb, and Si were found to have the most significant variability within the weld pools. While microhardness measurements mapped the geometric features of the weld quite well they did not capture the subtleties in weld structure that residual plastic strain measurements by EBSD did. The first part of this study was designed to fully characterize the alloy 182 weld metal prior to testing it in a 23 laboratory international round robin on the measurement of SCC growth rates in simulated BWR and PWR environments. For round robin testing 0.5T CT specimens were extracted from the same weldment. All CT specimens were identically oriented within the weldment so that the crack paths would capture specifically defined and measured compositional and plastic strain fields within the weld metal. A report on the results from this laboratory's SCC growth rate testing under simulated BWR conditions, high purity water containing 2000 ppb O₂ at 288°C, is presented in the second half of this study. Mechanical test parameters followed the test protocol developed for the round robin.

11:20 AM

The Effect of Grain Orientation on the Cracking Behavior of Alloy 182 Weld in PWR Environment: *Bogdan Alexandreanu*¹; Omesh K. Chopra¹; William J. Shack¹; ¹Argonne National Laboratory

The objective of this work is to study the influence of grain orientation on the cracking behavior of Alloy 182 weldments. The study involved two laboratory-prepared welds, a double-J weld and a deep-groove-filled weld. The grain boundary character distributions and grain orientations were examined by Orientation Imaging Microscopy (OIM). The microstructures of the two weld alloys are similar, with high proportions of cracking-susceptible high angle boundaries (0.70).

In addition, the OIM maps show the presence of clusters of grains sharing similar orientations. It is hypothesized that a boundary with a weak Taylor factor mismatch, as would be the case of two neighboring grains sharing a similar orientation, would be less susceptible to fracture. By contrast, a strong mismatch in Taylor factor across a grain boundary suggests that a strain incompatibility would exist at that boundary, thus making it susceptible to fracture. In order to test the hypothesis, crack growth rate (CGR) tests on the two weld alloys were conducted on 1-T compact tension specimens exposing different alloy orientations in simulated PWR environment. Following CGR testing, OIM maps were obtained along the crack paths to help determine whether cracking occurred more readily along grain boundaries separating dissimilarly oriented grains.

11:45 AM

SCC Behavior in the Transition Region of an Alloy 182-SA 508 Cl.2 Dissimilar Weld Joint under Simulated BWR-NWC Conditions: *Qunjia Peng*¹; Tetsuo Shoji²; Stefan Ritter³; Hans-Peter Seifert³; ¹University of Michigan; ²Tohoku University; ³Paul Scherrer Institute

Alloy 182-Low Alloy Steel (LAS) dissimilar weld joints contain the transition region that has complex microstructure. Recent incidents of stress corrosion cracking (SCC) in the weld metal of bottom head penetration housing of Boiling Water Reactors (BWR) have drawn the attention to the SCC behavior in the transition region of Alloy 182-LAS dissimilar weld joints, and, in particular, to the issue whether an intergranular SCC crack propagating in the weld metal could easily penetrate through the fusion line into the underlying LAS. In this study, following a microstructural characterization of the transition region of an Alloy 182-SA 508 Cl.2 dissimilar weld joint, the SCC behavior in the transition region in a simulated BWR-Normal Water Chemistry (NWC) environment was investigated. The results showed that the microstructure had a sharp change across the fusion line, and that the SCC propagation tended to cease at the fusion line under near-constant loading conditions. Such a SCC behavior shows consistency with the well-known SCC behavior of LAS, and with the field experience where SCC is usually confined to the Alloy 182 weld metal.

Waste Materials and Mechanical Properties

Thursday PM Room: Ballroom I
August 18, 2005 Location: Cliff Lodge

Session Chairs: Peter L. Andresen, GE Global Research Center; Renate Kilian, Framatome ANP

1:30 PM

Dynamic Strain Aging of Nickel-Base Alloys and Nitrogen Alloyed Stainless Steels: *Hannu Eelis Hänninen*¹; Mykola Ivanchenko¹; Yuriy Yagodzinskyy¹; Vitaliy Nevdacha¹; Ulla Ehrnsten²; Pertti Aaltonen²; ¹Helsinki University of Technology; ²VTT Technical Research Centre of Finland

Dynamic strain aging (DSA) and jerky flow phenomena in the commercial Ni-base alloys Inconel 600 and 690 have been investigated. Tensile tests were performed in the strain rate range of 10^{-3} to 10^{-6} s⁻¹ at temperatures of 100 – 400°C. A remarkable difference in the DSA behaviour of Inconel 600 and Inconel 690 alloys was observed. Tensile properties of the studied alloys in the DSA temperature range, and type and characteristics of jerky flow were obtained and analysed. The maps for occurrence of serrated flow as a function of strain rate and temperature were produced for Inconel 600 and 690 alloys and the activation enthalpies of DSA appearance were obtained (1.6 eV). The enthalpies of DSA appearance were compared with enthalpies of carbon diffusion, which were estimated by means of internal friction measurements of the studied alloys. If the obtained results are compared to the DSA occurrence in commercial AISI 316 NG stainless steel, the beginning of DSA in Inconel 600 and 690 alloys is shifted to a lower temperature range. The mechanisms of the DSA based on interstitial atom interactions with dislocations in the studied alloys are discussed and the results are analysed based on the susceptibility of these alloys to EAC.

1:55 PM

Stiffing of Crevice Corrosion in Alloy 22: Venkataraman Pasupathi¹; Gerald M. Gordon²; Kevin G. Mon²; Ahmet Yilmaz³; Gregory E. Gdowski³; *Raul B. Rebak*³; ¹Bechtel BSC; ²BSC/Framatome; ³Lawrence Livermore National Laboratory

Artificially creviced Alloy 22 (N06022) may be susceptible to crevice corrosion in presence of high chloride aqueous solution when high temperatures and high anodic potentials are applied. The presence of oxyanions in the electrolyte, especially nitrate, inhibits the nucleation and growth of crevice corrosion. Both potentiostatic and cyclic potentiodynamic tests were used to determine crevice corrosion initiation and growth. Results show that the occurrence of crevice corrosion can be divided into three characteristic periods: (1) nucleation, (2) growth and (3) stifling and arrest. That is, after a certain nucleation period, the crevice corrosion attack may initiate and progress until a critical stage is reached above which the crevice corrosion grow rate is reversed and the testing specimens regain the passive dissolution behavior. Effects of applied potential, temperature and composition of electrolyte were studied.

2:20 PM

Materials Degradation Issues in the U.S. High-Level Nuclear Waste Repository: *Kevin Mon*¹; Fred H. Hua²; ¹Framatome ANP; ²Bechtel SAIC Company, LLC

The safe disposal of radioactive waste requires that the waste be isolated from the environment until radioactive decay has reduced its toxicity to innocuous levels for plants, animals, and humans. All of the countries currently studying the options for disposing of high-level nuclear waste (HLW) have selected deep geologic formations to be the primary barrier for accomplishing this isolation. In U.S.A., the Nuclear Waste Policy Act of 1982 (as amended in 1987) designated Yucca Mountain in Nevada as the potential site to be characterized for high-level nuclear waste (HLW) disposal. Long-term containment of waste and subsequent slow release of radionuclides into the geosphere will rely on a system of natural and engineered barriers including a robust waste containment design. The waste package design consists of a highly corrosion resistant Ni-based Alloy 22 (N06022) cylindrical barrier surrounding a Type 316 stainless steel inner structural vessel. The waste package is covered by a mailbox-shaped drip shield composed predominantly of Ti Grade 7 (R52400) with Ti Grade 24 (R56405) structural support members. The U.S. Yucca Mountain Project has been studying and modeling the degradation issues of the relevant materials for some 20 years. This paper reviews the state-of-the-art in the past 20 years studies on Yucca Mountain Project (YMP) materials degradation issues with focus on interaction between the in-drift environmental conditions and long-term materials degradation of waste packages and drip shields within the repository system during the 10,000 years regulatory period. This paper provides an overview of the current understanding of the likely degradation behavior of the waste package and drip shield in the repository after the permanent closure of the facility. The degradation scenario discussed in this paper include aging and phase instability, dry oxidation, general and localized corrosion, stress corrosion crack-

ing and hydrogen induced cracking of Alloy 22 and titanium alloys. The effects of microbial activities and radiation on the degradation of Alloy 22 and titanium alloys are also discussed. Further, for titanium alloys, the effects of fluorides, bromides, calcium ions, and galvanic coupling to less noble metals are further considered. It is concluded that, as far as materials degradation is concerned, the materials and design adopted in the U.S. Yucca Mountain Project will provide sufficient safety margins within the regulated 10,000 year period.

2:45 PM

SCC Initiation and Growth in Alloy 22 and Titanium Alloys Concentrated Groundwater: *Peter L. Andresen*¹; Gerald M. Gordon²; ¹GE Global Research Center; ²Areva

The stress corrosion crack initiation and growth rate response was evaluated on as-received, cold worked and aged Alloy 22 (UNS N06022) and titanium Grade 7 in 105–200°C, aerated, concentrated, high pH groundwater environments. Time-to-failure experiments on actively-loaded tensile specimens evaluated the effects of applied stress, welding, surface finish, shot peening, cold work, crevicing, and aging treatments in Alloy 22 (UNS N06022). Titanium Grade 7 and stainless steels were also included in the matrix. Long term crack growth rate data showed stable crack growth in titanium Grade 7. Alloy 22 exhibited stable growth rates under “gentle” cyclic loading, but was prone to crack arrest at fully static loading. No effect of Pb additions was observed.

Nickel-Base Alloys – III

Thursday PM Room: Ballroom II
August 18, 2005 Location: Cliff Lodge

Session Chairs: William J. Mills, Bechtel Bettis Inc; Glenn A. White, Dominion Engineering, Inc

1:30 PM

Effects of Defect Acuity and Load Path on the Fracture Toughness of Alloy 82H and 52 Welds in Low Temperature Water: *Catherine M. Brown*¹; *William J. Mills*¹; ¹Bechtel Bettis Inc

Nickel-base welds experience a severe reduction in fracture resistance in low temperature (<150°C) water due to a hydrogen-induced intergranular cracking mechanism. In this study, fracture toughness testing of Alloy 82H and 52 welds was performed in 54°C hydrogenated water to characterize the effects of defect acuity and load path on the low temperature crack propagation (LTCP) behavior. Defect acuity effects were evaluated by conducting J_{IC} tests on weld specimens with either as-machined notches or natural weld defects and comparing the fracture response with that obtained using fatigue precracked specimens. Intergranular LTCP did not initiate from an as-machined notch; however, once a ductile tear initiated at a notch, it served as a sharp crack from which LTCP initiated. Rapid intergranular cracking was found to initiate from sharp weld defects, although the fracture resistance for specimens with weld defects was somewhat greater than that for fatigue precracked specimens. Load path effects were studied by performing constant-load tests at 54°C and cooldown tests from 288°C to 54°C under constant-displacement conditions. LTCP occurred under constant-load conditions, but only at K levels well above K_{JIC} from fracture toughness tests in water. During cooldowns under constant-displacement conditions, two Alloy 82H welds resisted LTCP at K levels well above K_{JIC} , but a third weld exhibited rapid cracking at K levels comparable to K_{JIC} . These findings demonstrate that although the resistance to LTCP tends to be enhanced under constant-load and constant-displacement conditions, the possibility of LTCP during cooldown under constant-displacement conditions cannot be ruled out.

1:55 PM

Reduction of Toughness Results for Weld Metal 182 in a PWR Primary Water Environment with Varying Dissolved Hydrogen, Lithium Hydroxide and Boric Acid Concentrations: *Bruce A. Young*¹; Allan R. McIlree²; Peter J. King³; ¹Babcock & Wilcox Company; ²Electric Power Research Institute; ³Babcock & Wilcox Canada

Primary Water Stress Corrosion Cracking (PWSCC) of Alloy 600, and its weld metals 182 and 82, has recently been experienced in Control Rod Drive Mechanisms (CRDMs) at Oconee units and in reactor vessel (RV) hot leg nozzles at V.C. Summer station. Recent publications by Bettis Laboratory has shown Alloy 600 and weld metal 82, as well as higher chrome weld metal 52 and high chrome base metal Alloy 690, has shown susceptibility to a reduction in toughness due to a hydrogen cracking mechanism at relatively low temperatures between 50°C and 100°C. Although the above failures have not lead investigators to the conclusion of the low temperature hydrogen cracking (LTHC) mechanism directly, the understanding of how to recognize the difference between high temperature PWSCC and low temperature hydrogen cracking (LTHC) due to toughness loss has not been developed. Since Bettis Laboratory has shown the LTHC phenomenon for Alloy 600 and weld metal 82, it was believed weld metal 182

THURSDAY PM

was also susceptible to this method of cracking. The work described in this paper focused on reproducing the Bettis results for weld metal 82 and addressed the lack of data for weld metal 182. The tests focused on a test temperature of 54°C in varying concentrations of dissolved hydrogen, lithium hydroxide and boric acid concentrations. The conclusions to date have shown in high hydrogen water (100 to 150 cc H₂/kg H₂O) both weld metal 82 and weld metal 182 exhibit and order of magnitude reduction in toughness in comparison to the air data at the same temperature. As dissolved hydrogen concentrations are reduced, the toughness recovers to some degree, but not fully. Fracture surfaces were examined after testing with an SEM. These surfaces have revealed predominantly intergranular failure along the dendrites under high strain with some evidence of ductility in the surrounding matrix.

2:20 PM

Low Temperature Crack Propagation in PWR Service?: *Allan R. McIlree¹; Anne Demma¹; ¹Electric Power Research Institute*

Low Temperature Crack Propagation (LTCP) is a form of hydrogen embrittlement which has yet to be definitively identified in PWR service, but which has been demonstrated in laboratory tests to cause severe degradation of the fracture resistance of certain nickel-base alloys. Currently available laboratory test data were reviewed to assess whether or not LTCP of nickel-alloy components is possible under PWR primary system service conditions. LTCP is not considered an important degradation mechanism for Alloys 600 and 690. However, Alloys X-750, 182/82, and 152/52 all suffer substantial degradation of fracture toughness and tearing resistance in laboratory tests in hydrogenated water. LTCP only occurs at temperatures below 150°C and should not be an issue either during normal power operation or during those stages of plant cool-down and start-up when the temperature of the primary coolant is above 150°C. LTCP is very unlikely to occur during either the stages of plant shut-down when the system is depressurized and after the hydrogen peroxide is added or those stages of plant start-up when the temperature is below 150°C, because the primary coolant is not hydrogenated during these periods and the calculated local hydrogen concentrations resulting from residual hydrogen in the material are a factor of 10 or more below the concentration required for LTCP. Although most of the conditions required for LTCP are (or, potentially, could be) satisfied during the stages of cool-down when the coolant is hydrogenated and the temperature is below 150°C, additional stress analyses are required to determine whether or not the mechanical requirements for LTCP identified in the laboratory tests are likely to be met in any nickel-alloy components. Stress analyses of specific components in relevant shutdown conditions will be presented. Additional laboratory tests and plant impact assessments should be considered to determine whether stopping hydrogenation of the primary coolant at an earlier stage of plant cool-down would be an effective and acceptable countermeasure to LTCP in nickel alloy primary system components in PWRs.

2:45 PM

Establishment of Experimental Conditions for the SCC Growth Rate Test of Alloy 600 and Ni Base Weld Metal in High Temperature Oxygenated Water: *Masayoshi Ozawa¹; Yutaka Yamamoto¹; Kiyotomo Nakata¹; Michiyoshi Yamamoto²; Zenmi Sagawa³; Jiro Kuniya²; Mikiro Itow⁴; Masaaki Kikuchi⁵; Norihiko Tanaka⁴; ¹Japan Nuclear Energy Safety Organization; ²Hitachi, Ltd.; ³Hitachi Engineering Company; ⁴Toshiba Corporation*

Experimental conditions for conducting long term SCC growth test of Alloy 600 and Ni base weld metal in high temperature oxygenated water have been studied. The following items were discussed in this report. (1) Effect of test interruption: In case of long term SCC growth test, the test can not help interrupting due to regular inspection for autoclave and so on, effect of test interruption on the SCC growth rate was evaluated. (2) Correction of PDM value: In case of Ni base weld metal, SCC length obtained from PDM measurement is generally shorter than actual SCC length because of its irregularity. Correction method of PDM value was defined here. (3) Evaluation of secondary cracks: In some cases, secondary cracks were observed in Alloy 600 heat affected CT specimens. Effect of secondary crack growth on primary SCC growth rate was evaluated using FEM analysis. (4) Activation condition for re-starting of arrested SCC: When SCC growth is arrested during long term test, some activation for re-starting arrested SCC will be needed. Periodical unloading method is used in this study and the conditions were evaluated. (5) Inter-dendritic crack introduction condition in high temperature water: In order to shorten incubation period for which inter-dendritic SCC growth starts from pre-crack tip, pre-crack introduction conditions in high temperature water was examined. (6) Detection limit of PDM method: PDM value shows some scattering so that detection limit of PDM value was evaluated based on the PDM value distribution.

3:10 PM Break

Nickel-Base Alloys – IV

Thursday PM
August 18, 2005

Room: Ballroom II
Location: Cliff Lodge

Session Chairs: William J. Mills, Bechtel Bettis Inc; Glenn A. White, Dominion Engineering, Inc

4:00 PM

Evaluation of SCC Crack Growth Rate in Alloy 600 and Its Weld Metals in Simulated BWR Environments: *Masayoshi Ozawa¹; Yutaka Yamamoto¹; Kiyotomo Nakata¹; ¹Japan Nuclear Energy Safety Organization*

SCC growth rates of nickel base alloys are important values to evaluate the integrity of pressure boundary components in nuclear power plants. In Japan, JNES is promoting a project, "Evaluation Technology for Stress Corrosion Crack Growth of Ni Base Alloys" (NiSCC, 2000-2005), to design "Crack growth rate (CGR) vs stress intensity factor (K)" curves in nickel base alloys that construct nozzles, core internals, etc. in BWR and PWR. The disposition curves require high quality CGR data in order to provide the evaluation of integrity of the components that can be used efficiently and with high confidence. However, the CGRs of nickel base alloys are variable, therefore the SCC growth rate decided carefully in the NiSCC project. In this paper, the CGRs in BWR environment of the NiSCC project were discussed on K value and environment (ECP) in SMAW weld metals, GTAW weld metal, and HAZ of alloy 600. The SCC growth tests were carried out for each alloys, Alloy 182, D-NiCrFe-1J, alloy 82 and alloy 600 (HAZ). Alloy 600 plates were welded under a constrained condition by shielded metal arc welding (SMAW) with alloy 182 and D-NiCrFe-1J(JIS) electrodes, and gas tungsten arc welding (GTAW) with alloy 82 filler metal. Chemical compositions of materials, welding conditions and post weld heat-treatments (PWHT) were chosen based on the fabrication condition of plants. The specimens of ITCT with side grooves were machined from the weld joints. Prior to tests in high temperature water, fatigue pre-cracks were induced at room temperature in air. The pre-crack in weld metals was parallel to the dendrite direction, and it in HAZ was along to fusion line. The tests were conducted in an autoclave equipped with a re-circulating loop at 288°C and approximately 8.8 MPa. Inlet and outlet water conductivity were controlled to less than 0.1uS/cm and 0.2uS/cm respectively. The crack length was monitored by means of the reversing DC Potential Drop Method (PDM). Environmental conditions of the test were represented by ECP, 150 to 200 mVSHE (NWC), -100 to 0 mVSHE (HWC(1)) and -300 mVSHE (HWC(2)). The inter-dendritic (ID) pre-crack by a gentle cycle loading was induced in the NWC before SCC growth test under a constant load. The tests were continued for up to about 6000 hours, at stress intensity factors, K, from 15 to 50 MPa-m^{0.5}. The SCC growth rate (CGR) was evaluated by the results of PDM that was revised by fracture surface measurement. The CGRs in alloy 182 in NWC were almost the same as the CGR in HWC (1). The CGRs in HWC(1) and HWC(2) depend on K value. The CGRs at k of 15 to 40 MPa-m^{0.5} in HWC(1) were about ten times larger than those in HWC(2). The CGRs in alloy 182 in NWC were almost the same as the CGR in HWC (1). The CGRs in D-NiCrFe-1J showed the same trend in dependence on the test condition in alloy 182. However, the values of CGRs in D-NiCrFe-1J were slightly larger than as those in alloy 182. The CGRs in alloy 82 showed approximately 1/10 of the CGRs in alloy 182. The CGRs in HAZ of alloy 600 in NWC were almost the same as the CGR in HWC (1). The CGRs in HWC(1) and HWC(2) showed the small dependence on K. The CGRs at k of 20 to 40 MPa-m^{0.5} in HWC(1) were about fifty times as those in HWC(2). The CGRs in the HAZ at K of about 40 MPa-m^{0.5} in NWC and HWC(1) were almost the same as those in alloy 182. However, the CGRs in the HAZ at K of 30 MPa-m^{0.5} and under were larger than those in alloy 182. In case of HWC(2), the CGRs in the HAZ at K of 20 to 40 MPa-m^{0.5} were almost the same as those in alloy 182. The CGRs in this study were compared with SKIF curves in alloy 182 and Morin's curves in Alloy 182 and 600. The CGRs in alloy 182 showed approximately 1/5 of the SKIF curves. The CGRs of K of 40 to 50 MPa-m^{0.5} in NWC and HWC(1) were smaller than the Morin's curves. However, the CGRs of K of 15 to 20 MPa-m^{0.5} in HWC(1) were slightly large as the Morin's curves. In case of HAZ of alloy 600, the CGRs showed 2 to 4 times as the Morin's curves. It was found that the SKIF curves were over conservative and the Morin's curves had some risks. This study is supported by the Ministry of Economy, Trade and Industry.

4:25 PM

Evaluation of Mechanical and Environmental Parameters Affecting Primary Water Stress Corrosion Cracking of Nickel-Based Alloys: *Junhyun Kwon¹; Yong-Sun Yi¹; Seolhwan Eom¹; Yun Soo Lim¹; Joung-Soo Kim¹; ¹Korea Atomic Energy Research Institute*

Primary water stress corrosion cracking (PWSCC) is one of the main degradation processes of nickel-based alloys in the pressurized water reactor environments. This paper evaluates the quantitative influences of mechanical and envi-

ronmental factors on the SCC crack growth rate (CGR) of nickel-based alloys in the high temperature water environments. The exact mechanism of the phenomenon is still debatable and no theoretical description of the CGR estimation is available. In this study, the theoretical equation which takes the crack-tip strain distribution for the growing cracks into account was applied in estimating the CGR. The theoretical equation was developed on the basis of the slip/dissolution model. In order to complement the theoretical calculations, SCC tests were performed to obtain the CGR of Alloy 182 in high temperature water. We investigate the significance of each factor on SCC rate through the numerical calculations. It is shown that mechanical properties of material, as well as the environmental factors related to current-density curve, are of importance to determine the CGR. The increase in the yield strength and the decrease in the repassivation rate enhance the CGR.

4:50 PM

Fracture Surface Morphology of Stress Corrosion Cracks in Nickel-Base Welds: *William J. Mills*¹; ¹Bechtel Bettis Inc

The stress corrosion cracking behavior of Alloy 82H welds was characterized in 316°C to 360°C water. Tests were conducted under constant-load conditions, with periodic unload-reload cycles every 10 or 100 minutes and with a small-amplitude flutter cycle. Crack growth rates (CGRs) exhibited an Arrhenius relationship with an activation energy of 33 kcal/mol and a power-law stress dependency with a K_I exponent of 1.8. Periodic unload-reload cycles every 100 minutes did not significantly affect CGRs, whereas unload-reload cycles every 10 minutes caused a small to modest acceleration in CGRs. In this study, the fracture surface morphology and microstructural aspects of cracking were studied. Specimens tested under constant load, with a 100-minute unload-reload cycle, and with a flutter cycle exhibited very similar fracture surface morphologies where cracking was predominantly intergranular and very uneven. The degree of unevenness ($\Delta a_{MAX} - \Delta a_{AVE}$) increases with increasing crack extension and then remains constant for crack extensions greater than 1 mm. Uneven cracking is caused primarily by the heterogeneous nature of welds. Specifically, the most susceptible grain boundaries readily separate producing SCC fingers ahead of a crack, while the most resistant boundaries do not separate thereby causing unbroken ligaments behind an advancing crack front. A 10-minute unload-reload cycle produces uniform crack extension and comparable amounts of intergranular and transgranular cracking. While intergranular cracking occurs first along the most susceptible grain boundaries, ligaments between the intergranular segments fail by local separation along persistent slip bands. Even though 10-minute unload-reload cycles cause only a small to modest acceleration in CGRs, they should not be used to estimate SCC performance because the cracking mechanisms are different.

Index

A

Aaltonen, P	20, 29
Aizawa, M	17
Alexandreaanu, B	19, 28
Allen, T R	15, 26
Ampornrat, P	15
Amzallag, C	13, 27
Anada, H	23
Andresen, P L	9, 10, 17, 18, 23, 29
Andrieu, E	7
Arioka, K	13
Armson, I	9
Attanasio, S	10
Atzmon, M	14

B

Bagli, K	16
Bahn, C	10, 15
Ballinger, R G	20
Bamford, W	10
Baum, A	21
Bennett, P	16, 22
Borodin, O V	26
Boursier, J	11, 13, 27
Boyers, G	23
Brabec, P	22
Brechet, Y	26
Brennenstuhl, A M	25
Brown, C M	29
Bruemmer, S	19, 21, 23, 26, 28
Brugier, B	27
Bryk, V V	26
Busby, J T	19, 22, 26

C

Cai, Z	13
Carcea, A	21
Carpenter, C E	12, 16
Castano, M	19
Cattant, F	16
Chatani, K	22
Chen, Y	14, 15
Chiba, G	13
Choi, H	10
Chopra, O	12, 19, 28
Chu, K	15
Chung, H	24
Cintas, J	9
Combrade, P	7
Comstock, R	13, 14
Conermann, J	19
Couvant, T	11, 13, 27
Cullen, W	12

D

Daret, J	8
Davidson, R D	25
de Bouvier, O	23
De Lair, R	13
Deconinck, J	9
Delabrouille, F	7, 23
Demma, A	30
Devine, T M	7
Devrient, B	12
Diaz, T P	17

Dozaki, K	20
Dubuisson, P	22, 26
Dymarski, M	16

E

Eaker, R	21
Eason, E D	9
Edwards, D J	26
Efsing, P	7, 16
Ehrnstén, U	12, 20, 29
Eom, S	30
Ernestová, M	12
Esselman, T	20
Evans, K	21

F

Fairbrother, H	11
Faulkner, R	9
Föhl, J	12
Forssgren, B	16
Foucault, M	7, 27
Fruzzetti, K	24
Fujii, K	26
Fujimoto, K	19
Fukuchi, S	23
Fukuya, K	26
Fyfitch, S	16

G

Garner, F A	26, 27
Gartner, E	14
Garud, Y	23
Gavillet, D	19
Gavrilov, S	9
Gdowski, G E	29
Gendron, T S	13
Gold, R	8
Gold, R E	10
Gómez-Briceño, D	12
Good, G M	25
Gordon, G M	29
Gorman, J A	20, 21
Guerre, C	10
Gupta, G	14
Guzonas, D	14, 15

H

Hackett, M J	19
Hall, J F	10
Hänninen, H E	29
Harrington, C	27
Heaslip, K	15
Herms, E	11
Hettiarachchi, S	6, 17
Hickling, J	10, 13, 27
Hoffmann, H	16
Høgberg, N W	22
Hong, J	12
Horn, R M	23, 27, 28
Horner, O	23
Hua, F H	29
Hwang, I	10, 13, 24
Hwang, S	12
Hyres, J W	16

I

Ichikawa, N	17
Ilg, U	13, 16
Inada, F	14
Ishida, K	17

Ishiyama, N	6
Itatani, M	7
Itow, M	7, 30
Ivanchenko, M	29

J

Jacko, R	8, 10
Jansson, C	12, 16, 22
Jenssen, A	7, 9, 22
Jeong, Y H	13, 14
Jeremy, B	14
Jevec, J M	24
Jiao, Z	14, 26
Jung, M	24
Jung, Y	14

K

Kaji, Y	20
Kalchenko, A S	26
Kanbe, H	14
Kaneda, J	14, 15
Kano, F	15
Kanzaki, M	23
Karlsen, T	22
Karlsen, W	20
Kasahara, S	15
Katayama, Y	6, 9
Kato, T	22
Kawamata, K	20
Kawamura, H	14
Kenik, E A	19
Kikuchi, M	7, 30
Kilian, R	16, 29, 30
Kim, D	12
Kim, H	9, 12, 14
Kim, H G	13
Kim, J	10, 24, 30
Kim, W	14
Kim, Y J	17
Kimura, A	6
King, P	12, 24, 25, 29
Kitsunai, Y	22, 26
Klymyshym, N	27
Koba, K	23
Kodama, M	22
Konig, M	27
Konobeev, Y V	27
Kuester, K	16
Kuniya, J	15, 30
Kwon, J	30
Kwon, O	24

L

Lagerstrom, J	27
Lai, B	13
Lapeña, J	12
Lee, B	12
Lee, H	14
Lee, T	24
Legras, L	7
Lewis, N	8
Lieder, R	20
Lim, Y	24, 30
Lin, P	25
Liu, C	17
Lloyd, A C	24
Lu, Y	21
Lumsden, J B	21, 23, 24

M			
Macdonald, D D	9, 14	Pavageau, E	23
Mager, T R	19	Pearce, C	24
Maksimkin, O P	27	Peng, Q	28
Marcus, P	7	Platts, N	11
Massoud, J	19, 20, 22, 26	Pokor, C	26
Matsui, Y	20	Pollick, M	18
Mayuzumi, M	6	Porollo, S I	27
McBrine, W	20	Prabhu, P	20
McGrath, M	16	Prokhorov, V	22
McIlree, A	16, 20, 21, 23, 24, 27, 29, 30	R	
McIntyre, N	25	Radhakrishnan, H	21
McKrell, T	20	Ramamurthy, S	25
McRae, G	15	Raquet, O	10, 11
Miller, M K	12	Rebak, R B	29
Mills, W J	29, 30, 31	Richey, E	8, 10
Mintz, T S	7	Rigby, K	11
Miwa, Y	19	Ritter, S	12, 28
Mizutani, Y	6	Roth, A	12, 13, 19
Mon, K	29	Rouillon, Y	13
Montes, M	9	S	
Moreton, P	9	Sagawa, Z	30
Morita, R	14	Saito, N	15
Moriya, K	15	Saito, Y	6, 22
Morra, M M	9, 10, 18, 23, 28	Sakaguchi, K	6
Morton, D	7, 8, 10	Sakamoto, H	22
Moshier, W C	27	Sarver, J	24, 25
Motta, A T	13, 14	Sato, M	23
Mullen, J	8	Satoh, T	6
N		Satoh, Y	6
Nagata, N	20	Scenini, F	7
Nakamura, T	22	Schurman, M	8
Nakano, J	20	Scott, P	7, 10, 27
Nakano, M	19	Seifert, H	12, 28
Nakata, K	10, 23, 30	Shack, W J	12, 19, 28
Namduri, H	20	Shamardin, V	22
Nanstad, R K	12	Shibayama, T	15
Nasrazadani, S	20	Shioiri, A	15
Natesan, K	12	Shogan, R	19
Nelson, L	6	Shoji, T	6, 9, 22, 28
Nevdacha, V	29	Silva, M	14
Newman, R	7, 21	Simonen, E P	22, 26, 27
Noda, T	6	Slade, J P	13
Norring, K	27	Sokolov, M A	12
Nowak, E	13, 16	Solomon, H D	13
O		Sridharan, K	15
Obata, R	26	Stachle, R W	21
Ogundele, G	24	Stairmand, J	11
Ohkubo, H	6	Stevens, J	20
Ohms, C	19	Stoenescu, R	19
Okabe, T	23	Stone, M	15
Okamura, M	17	Sundberg, J	7, 22
Okuda, J	10	Suzuki, J	17
Ooki, S	22	Suzuki, S	17, 22
Osato, T	17	T	
Othon, M	28	Tachibana, M	17
Ozawa, M	10, 23, 30	Takahashi, H	15
P		Takamori, K	6, 17, 22
Pagan, S	24	Takeda, Y	6
Palumbo, G	25	Takiguchi, H	20
Paraventi, D J	27, 28	Tan, L	15
Pareige, P	26	Tanaka, N	7, 30
Park, J	12, 24	Tanaka, S	22
Park, J Y	13, 14	Tanaka, Y	22
Parkhomenko, A A	26	Tani, J	6
Pasupathi, V	29	Terachi, T	13
Pathania, R	9	Teyseyre, S	14
		Theimer, R	20
		Thomas, L E	21, 23, 28
		Thompson, R H	20
		Tice, D R	11
		Toivonen, A	20
		Toloczko, M	27
		Tolstolutsкая, G D	26
		Toyoda, M	10
		Tsai, C	17
		Tsubota, M	6, 9
		Tsukada, T	19, 20
		Tsuruta, T	23
		Turluer, G	10
U		U	
		Uchida, S	6
		Ugachi, H	20
		Urquidi-Macdonald, M	9
		Usui, N	6
V		V	
		Vaia, A R	20
		Vaillant, F	7, 11, 13, 20, 21, 23, 27
		Vallee, A J	13
		van der Schaaf, B	19
		Van Dyck, S	19
		Vankeerberghen, M	9
		Vetrano, J	28
		Viguier, B	7
		Voyevodin, V N	26
W		W	
		Wachi, E	19
		Wada, Y	6, 17
		Wang, S	6
		Was, G S	13, 14, 15, 19, 22, 26
		Weißberg, T	12
		Wesseling, U	13, 16
		White, G A	27, 29
		White, R	20
		Widera, M	13, 16
		Wilkening, W	8
		Wills, J	15
		Woodman, B	23
		Wuthrich, J	8
X		X	
		Xu, H	16
Y		Y	
		Yagodzinskyy, Y	29
		Yamada, T	13
		Yamaguchi, Y	19
		Yamamoto, M	30
		Yamamoto, Y	10, 23, 30
		Yeh, T	17
		Yeon, J	14
		Yi, Y	24, 30
		Yilmaz, A	29
		Yilmazbayhan, A	13
		Yin, Y	9
		Yonezawa, T	7, 8, 19
		Yoshimoto, K	10
		Yotsuyanagi, T	17
		Young, B A	29
		Young, G	8, 10
		Yun, M	14
Z		Z	
		Zamboch, M	12, 22
		Zimmer, R	13

CONFERENCE AT A GLANCE

12th International Conference on Environmental Degradation of Materials in Nuclear Power Systems-Water Reactors

	Sunday August 14, 2005	Monday August 15, 2005	Tuesday August 16, 2005	Wednesday August 17, 2005	Thursday August 18, 2005
Ballroom Lobby	<i>Registration</i> 2:00 – 7:00 PM	<i>Registration</i> 7:30 AM – 5:00 PM	<i>Registration</i> 7:30 AM – 12:30 PM 6:00 – 8:00 PM	<i>Registration</i> 7:30 AM – 5:00 PM	<i>Registration</i> 7:30 AM – 2:00 PM
Magpie A/B		<i>Authors' Breakfast</i> 7:00 – 8:00 AM	<i>Authors' Breakfast</i> 7:00 – 8:00 AM	<i>Authors' Breakfast</i> 7:00 – 8:00 AM	<i>Authors' Breakfast</i> 7:00 – 8:00 AM
Ballroom I		<i>BWR SCC and Modeling – I & II</i> 8:00 AM – 12:10 PM <i>BWR SCC and Modeling – III & IV</i> 1:30 – 4:25 PM	<i>LAS and RPV Steel</i> 8:00 – 10:05 AM <i>Operational Experience - I</i> 10:30 AM – 12:10 PM <i>Operational Experience - II</i> 6:00 – 8:55 PM	<i>Irradiation Assisted Stress Corrosion Cracking – I & II</i> 8:00 AM – 12:10 PM <i>Irradiation Assisted Stress Corrosion Cracking – III</i> 1:30 – 3:10 PM <i>Crack Growth</i> 4:00 – 5:40 PM	<i>Irradiation Effects I & II</i> 8:00 AM – 12:10 PM <i>Waste Materials and Mechanical Properties</i> 1:30 – 3:10 PM
Ballroom II		<i>PWR Primary – I & II</i> 8:00 AM – 12:10 PM <i>PWR Primary – III & IV</i> 1:30 – 5:40 PM	<i>PWR Primary – V</i> 8:00 – 9:40 AM <i>Zircaloy</i> 10:30 AM – 12:10 PM <i>Noble Metal and SCC Mitigation</i> 6:00 – 8:55 PM	<i>PWR Secondary – I & II</i> 8:00 AM – 12:35 PM <i>PWR Secondary – III & IV</i> 1:30 – 6:05 PM	<i>Nickel-Base Alloys – I & II</i> 8:00 AM – 12:10 PM <i>Nickel-Base Alloys – III & IV</i> 1:30 – 5:15 PM
Ballroom III			<i>Super-Critical Water-Cooled Reactors I & II</i> 8:00 AM – 12:10 PM		
Superior Room					<i>Organizing Committee Lunch</i> Noon – 1:30 PM
Golden Cliff/ Eagle's Nest	<i>Welcome Reception</i> 6:00 – 7:00 PM				
La Caille Restaurant				<i>Conference Banquet</i> 6:30 – 9:30 PM	